TAMPEREEN TEKNILLINEN YLIOPISTO
TAMPERE UNIVERSITY OF TECHNOLOGY

Alper Cömert

The Assessment and Reduction of Motion Artifact in Dry Contact Biopotential Electrodes

Julkaisu 1319 • Publication 1319

Tampere 2015

Tampereen teknillinen yliopisto. Julkaisu 1319
Tampere University of Technology. Publication 1319

Alper Cömert

The Assessment and Reduction of Motion Artifact in Dry Contact Biopotential Electrodes

Thesis for the degree of Doctor of Science in Technology to be presented with due permission for public examination and criticism in Tietotalo Building, Auditorium TB109, at Tampere University of Technology, on the 10th of September 2015, at 12 noon.

Tampereen teknillinen yliopisto - Tampere University of Technology
Tampere 2015

ISBN 978-952-15-3563-5 (printed)
ISBN 978-952-15-3575-8 (PDF)
ISSN 1459-2045

Abstract

The connecting interface between biopotential monitoring systems and the human body is the electrode. Conventional medical electrodes use gel to improve skin-electrode contact and glue to provide secure attachment of the electrode to the skin. However, this type of electrode is neither reusable nor user-friendly when implemented in wearable monitoring systems. For wearable monitoring systems, the best type of electrode to use, as seen from the point of view of user comfort and ease of use of the wearable system, is the un-gelled electrode. The un-gelled electrode foregoes conductive gel and attachment glue and instead uses body moisture and clothing pressure to provide contact and secure attachment. The drawback of un-gelled electrodes is that they are susceptible to the wearer's movements, namely, to motion artifact.

Solving the issue of motion artifact will improve signal quality and reliability for wearable systems and, due to integration and reusability, would reduce costs. These two factors, when combined, would enable the widespread use of wearable monitoring systems in both the medical context and the consumer-user context. One effect of this will be a reduction in load and costs on health care systems due to improved preventive monitoring and better monitoring of patients in the recovery and rehabilitation phase. A second effect, combined with the information exchanging channels between individuals, will be unforeseen developments in health science due to what can be called the crowdsourcing of some aspect of physical and mental health and fitness.

This thesis aims to further state-of-the art wearable physiological monitoring by aiding motion artifact research and electrode design. To accomplish this aim, investigations into the programmable and repeatable generation of electrode movement in order to generate motion artifact, the effect of impedance current frequency on the relationship between skin-electrode interface impedance and electrode movement and motion artifact, the effect of using an electrode support structure and how its design affects the motion artifact, and the effects of garment parameters such as tightness are presented in this thesis.

A system that generates known and programmable motion of the electrode under controlled circumstances was designed, tested, and after the verification of system functionality, used in subsequent investigations. The presented system generates accurate motion of the electrode and the electrode motion can be observed as both motion artifact and skin-electrode impedance changes.

A real time impedance spectroscopy study of 24 impedance current frequencies between 25 Hz and 1 MHz was done on electrodes subject to accurately known motion generated by the designed system in order to find the impedance current frequencies most suited to motion artifact studies.

During this research, a hypothesis was formed that states that an electrode with a structural design that restricts epidermis deformation by trapping the epidermis under the electrode area can reduce motion artifact. Different electrode support structures were designed in order to test this hypothesis. The electrodes with support structures were subjected to system-generated motion and the resulting data were analyzed for the verification of support structure functionality and the hypothesis.

Electrodes that were supported by a tight garment-mimicking elastic straps were studied under subject-generated movement and at various clothing tightness levels. The same study was used to understand the effect of using padding between the garment and the electrode.

The motion artifact generation system was seen to be successful in accurately generating electrode motion, thus motion artifact, which was programmable and repeatable. The electrode mounting force monitoring proved to be an important functionality as the mounting force was seen to affect the motion artifact.

Skin-electrode impedance was found to correlate well with electrode motion in current frequencies between 17 kHz and 1 MHz. While the correlation between impedance and motion artifact was lower than the correlation between impedance and electrode motion, it was also highest in this frequency band.

Electrode support structure design is seen to be an important factor to consider when designing the electrode, and the electrodes that came closest to fulfilling the design criteria of the hypothesis were the best functioning electrodes. The hypothesis is seen to be promising and electrodes that distributed skin deformation over a large area and/or restrict epidermis deformation were found to reduce motion artifact.

In the presented studies, the pressures under those electrodes that were found to be the most effective in reducing motion artifact differed between experiments yet stayed in a range between 5 mmHg -36 mmHg (0.66 kPa – 4.80 kPa). A simple guideline is that the electrode should be attached firmly but not so firmly that it becomes uncomfortable. This guideline fitted well with the pressure levels found for each experiment.

The presented Motion Artifact Generation and Assessment System can be used for research or commercial purposes, furthering the research on motion artifact and aiding in the successful design of motion artifact resilient electrodes. The issue of which are the best current frequencies to use to measure skin-electrode interface impedance in motion artifact research has been clarified. Possible means of reducing motion artifact at its origin by using structural electrode designs that restrict epidermis deformation is hypothesized and proven worthy of further research. The importance of garment design and guidelines for use are given and tightness recommendations presented. The thesis presents methodology for the furthering of the understanding of motion artifact and electrode design that will eventually make wearable monitoring systems widespread over a large range of applications and a large number of users.

Preface

The work presented in this thesis was carried out at the Tampere University of Technology. It was started in the Ragnar Granit Institute, and after a number of structural changes in the university, was finalized in the Electronics and Communications Engineering.

In 2003, a TEKES project about wearable group exercise monitoring that was a collaboration of CorusFit OY and TUT was launched, and started my long journey towards the thesis. This project made it clear that motion artifacts are a problem that prevent the wide spread use of wearable monitoring devices, and so my work began. After this project ended, I took part in a number of smaller projects which all added to my knowledge and experience. Here I would like to thank many people who made it possible for this thesis to come to life.

I would like to give my deepest thanks to Prof. Jari Hyttinen, who provided me with the opportunity to work on this topic, guided me in scientific matters and provided financial means for me to continue this work.

I thank my pre examiners Dr. André C. Linnenbank and Prof. Reijo Lappalainen for their extensive review of the thesis. Their comments and suggestions have made the thesis scientifically stronger and also provided personal lessons for me to use in the future.

People I worked with, I would like to acknowledge in no particular order: Juhani and Merja Perhonen for their collaboration and financing opportunities, Markku Honkala for his never ending creativity, Juho Nousiainen, Jari Viik and Hannu Eskola for their teachings and support, Antti Vehkaoja and Merja Puurtinen for our work together, Baran Aydoğan for jumping in to help, Jarmo Verho and Timo Salpavaara for their electronics expertise, Peter Heath for his thorough language work on all my publications, Soile Lönnqvist for her always present readiness to aid in formal matters, the personnel of Projo for building the first motion artifact generation device prototype, all my experiment subjects that sat for hours without a complaint, and all my colleagues at the department which made work life an opportunity for growth and enjoyment.

I would also like to thank the Pirkanmaa Cultural Fund for providing me with a grant, which not only was a financial factor but also an encouragement for me to continue this work.

Now that this journey is closing to an end, I am starting to realize that it was more about human nature, the nature of thoughts and beliefs, and life itself. I will carry these lessons throughout my life, and will impart them on people who need them for their own journeys.

None of this would have been possible without my parents' emotional and financial support, and I would extend a deep gratitude to Arif and Lydia Cömert. My siblings, Sibel Ece (Cömert) and Bertan Cömert have been there to support me, to encourage me, or just be, and I am happy to have them in my life. My sister's husband, Altuğ Ece, and their little daughter Suzan have added to the joy in my life. Maybe the most important lesson I have learned is that the people in our lives are our most precious parts of our lives.

Tampere, 16 July 2015

Alper Cömert

Table of contents

List of Publications

Parts of this thesis have been previously published. These following publications are included in the thesis:

Paper 1

Cömert A, Honkala M, Hyttinen J: Effect of pressure and padding on motion artifact of textile electrodes. *Biomed Eng Online* 2013, 12:26.

Paper 2

Cömert A, Hyttinen J: A motion artifact generation and assessment system for the rapid testing of surface biopotential electrodes. *Physiol Meas* 2015, 36:1.

Paper 3

Cömert A, Hyttinen J: Impedance spectroscopy of changes in skin-electrode impedance induced by motion. *BioMedical Engineering OnLine* 2014, 13:149.

Paper 4

Cömert A, Hyttinen J: Investigating the Possible Effect of Electrode Support Structure on Motion Artifact in Wearable Bioelectric Signal Monitoring. *BioMedical Engineering OnLine* 2015, 14:44

Contributions of the author

Paper 1

The author designed the study protocol and the overall concept of the paper was designed with coauthors. The author designed and selected the materials and study methods. The analyses, conclusions, and writing of the paper were done by the author. This paper was collaboration between the author, Professor Jari Hyttinen, and Markku Honkala.

Paper 2

The author designed the presented system and the study protocol. The overall concept of the paper was designed with the coauthor. The design and selection of system components, the construction of the system, and study methods as well as the analyses, conclusions, and writing was done by the author. The author wrote the paper in collaboration with Professor Jari Hyttinen.

Paper 3

The author designed the study protocol and the overall concept of the paper was designed with the coauthor. The author designed and selected the materials, impedance current frequency parameters, and study methods and carried out the analyses and conclusions. The author wrote the paper in collaboration with Professor Jari Hyttinen.

Paper 4

The author designed the study protocol and the overall concept of the paper was designed with the coauthor. The design and selection of materials and study methods as well as the construction of electrode paddings, analyses, conclusions and writing was done by the author. The paper was written in collaboration with Professor Jari Hyttinen.

List of Abbreviations and Symbols

Δdeg	Servo rotation magnitude
Δx	Electrode movement in the x-axis
Δy	Electrode movement in the y-axis
Ag/AgCl	Silver/silver chloride
BMI	Body mass index
C_{cm}	Capacitance of the cell membrane
C_{el}	Capacitance of electrode-electrolyte interface
C_{ep}	Capacitance of the epidermis
C_i	Capacitance of the skin-electrode interface in the absence of electrode gel
C_{sw}	Capacitance of the sweat ducts
CMRR	The common-mode rejection ratio
E_{ep}	The potential across the epidermis
E_{hc}	Half-cell potential
E_{sw}	Potential difference between the inside and outside of the sweat ducts
ECG	Electrocardiography/ Electrocardiogram
EEG	Electroencephalography
EMG	Electromyography/ Electromyogram
NaCl	Sodium chloride
PSD	Power spectrum density
R_c	Resistance of the cell
R_d	Resistance of the dermis
R_{el}	Resistance of electrode-electrolyte interface
R_{em}	Resistance of the extracellular medium
R_{ep}	Resistance of the epidermis
R_g	Resistance of electrode gel

R_i Resistance of the skin-electrode interface in the absence of electrode gel

R_{sw} Resistance of the sweat ducts

RMS Root mean square

SNR Signal-to-noise ratio

1. Introduction

With the increase in the percentage of the elderly in the population, the increase in obesity, and the increase in chronic and lifestyle-related diseases, the load on already over-stretched medical services and medical personnel is increasing, as are the costs. Health care costs in the U.S.A. are predicted to increase from 17.9 % to 19.9 % of the gross domestic product (GDP) from 2010 to 2022 (Cuckler et al., 2013). This amounts to an estimated increase in the health care costs from $2.6 trillion to $5 trillion dollars while the GDP is estimated to rise from $14.5 trillion to $25.2 trillion. In the EU countries, health care costs are expected to rise from 6.8 % of the GDP to 7.4 % of the GDP from 2010 to 2030 (Przywara, 2010). This projected rise in health care costs is much more optimistic than the one put forward by *The Economist*, based on World Bank numbers, which states that health care costs in the EU countries will rise from 8% to 14% of GDP by 2030, and that the costs of health care will rise at a faster rate than the amount of funding available (*The Future Of Healthcare In Europe*, 2011). It is not only the number of patients that causes problems; it is also the likelihood that many elderly and obese patients will suffer from reduced mobility. Reduced mobility makes it more difficult to transport these patients to medical facilities or to transport medical-grade equipment and services to these patients. This brings forth the need and the increased interest in the development of highly mobile physiological monitoring systems with high signal quality and processing power. Such systems can be used in medical environments, in daily life, on the sports field, and in a variety of other applications or monitoring areas without the need for medical personnel to be present, the necessity of large-sized peripheral systems, or the need for the subject to be immobile.

In addition to the present and future needs of the health care industry, further drivers of the mobile physiological signal monitoring market are health and sports enthusiasts, sports professionals, and other non-medical setting users. The use of wearable physiological signal monitoring devices in the professional sports industry is increasing in many areas. Such uses range from simple heart rate monitoring and the more detailed electrocardiographic (ECG) monitoring of athletes to more complicated muscle contraction measurements taken during physical activity. One recent development in the mobile physiological signal monitoring market is the emergence of so-called body-hackers and mind-hackers. These are enthusiasts who use physiological signal monitoring and biofeedback to improve their mental states, health, sports performance, professional performance, and even their mental capabilities. The rise in popularity of heart rate monitors and heart rate variability analyzers has shown the large market potential of this group.

In recent years, the development of mobile monitoring systems has been aided by extensive developments in electronics that have resulted in devices becoming smaller, less power consuming, yet more powerful, and that have also enabled batteries to be smaller in size but larger in capacity. Of special importance are the developments in smart phones that now possess enormous processing power compared to only five years ago together with the possibilities of large on-device data storage,

high speed data transfer and computing, and data storage in the cloud. Because of these advancements, monitoring devices can now be made more unobtrusive, long-term usable, able to communicate with a medical center, and potentially provide medical grade data. As a result, a boom in wearable monitoring devices can be expected.

Electrocardiography (ECG), electromyography (EMG), and electroencephalography (EEG) are most likely to be the first methods to become widespread, but the possibilities are not limited to only these, as the developments in monitoring devices might open the way for new monitoring or diagnostic methodologies. There are, for example, devices such as heart rate monitors currently on the market that can also measure heart rate variability, EMG devices that can analyze muscle activation sequence, and consumer-grade EEG devices.

The aim of this thesis is to aid in the design of wearable monitoring systems by increasing our understanding of the skin-electrode interface under motion and by looking for ways to reduce problems that arise at this system layer due to subject movement. This task is approached from a practical electrode design perspective, from a theoretical perspective of motion artifact generation, and by developing robust and repeatable methods that can lead to a standardized research methodology for analyzing electrode design in relation to motion artifact.

The need for this thesis arises from one issue with wearable monitoring systems that remains unsolved: the problem arising at the skin-electrode interface in non-stationary monitoring caused by subject movement. The use of electrodes allows for the measurement of the electrical activity at the skin surface caused by physiological events such as muscle activity, heartbeat, and brain activity. Since this electrical activity generates a potential on the skin and this potential is measured by the electrode in contact with the skin, it can be said that the skin-electrode interface is the input point for the electrical measurement system (Webster, 2009). Therefore, as an input, any disturbance in this skin-electrode interface will be disruptive to the biopotential that the monitoring system intends to measure. When the subject moves, the electrode moves and results in changes in the anatomical tissue. Movement of the electrode causes deformation of the skin and changes in the physical and electrical properties of the skin-electrode interface, resulting in motion-related electrical potentials. These unwanted electrical signals are called motion artifact. A motion artifact can be larger than the measured signals and most often is in the same frequency band as the signals that are being measured. Thus, motion artifact can be very disruptive to signal quality (Webster, 2009).

In the case of wearable devices designed to be used for long-term monitoring and possibly by the medically untrained persons, reusable electrodes integrated into monitoring garments are preferable to the use of disposable medical-grade electrodes (Beckmann et al., 2010; Lymberis and Paradiso, 2008). These integrated electrodes do not usually use conductive gel or glue in their application and are called dry or un-gelled electrodes. Although user-friendly and reusable, they have generally been found to have inferior signal quality (Langenhove, 2007) and to be more susceptible to motion artifacts (Merritt et al., 2009). Therefore, if the use of wearable devices is to become more widespread without sacrificing user-friendliness or data reliability, the motion artifact of un-gelled electrodes must be reduced to a level close to that of commercial medical electrodes.

Many researchers have studied the motion artifact in order to detect its presence or to develop methods to reduce it. In order to study motion artifact, methods are needed to generate motion, to measure the motion artifact, and to assess the resulting signals. Motion can be generated in various ways, and these methods can be grouped in three categories: motion generated by subject movement, electrode motion generated by operator action, and motion generated by mechanical means. Research done by using subject-generated motion use the subject moving in predetermined ways such as swinging arms and other single or multi-joint movements (Cho et al., 2009; Kearney et al., 2007; Lee et al., 2010; Muhlsteff et al., 2004; Pengjun et al., 2011; Pola and Vanhala, 2007; Sweeney et al., 2010), walking or running (Di Rienzo et al., 2007; Kang et al., 2008; Lee et al., 2008, 2010; Merritt et al., 2009; Jorg Ottenbacher et al., 2008), jumping (Laferriere et al., 2011), sitting, cycling (Raya and Sison, 2002), training on an elliptical trainer (Marozas et al., 2011), mechanically restricted voluntary limb movement (Roy et al., 2007), or in random movement patterns (Romero et al., 2012, 2011) in order to generate motion artifact at electrodes worn on the body using some form of garment or belt system. In some studies, the operators generate motion by pressing on the electrode and moving the electrode with their fingers (Buxi et al., 2012; Hamilton et al., 2000; Tong et al., 2002), and by pulling the skin around the electrode (Hamilton and Curley, 1997; Liu, 2007). Mechanical generation of motion is achieved by increasing the force on the electrode by changing weights or with pulley systems (Beckmann et al., 2010; Talhouet and Webster, 1996; Vos et al., 2003), by vibrating the body or the electrode (Fratini et al., 2009; Searle and Kirkup, 2000), and by lateral electrode motion created by motorized systems (Hokajärvi, 2012; Liu et al., 2013; Ödman and Öberg, 1982). Some studies forego the subject and test the electrodes on a skin simulator. One factor affecting these studies is that for most the motion created is constrained by the human factor in both accuracy and repeatability. Furthermore, the contribution of garment and electrode design to the motion artifact is not separated, and the exact pattern of electrode motion might not be known. These two factors could affect experiment standardization and repeatability and the depth of motion artifact analysis in relation to motion.

Surprisingly, with the exception of the paper by Liu et al., which presents results for dry electrodes on skin, none of the introduced studies or other studies used a motorized system for the elaborated motion artifact study of un-gelled electrodes on human skin. It is understandable that the researchers preferred to test electrodes already integrated into garments as the garment and the electrode act together in the creation of the motion artifact in wearable monitoring systems. Nevertheless, the lack of research on motion artifact using controlled motion directly applied to the electrode shows that there is an area where large improvements in un-gelled electrode design are possible. When achieved, these improvements will carry over to wearable system functionality, when the electrode is integrated into the garment.

Various methods for the detection and reduction of motion artifact have also been proposed and shown to have varying degrees of success. Among these are adaptive filtering methods that use sensors to detect electrode motion (Di Rienzo et al., 2007; Kim et al., 2008; Lee et al., 2010; Luprano et al., 2013; Raya and Sison, 2002; Romero et al., 2012; Sweeney et al., 2010; Tong et al., 2002), to detect skin deformation (Hamilton et al., 2000; Hamilton and Curley, 1997; Lee et al., 2010; Liu, 2007; Pengjun et al., 2011), to detect skin-electrode contact pressure changes (Kim et al., 2008; Pengjun et al., 2011), to

detect additional biopotentials between electrodes separate from the studied electrode (Kearney et al., 2007; Luo and Tompkins, 1995), and skin-electrode impedance as input signals to reduce motion artifact (Hamilton et al., 2000; Laferriere et al., 2011; Luprano et al., 2013; J. Ottenbacher et al., 2008; Romero et al., 2012, 2011). Skin-electrode impedance has been further studied in relation to motion and has shown varying degrees of relation to motion and motion artifact (Albulbul and Chan, 2012; Beckmann et al., 2010; Buxi et al., 2012; Ödman, 1981; Ödman and Öberg, 1982; Talhouet and Webster, 1996). In addition, active electrodes have been shown to be successful in the reduction of the motion artifact (Kang et al., 2008; Merritt et al., 2009)

During the literature review, it was noted that the skin-electrode interface impedance studies used largely varying impedance frequencies for their impedance measurements. It remains unclear if the impedance current frequencies are a factor in the relationship between impedance and motion, or between impedance and motion artifact.

Different textile electrode manufacturing methods that create different electrode surfaces such as knitting, weaving, or embroidering have all been investigated. (Beckmann et al., 2010; Cho et al., 2009; Fratini et al., 2009; Marozas et al., 2011; Marquez et al., 2013; M. Catrysse, 2003; Mestrovic et al., 2007; Pola and Vanhala, 2007; Puurtinen et al., 2006; Rattfält et al., 2007). Other materials such as rubber, conductive polymers, silicone, and silver paste have also been used (Buxi et al., 2012; Chan and Lemaire, 2010; Garcia et al., 2007; Gruetzmann et al., 2007; Laferriere et al., 2011; Muhlsteff et al., 2004; Muhlsteff and Such, 2004; Pandian et al., 2008; Pylatiuk et al., 2009; Yoo et al., 2009). All the presented electrodes successfully measured the biopotentials, which was the scope of their respective studies, yet still remained susceptible to motion artifact in various ways. However, due to the different methods used, the results have been difficult to compare.

Various electrode designs that aim to reduce the motion artifact have been investigated. These include designs such as inserting a pillow between the garment and electrode (Cho et al., 2009; Lin et al., 2011; Löfhede et al., 2012; Seoane et al., 2014, 2013; Tseng et al., 2013) , making a textile electrode that has the design of a Velcro textile (Marquez et al., 2013), using a telescope-like structure to attach the electrode to the skin (Griebel et al., 2009), and designing the electrode surface to have small bumps (Buxi et al., 2012; Laferriere et al., 2011). For non-textile dry electrodes, simple 3-dimensional shapes such as circular and oval discs have been studied (Chan and Lemaire, 2010; Garcia et al., 2007; Gruetzmann et al., 2007; Laferriere et al., 2011; Muhlsteff et al., 2004; Muhlsteff and Such, 2004; Pandian et al., 2008; Pylatiuk et al., 2009). All designs claim an improvement of the electrode in relation to motion artifact. In addition to the electrode with the small bumps and studies that compare different textile electrode manufacturing processes that have found that embroidered electrodes are more stable against motion, most of these designs have not tried to affect the deformation of the epidermis, the upmost layer of skin, where the motion artifact originates. Most effort is being made to ensure that there is adequate contact between electrode and skin, yet this may be insufficient for the design of a motion artifact-resilient electrode.

Overall, previous research shows that motion of the electrode creates motion artifact and that motion also causes detectable changes in the signals obtained by impedance, acceleration, or other secondary

sensors, and that the studied methods in motion artifact reduction are all successful to some degree. Yet, further improvement is needed to make studies repeatable and comparable with each other.

In this thesis, an investigation aimed at better understanding motion artifact is undertaken.

In order to be able to directly analyze the relationship between changes in the electrical properties of the skin-electrode interface, the generated potential and impedance, and the accurately known motion and to have repeatable experiments, a device that mechanically generates exactly known motion of the electrode was designed and constructed. In this thesis, the studies leading up to the design of this device, the device and the studies done with this device are presented.

The electrode structure and its effect on the motion artifact are investigated to gain a better understanding of the practical aspects of motion artifact generation and reduction. A further aim is to provide guidelines for the design of electrodes that mechanically reduce the motion artifact at its source.

Using both subject-generated motion and mechanically-generated motion, electrode motion and the forces acting on the electrode are investigated. Because the design of a garment affects how the subject movement is translated into electrode motion and force applied to the electrode, knowing how these factors affect the electrode in the context of motion artifact could lead to guidelines for garment and overall system design.

To answer the questions about the effect impedance current frequency has on the relationship between skin-electrode interface and electrode motion and between skin-electrode impedance and motion artifact, an impedance spectroscopy study of frequencies from 25 Hz to 1 MHz was carried out.

This thesis introduces a Motion Artifact Generation and Assessment System that can help in the design of comparable research, a hypothesis on how electrode structure design can reduce the motion artifact, an electrode design that aims to physically reduce motion artifact, and answers the questions on what impedance frequencies to use when studying electrode motion and motion artifact.

1.1. Main Hypotheses, Objectives and Research Questions

The major aim of this thesis is to increase our understanding of the motion artifact, its generation, measurement, assessment, and reduction. Because motion artifact is tackled from the point of view of wearable systems, the focus is on un-gelled electrodes.

We can hypothesize that to study motion artifact we need to be able to know and control the motion acting on the electrode in order to make these studies repeatable, standardized, quantitative, and comparable. We could presume that directly applying the motion to the electrode is necessary for testing the electrode's susceptibility to motion itself, without considering the contributions of garment properties in the generation of motion. To investigate this hypothesis and assumption, a device for mechanically generating the motion artifact will be conceptualized, designed, built, and functionally tested.

Skin-electrode impedance measurements are not standardized, with different impedance frequencies being used in different studies. It is highly probable that different anatomical, physiological, and psychological changes in the skin-electrode interface and the tissue in the current pathway each have a major effect at different impedance frequencies. To provide clarity on this issue, an impedance spectroscopy study is undertaken in which multiple frequencies in a wide frequency band are measured simultaneously from an electrode subject to motion.

Due to the elastic properties of the skin and elasticity constraints and due to the electrical properties of skin, it is not clear how motion artifact and the skin-electrode interface are related to electrode motion magnitude and speed. To bring clarity to this issue, a device for mechanically generating motion artifact is used to study the frequency response and the amplitude response of these two signals to the electrode motion. As applied pressure affects the skin physically, we can assume that applied pressure will also affect the electrical behavior of skin under various levels of pressure. To investigate this assumption, motion artifact generated by directly applied motion is tested under various electrode-mounting forces. Because the tissue underlying the skin might affect the elastic properties of the skin or how the electrode pressure induces skin deformation, these investigations are carried out in two locations, each with different anatomical structures.

Following the widely accepted assertion that the motion artifact originates in the epidermis, I hypothesize that an electrode structure that physically restricts epidermis deformation at its origins by trapping the skin under the electrode area, and thereby constricting the skin, could effectively reduce the motion artifact at its source.

This hypothesis suggests the possibility that structural electrode design could physically affect the generation of motion artifact. For the study of the hypothesis and this follow-up reasoning, different electrode designs, including an epidermis-restricting design, are investigated in relation to their susceptibility to motion artifact.

Just as structural electrode design might affect the generation of motion artifact, the mere existence of padding between the inside of the garment and the electrode might also affect electrode susceptibility to motion artifact. Electrodes with and without the inserted padding are investigated to clarify this possibility. In these experiments, various garment tightness levels are used for the investigation of the effects of garment design on motion artifact.

1.2. Structure of the Thesis

The structure of the thesis follows the general principles of scientific reporting. The thesis starts out with the Background chapter in which the underlying mechanisms of surface biopotentials and bioimpedance measurements are introduced to present the reader with a brief overview of the theoretical background of the thesis. Major projects worldwide to augment wearable monitoring are presented to give a summary of recent developments in the field. In the same chapter, electrode types are introduced and un-gelled electrodes are discussed in more detail, as they are the most relevant to wearable monitoring systems. Major sources of noise are listed and the origin of motion artifact is studied in more detail.

In the Methods chapter, the testing of motion artifact generated by the voluntary movement of a subject in a garment-mimicking setup is first introduced, as this was the initial stage of research. This is followed by the introduction of a Motion Artifact Generation and Assessment System that was designed in this thesis with the aim of making motion artifact studies with known and programmable, mechanically-generated motion under controlled parameters such as pressure and electrode location. This is followed by the presentation of the electrode designs used in the studies and designed in this thesis. To conclude, the methods, subjects, and data analysis are presented.

The Results summarizes and organizes the experience and findings concerning the functionality of the introduced system, the impedance spectroscopy of the skin-electrode interface during applied electrode motion, the relationship between motion artifact and applied motion, the relationship between motion artifact and the peripheral conditions of electrode-mounting force and electrode location, the effect of using padding between the inside of the garment and the electrode, and the further implications of structural electrode design. The Discussion chapter elaborates on the important aspects of the results such as the functionality of the presented system, its advantages, shortcomings, and disadvantages, the best frequencies to use for impedance measurements in motion artifact studies, the knowledge gained on the motion artifact by using the system, and the understanding gained on reducing motion artifact by affecting the physical behavior of the skin by electrode structure design. Finally, guided by the Discussion chapter, the Conclusions chapter aims to provide guidance for future research.

2. Background

To better explain motion artifact and issues related to motion artifact, in this chapter the physiological signals and parameters that can be measured by surface electrodes are first discussed: what they are, how they are created, what they mean. After a generalized introduction into surface biopotentials, EMG and ECG are discussed as they are two of the most used wearable physiological monitoring methods and have great diagnostic, rehabilitative, and preventive importance. The bioimpedance measurement, which is not a biopotential measurement but a measurement of current conductance in the body and the electrodes, is then discussed at the end of chapter 2.1. Bioimpedance measurement also has widespread applications and is used in studies related to motion artifact as a separate signal input for methods aiming to reduce the effects of motion artifact or the motion artifact itself.

After the surface measurements are introduced, the most common wearable monitoring systems and the best-known research projects are listed to give the reader an idea of the current state of research. This is not a complete list but covers many of the major projects in the last ten years. In addition, some known and potentially promising present-day projects and products that are already on the market are introduced.

Next, the types of electrodes are discussed. Conventional gelled electrodes and non-contact capacitive electrodes are introduced, but the emphasis is given to un-gelled electrodes, also called dry electrodes, as this type of electrode is the one most suitable for wearable monitoring applications. Some examples of un-gelled electrode materials and designs are given in subchapter 2.3.2.1. Because in many instances dry electrodes are used by moistening with water, saline, salt water spray, or a hydrogel and are otherwise dependent on skin humidity and sweating, the use of the term “dry electrode” has come into question. For this reason, throughout this thesis the term “un-gelled electrode” is used to describe this type of electrode.

Electrode noise is introduced in 2.4. The major sources of electrode noise are introduced, as well as motion artifact. Motion artifact, as it is the topic of the thesis, is later expanded on in chapter 2.5. In chapter 2.5, the origin of motion artifact is discussed by presenting the events at the skin-electrode interface and how motion artifact is created at this interface. Furthermore, methods to generate motion artifact in previous studies are discussed and followed by research methods used for motion artifact detection and/or reduction.

2.1. Physiological Signals Measured on the Body Surface

There is a certain category of cells in the body that has large and fast enough electrochemical activity that can be measured from the skin surface as biopotentials. The measured biopotentials can originate from the activity of a single cell or from the activity of a collection of cells. This category of cells is made

up of nerve cells, muscle cells, and glandular cells. Nerves transfer information in the body, and this transfer of information can take many forms such as information transferred to the brain from touch-sensitive skin cells and commands from the brain to the muscles. Muscle cells cause voluntary and involuntary muscle contractions, cause movement and keep the body in the desired posture. Glandular cells are tasked with the secretion of various chemicals, for example, hormones. At rest, these cells possess a resting potential across their membrane, and when excited this potential changes and forms an action potential. An action potential functions in an on-off state. If the stimulus is large enough to cause the membrane potential to reach the threshold, the action potential is generated and reaches its set all-or-nothing level. The action potential, once generated, is independent from the level or duration of the stimulus and exceeds what is needed for the skin membrane potential to reach the threshold. (Webster, 2009)

Using a micropipette, the resting and action potentials of single cells can be recorded. The levels are slightly different for different types of cells, locations, and species. The resting potential lies between -50 and -100 mV, as measured from outside of the cell to the inside. As an example, a nerve fiber has an action potential of 120 mV with a duration of 1 ms. In the time during and immediately after an action potential is generated, a refractory period exists which can be divided into two parts: the absolute refractory period, which includes the action potential and no other action potential can be generated, and the relative refractory period, where an action potential can be generated only by an extra high stimulus. These aspects of the action potential are presented in Figure 1. The absolute refractory time for a nerve cell is 1 ms, making the maximum number of action potentials in a second to be limited by 1000 impulses/second. The strength of a nerve impulse train is determined by the frequency of the impulses. (Grimnes and Martinsen, 2000; Plonsey and Barr, n.d.)

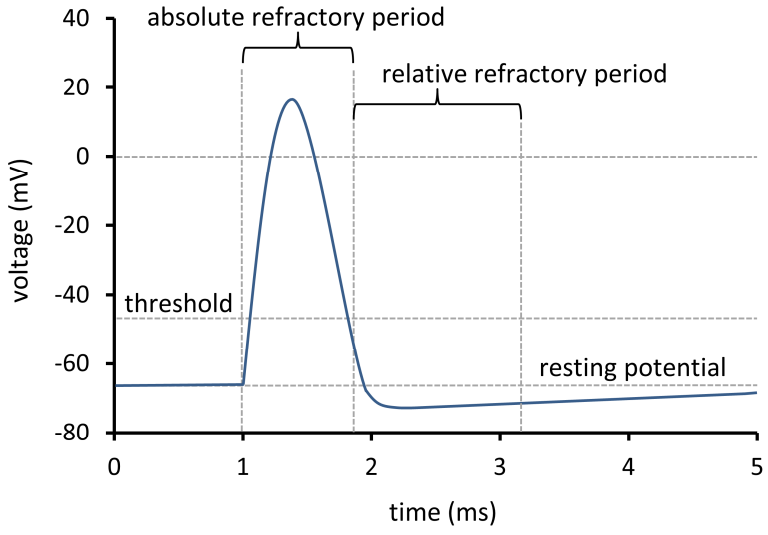

Figure 1. The action potential. During the absolute refractory period, no other action potential can be created. In the relative refractory period, additional action potentials might be created, but the required stimulus is larger than the threshold level. Modified from (Webster, 2009).

These individual action potentials of a single nerve or muscle cell, when present for the cells in a nerve fiber, muscle fiber, or a collection thereof, add up to an electrical potential or current that is generated inside body tissue, which is essentially a volume conductor. Since all the electrical activity of the cells is inside this volume conductor, the potentials and currents generated are conducted throughout this volume and can be measured on the skin. What is then measured is not a single action potential, but a collection of the action potentials of a nerve fiber or of a muscle fiber. This provides information on the physiological system that is being monitored. The best-known of these measurements are ECG, for measuring heart activity, EMG, for measuring muscle activity, EEG, for measuring brain activity, EOG, for measuring eye activity, and ENG, for measuring nerve activity. (Webster, 2009)

ECG and EMG signals, commonly focused on with wearable monitoring systems for use in non-medical settings, are greatly affected by motion artifact and are introduced below.

Following ECG and EMG, the bioimpedance measurement, which is not a biopotential in itself but a measurement of the electrical properties of body tissue, is introduced. The reason for the inclusion of bioimpedance is that it changes due to many factors such as tissue type, blood flow into the tissue, liquid accumulation in the tissue, and tissue volume. Thus, bioimpedance can be used in diagnosis and analysis.

2.1.1. EMG

A muscle comprises muscle fibers organized into motor units. A motor unit controls multitudes of muscle fibers and comprises the smallest muscle unit that can be activated by itself. How a single motor unit is connected to multiple muscle fibers is presented in Figure2. Once a motor unit is active, all its connected fibers are activated. Motor units are interconnected with other motor units at junction points so that, depending on the muscle activation strength or muscle fatigue, one or more motor units can act in harmony to achieve the muscle contraction command given by the nervous system.(Webster, 2009)

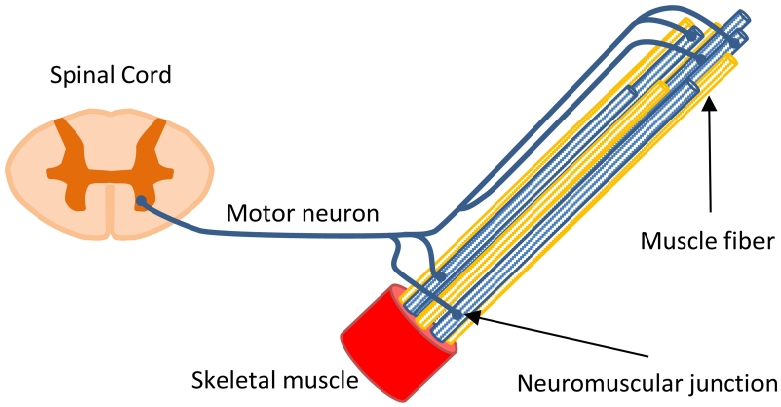

Figure 2. The motor unit. The motor unit comprises a single motor neuron and the muscle fibers it is connected to (Webster, 2009). A cross section of the spinal cord, the motor neuron, individual muscle fibers and the skeletal muscle made up of these fibers are depicted.

The nerve fibers of the single motor unit acting in unison are composed of a bioelectric source that can be measured on the skin close to the muscle. For a single motor unit, the measured potentials range between 20 µV and 2000 µV with discharge frequencies between 6 Hz and 30 Hz. (Webster, 2009)

Rarely is only one single motor unit activated, and thus the signal measured on the skin consists of the superimposition of multiple motor units and can look rather like noise and can be of a few millivolts with a frequency spanning 30-500 Hz (Kutz, 2003) or, in some applications, 50 to 5000 Hz (Grimnes and Martinsen, 2000).

Strong muscle contraction causes higher EMG amplitude, but this increase does not rise proportionally to the increase in contraction. Most of the increase in EMG happens during contraction increases spanning mid ranges, while during the small changes of contraction in the low levels or close to maximal levels, the EMG change is not as prominent. As the muscle fatigues, the frequency spectrum of the EMG shifts to the left, to lower frequencies, and its amplitude decreases. (Kutz, 2003) A depiction of how multiple active motor units give rise to the seemingly complex EMG signal is presented in Figure 3.

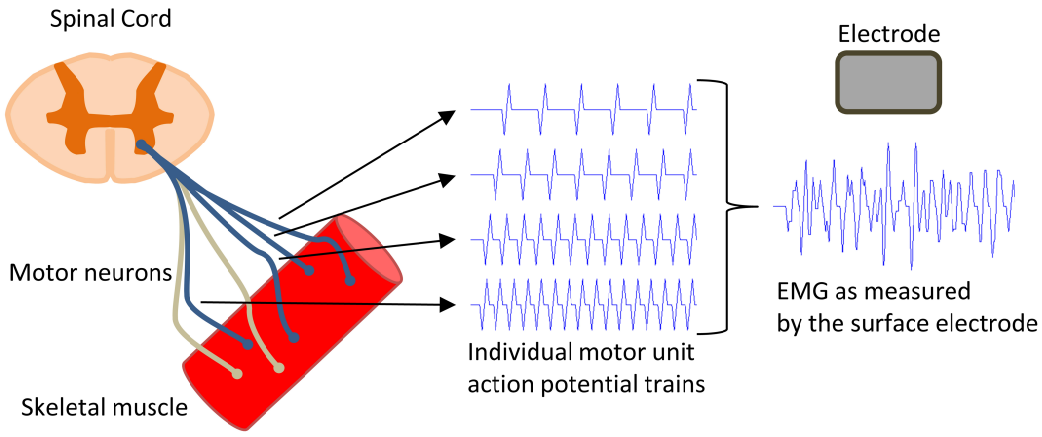

Figure 3. EMG generation. Potentials from individual motor units are summed up at the electrode. Active motor neurons are depicted in blue, inactive motor neurons are depicted in gray.

EMG is used in rehabilitation, sports, and other fields to mainly track the presence of muscle activation, muscle activation strength, muscle activation sequence, movement patterns, and other important aspects related to movement and posture. (Merletti et al., 2009)

2.1.2. ECG

The heart function is a precisely orchestrated coordination of nerve and muscle comprising four chambers. The two upper chambers, the atria, are tasked with filling the two lower chambers, the ventricles, which in turn are tasked with pumping blood into the circulatory system. (Webster, 2009)

ECG measures the combination of the activity of the cardiac cells that make up the muscular walls of the four chambers, the heart nervous system and the nerve conducting system, with the muscle cells dominating the signal. At each stage of the heart cycle, the corresponding nerve and muscle activity create potentials that are measurable by electrodes placed on the skin (Grimnes and Martinsen, 2000). The QRS complex, the most prominent feature of ECG, can have amplitudes up to 3 mV (Bailey et al., 1990; Wolthuis et al., 1979) with a diagnostic frequency band of 0.05 to 150, which can be more relaxed for just monitoring the patient or heart rate monitoring purposes (Bailey et al., 1990; Grimnes and Martinsen, 2000). The ECG and its main components are presented in Figure 4.

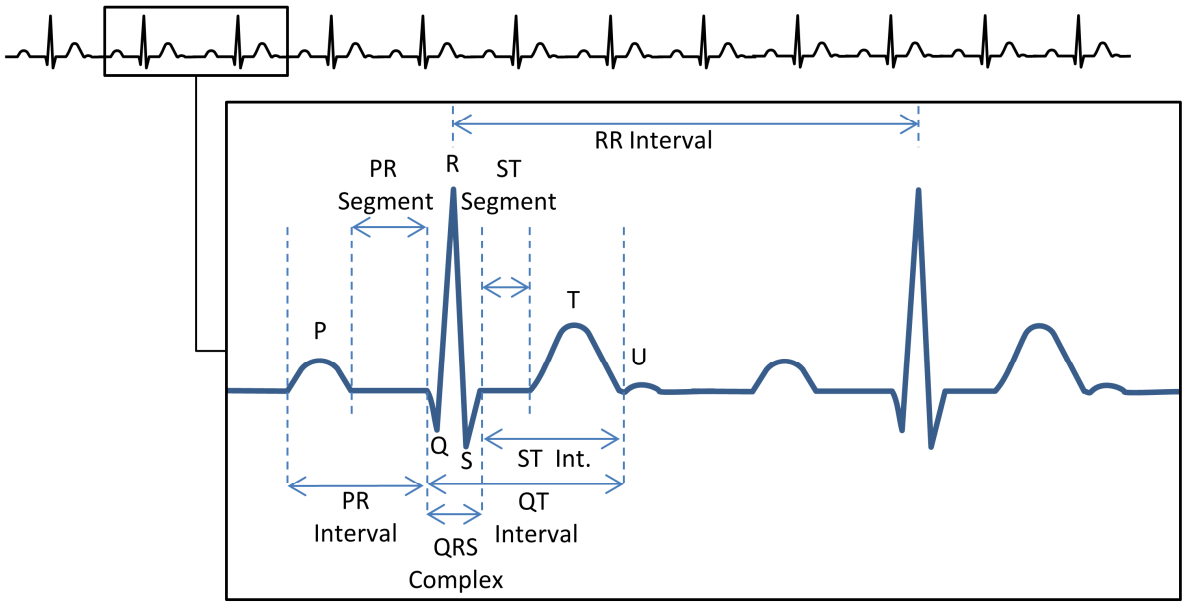

Figure 4. The ECG. P, Q, R, S, T and U waves and important segments and intervals are presented.

ECG is the most widely used diagnostic tool in medicine, and it will keep this place as the aging population and the increase in obesity continue to contribute to an increase in cardiac problems. This diagnostic use spans risk assessment, prevention, diagnosis, and rehabilitation. Besides the clinical application, heart rate derived from the ECG signal is widely used in sports, both professional and recreational, and in various bio-feedback applications. Recently, heart rate variability, the difference in the intervals between heart beats, has been a source of interest in sports and self-assessment applications as a means of measuring physical and mental fatigue, stress, and state of recovery.

The heart rate monitors and heart rate variability monitors that rely on detecting the QRS complex have less stringent criteria than diagnostic ECG monitors. The QRS complex can be detected with a signal filtered between 1 Hz and 30 Hz, and the amplitude of the QRS complex is up to around 3 mV. On the

other hand, for diagnostic ECG, signals of amplitude of 20 µV with duration of at least 6 ms are required as detected waveforms. As a result, the upper limit of acceptable noise is well below this level, as low as 5 µV. Moreover, the signal bandwidth is required to be between 0.05 Hz and 150 Hz for adults and between 0.05 Hz and 250 Hz for infants to preserve low and high frequency information. (Kligfield et al., 2007) These requirements highlight the importance of motion artifact reduction for a viable ECG signal. The necessary effectiveness of motion artifact reduction is different for different ECG applications because of the signal aspects measured in the application and the importance of the application readout. A heart rate monitor, for which the largest and most distinct component of the ECG, the QRS complex, is of interest, is more resilient to motion artifact than a diagnostic ECG monitor for which the smallest artifact can cause distortions that make it impossible to analyze the low amplitude components of an ECG waveform. At the time of writing, a standardized upper limit of motion artifact for heart rate monitors has not been defined to the best of the author's knowledge.

2.1.3. Bioimpedance

The two introduced methods, EMG and ECG, can be considered passive measurements because a potential is measured on the skin without active participation of the measurement system in the body systems. Biological tissue is an inhomogeneous conductor made up of different types of cells with differing electrical properties and the extracellular medium, and has resistive and capacitive properties. This tissue impedance can be measured by injecting current into the tissue and measuring the resulting voltage, or vice versa by applying a potential difference across the tissue and measuring the resulting current. (Grimnes and Martinsen, 2000)

Because the extracellular medium is mostly resistive and is composed of ions that flow freely in the fluid and the cellular medium has a dominant capacitive component because of the dielectric properties of the cell membrane, current at different frequencies flows through different pathways. A simplified depiction of this behavior and a simple electrical tissue model are presented in Figure 5.

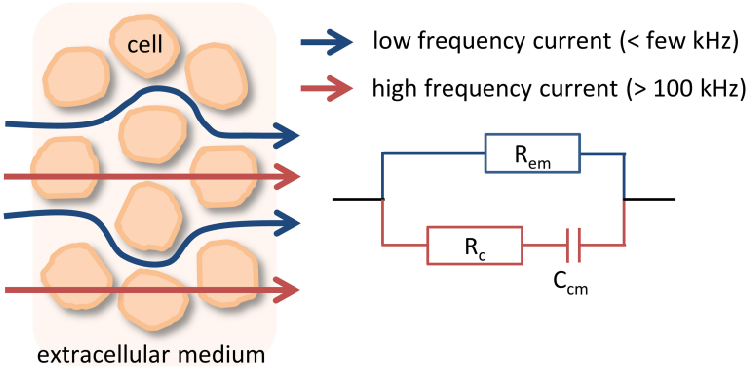

Figure 5. Frequency-dependent current pathways and simple electrical model of tissue. R_{em} is the resistance of the extracellular medium, R_c is the resistance of the cell, and C_{cm} is the capacitance of the cell membrane. Modified from (Grimnes and Martinsen, 2000)

This has application-specific importance as tissue impedance at different frequencies might attribute to different physiological systems and conditions.

Different tissue types have different conductivities and frequency-dependent impedances. Table 1 summarizes the tissue conductivities of most common tissue and seawater as an example (Grimnes and Martinsen, 2006). In the table, σ represents tissue conductivity. By comparing the low frequency values to the high frequency values, the differing behavior of tissue can be observed.

Table 1. Sample Conductivities

Tissue page 103	σ (S/m) @ 1 Hz – 10 kHz	σ (S/m) @ ca 1 MHz
Human skin, dry	10^-7	10^-4
Human skin, wet	10^-5	10^-4
Bone	0.005- 0.06	
Fat	0.02-0.05	0.02-0.05
Muscle	0.05-0.4	0.6
Blood	0.7	0.7
Seawater	5	5

The difference between the dermis and the epidermis conductivities as reported in two different sources is presented in Table 2. (He, 2010; Tavernier et al., 1993) He does not report the measurement frequency. Even though Tavernier et al. report different conductivities for dermis and epidermis, they report that the values stay constant from 1 Hz to 100 kHz (Tavernier et al., 1993).

Table 2. Conductivities of skin layers

	σ (S/m) (He, 2010)	σ (S/m) (plane/transverse) (Tavernier et al., 1993)
Dermis	0.22	2.57 / 1.62
Epidermis	0.026	0.95 / 0.15
Subcutaneous fat	0.08	

Another important factor in bioimpedance measurements is the electrode setup, which most commonly has three forms: two-electrode bioimpedance, three-electrode bioimpedance, and four-electrode bioimpedance. These setups each have a different sensitivity field, meaning they measure different regions of the tissue. (Grimnes and Martinsen, 2000; Kauppinen et al., 2006)

Figure 6 describes the sensitivity field of two-, three-, and four-electrode impedance measurement setups.

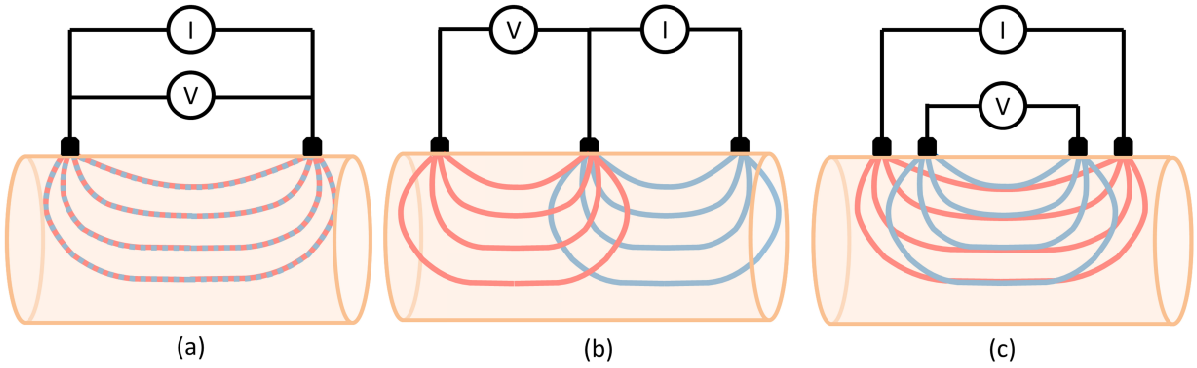

Figure 6. Example of sensitivity fields in bioimpedance measurements. (a) Two-electrode setup, (b) Three-electrode setup, and (c) Four-electrode setup. Due to reciprocity, these two fields can be used interchangeably for voltage and current, and the sensitivity field is defined as the area covered by both fields (Kauppinen et al., 2006). (c) is modified from (Kauppinen et al., 2006). The presented figure is different than the sensitivity distribution of the impedance measurement. The sensitivity distribution is the dot product of the current density fields of the current feeding electrodes and voltage measurement electrodes. The dot product of these vector fields is a scalar and is maximum when the fields are parallel, zero when the fields are perpendicular, and negative when the angle between the fields is larger than 90° (Geselowitz, 1971; Malmivuo and Plonsey, 1995). In the presented figure, the areas impacting the measurement are the intersection areas of the two fields.

In the two-electrode measurement setup, the electrode pair used for the current injection is also used for the voltage measurement. This measurement has a sensitivity field spanning the instrumentation, the skin-electrode interface at both electrode locations, and the tissue between these two locations. Because the upper layers of skin have higher resistance than underlying tissue, this type of measurement has more of a dependence on the electrode contact region of the tissue than the deeper layers of tissue. (McAdams et al., 1996)

The three-electrode measurement setup has one common electrode for the current injection and voltage measurement. The electrodes for the current sink and the other pole for the voltage measurement are separate. The main measured impedance is that of the common voltage/current electrode interface with the skin. This kind of measurement is dominated by the skin-electrode contact in the lower frequencies, and in the higher frequencies also measures tissue under the skin.(Grimnes and Martinsen, 2006, 2000)

For the four-electrode measurement setup, the electrode pair used for current injection is separate from the electrode pair used for voltage measurement, and this measurement is better suited for measuring the impedance of deeper tissue (Grimnes and Martinsen, 2000). This setup does not measure the electrode impedance and the electrode setup can be arranged for the sensitivity field to be specifically targeted to a tissue volume of interest. (Kauppinen et al., 2006)

Bioimpedance measurements can be done as a single frequency impedance measurement or as a multiple frequency impedance spectrum measurement. As different tissues have different dielectric

properties, the frequency of the impedance current affects which tissue in the measurement sensitivity field will be the dominant volume to be measured. Thus, a single frequency measurement cannot differentiate between the effects of geometry changes and the effects of tissue changes, while the impedance spectrum measurement can provide a better picture of what happens to tissues that lie in the sensitivity field.(Bronzino, 1995)

Impedance plethysmography is the electrical measurement of a specific volume. Measured from a limb, swelling due to blood flow, posture change, or edema, can be assessed. Measured from the thorax, various aspects of lung function and breathing parameters, the onset of pulmonary edema, and cardiac output can be investigated. Other applications are skin moisture, fingerprint with live finger detection, impedance tomography, monitoring of tissue ischemia, and death (Grimnes and Martinsen, 2006). Less well known applications are rheoencephalography, the measurement of the blood flow to the brain, urinary tissue characterization, and electrical impedance myography, the assessment of the condition of muscles (Grimnes and Martinsen, 2000). These measurements usually are done as a single frequency impedance measurement.

The most commonly known multi-frequency bioimpedance measurements are the commercially available body composition analyzers.

2.2. Mobile Monitoring of Physiological Systems

Since the early nineties when researchers were walking around with computers in their backpacks, wearable vital sign monitoring has been of interest, and this interest has continued to this day. At the beginning of the 2000s, heart rate monitors in the form of chest belts were the forerunners of physiological signal monitoring, but many other forms and many other parameters have since been investigated. Below, in Table 3, I present an alphabetically ordered compilation of the best-known and most influential projects in the field of physiological signal monitoring. This is not an exhaustive list as many smaller projects and projects that have just launched and products not yet on the market have been excluded.

Table 3. Wearable physiological signal monitoring systems

Name/Ref	Date	Type	Description	Electrode Type	General Purpose
Alive Bluetooth Heart and Activity Monitor (Alive Technologies, Queensland, Australia)("Alive Bluetooth Heart & Activity Monitor — Alive Technologies," n.d.)	Present	Pebble	Measures 1-channel ECG and activity and transfers data to a smartphone via Bluetooth	Gelled	Clinical screening, diagnosis and monitoring Consumer health and fitness
AMON (Anliker et al., 2004)(Zurich,	2004	Wrist-device	Long-term monitoring of 1-channel ECG, SpO2, blood pressure, skin	Metal (Gold)	Clinical monitoring

Switzerland)			temperature and activity. Has integrated GSM connectivity. ECG needs the user to touch the electrodes on the wrist device.		Alert
ATREC (Seoane et al., 2014, 2013)	Present	Garment Glove and armband	Measures the wearer's psychological state by measuring the galvanic skin response, skin temperature (and environment temperature), 1-channel ECG, and using bioimpedance measurement, respiration.	Textile	Military stress level monitoring
Aubade 2006 (Katsis et al., 2006)	2006	Chest belt, mask, glove	Measures the wearer's psychological state by facial EMG, ECG, respiration and galvanic skin response, and transmits wirelessly to a base station	Not given	Emotional state monitoring
BioHarness (Zephyr Technologies, Maryland, USA)("BioHarness 3 - Wireless Professional Heart Rate Monitor & Physiological Monitor with Bluetooth - Zephyr Technology Corporation," n.d.)	Present	Chest Belt / Shirt	Measures the heart rate, breathing rate, and via acceleration sensors, the posture and activity levels. Transmits the data by Bluetooth to analysis device.	Textile	Physiological monitoring for research Consumer health and fitness
CardioShirt (Numetrex, Philadelphia, USA)("Heart Rate Monitors, Workout Clothes and Fitness Gear - NuMetrex," n.d.)	2006-Present At present, it is known as Adidas miCoach	Shirt	A shirt for heart rate monitoring from a 1-channel ECG, compatible with modern hear rate monitors	Textile	Consumer health and fitness
CorusFit SensorWear (CorusFit Oy, Jyväskylä, Finland)("Corusfit - Invest in the health of your heart," n.d.)	Present	Garment	Measures 2-channel ECG during group exercise, the data is transmitted wirelessly to supervisor station	Textile	Monitored preventative and rehabilitative group exercise
Fitness Shirt (Fraunhofer Institute, Erlangen, Germany)("Intelli-gent training with a Fitness Shirt and an E-bike," n.d.)	Remove ? Development	Garment	Heart rate and breathing, connects wirelessly to a table or smartphone	Textile	Training assessment for cycling
Generic Heart Rate Monitors	Present	Chest Belt	Measures the heart rate from electrodes located on a chest belt and wirelessly transmits the data	Textile	Consumer health and fitness

			to a wrist worn display. Newer versions also measure 1-channel ECG. Polar(Polar OY, Kuopio, Finland), Suunto (Suunto OY, Kempele, Finland), Numetrex (Textronics, Philadelphia, US)		
HeartCycle(Luprano et al., 2013)	2013	Garment	Measures 1-channel ECG, photoplethysmography, and heart sounds, connects to a smartphone via Bluetooth	Capacitive	Clinical monitoring
Hexoskin("Biometric shirts for performance improvement and sleep tracking," n.d.)	Present (new)	Garment	Monitors the heart rate, breathing and activity and transmits to a smartphone or tablet.	Textile	Consumer health and fitness
LifeGuard (Mundt et al., 2005) (NASA, California, USA)	2004	Patch	2-channel ECG, breathing rate, and pulse oximetry, blood pressure and skin temperature measurements of 1-2 days duration. Wireless communication with a base station.	Gelled	Medical and non-medical monitoring in extreme environ-ments
LifeShirt (VivoMetrics/Vivonoetics, San Diego, California, USA) ("LifeShirt - Vivonoetics," n.d.)	2000 – Recently discon-tinued (See Smartex for newer model)	Garment	A shirt that measured many parameters from 1-channel ECG, breathing rate, and acceleration to blood pressure and temperature by the addition of peripherals. The data was stored on a memory card.	Textile	Clinical monitoring
MagIc (Di Rienzo et al., 2007, 2006, 2005)	2005	Garment	1-channel ECG, respiration, skin temperature, and activity, connects via Bluetooth	Textile Woven	Clinical monitoring Elderly monitoring
MyHeart (Harris and Habetha, 2007; Luprano et al., 2006; Muhlsteff et al., 2004; Pacelli et al., 2006; Paradiso and De Rossi, 2006; Paradiso and Pacelli, 2011; Zaunseder et al., 2007)(Coordinator: Philips, Aachen, Germany)	2004-2008	Garment	A large EU project with over thirty partners. Measures 3-channel ECG, breathing and movement	Textile Knitted	Clinical monitoring for prevention and disease manage-ment
Myontec (Myontec, Kuopio, Finland)("Myontec | Know Your Muscles," n.d.)	Present (new)	Shorts	Measures EMG for muscle activity from tight shorts. Stores data on the on-clothing device and transmits the data wirelessly to a smartphone or the cloud.	Textile	Consumer fitness

Physio Glove (Crommwell Inc., Evanston USA)("PRODUCTS PhysioGlove," n.d.)	Present	Glove	A glove with 10 electrodes worn on the left arm that produces a 12-lead ECG when placed on the chest.	Not glued but no further information	Intermittent ECG monitoring
Physiological Status Monitor (Quantum Applied Science and Research, Inc., San Diego, California, USA)("PSM | Quasar USA," n.d.)	Present	Belt	Measures 1-channel ECG, skin temperature and acceleration. Can store 72 hours of data on a memory card, or can transmit the data wirelessly	Dry Contact	Consumer health and fitness
Quasar ECG Shirt (Park et al., 2006) (Quantum Applied Science and Research, Inc., San Diego, California, USA)	2004-2007 (Also see Physiological Status Monitor)	Garment	Using capacitive electrodes, measures 1-channel ECG.	Capacitive	Consumer health and fitness
SmarTex(Vivonoetics, San Diego, California, USA) ("Smartex WWS - Vivonoetics," n.d.)	Present	Garment	Measures 1-channel ECG, heart rate, respiration rate, activity and posture. The data can be stored on device or streamed.	Textile	Long-term physiological signal monitoring
SmartShirt (Georgia Institute of Technology, Atlanta, Georgia, USA) ("Georgia Tech Wearable Motherboard," n.d.)	1996-2001	Garment	Possibly the grandfather of mobile monitoring garments. Measures 3-channel ECG, heart rate, respiration rate, and body temperature, and communicates via Bluetooth or ZigBee. Is also capable of detecting penetration through the garment.	Gelled	Military monitoring
SmartVest (Pandian et al., 2008)	2008	Garment	Measures ECG, photoplethysmography, body temperature, galvanic skin response. Implements an algorithm to derive blood pressure from the PPT signal. Transmits data wirelessly to a base station	Dry contact	Clinical Monitoring
Wealthy (Lymberis and Paradiso, 2008; Paradiso et al., 2005a, 2005b; Paradiso and Pacelli, 2011; Scilingo et al., 2005)(Italy)	2002-2005	Garment	Measures 3-channel ECG, EMG on arms, respiration, temperature and activity. Wirelessly transmits the data using Bluetooth or GPRS	Textile (Hydrogel); Knitted	Clinical Monitoring Consumer health
Zensor (Intelesens, Belfast, Northern Ireland, UK)("Intelesens | Responsive Healthcare - zensor,"	Present	Patch	Measures 1-Channel ECG, heart rate, breathing rate, motion, for up to 7 days. In this sense, it is similar to a common Holter monitor, but smaller and less obtrusive.	Gelled/ No info, Glued	Clinical diagnostic monitoring

n.d.)					

2.3. Surface Electrodes

The surface potentials created by physiological processes are usually in the millivolt range, with some even lower (Kutz, 2003). Many different types of electrodes can be used to measure surface potentials: flat surface electrodes, needle electrodes, suction cup electrodes, and implantable electrodes (Grimnes and Martinsen, 2000). In the context of the topic of this thesis, surface electrodes are of interest.

Surface electrodes suitable for wearable monitoring can be roughly divided into three groups: electrodes with conductive paste, electrodes without conductive paste, and non-contact capacitive electrodes. Electrodes with conductive paste are commonly referred to as gelled electrodes, and medical electrodes are mainly of this type. Electrodes without conductive paste are called dry electrodes, and most wearable systems aim to incorporate this kind of electrode. A less known electrode is the capacitive electrode, which measures potentials without galvanic coupling, and these are best-known as sensors in automotive seats. (Neuman, 1997)

These three types are briefly summarized below and the details of the skin-electrode interface are investigated in more detail in the Skin-Electrode-Interface Model chapter 2.5.1 and the in the Sources of Motion Artifact chapter 2.5.2.

2.3.1. Gelled Electrodes

A simple way of looking at surface contact electrodes is that they simply measure voltage, yet this is oversimplified. Electrodes conduct current while measuring voltage, and this means transducing ionic current into electronic current.(Grimnes and Martinsen, 2000; Kutz, 2003; Webster, 2009)

Gelled electrodes achieve contact between electrode and skin by a conductive medium, an electrolyte. This electrolyte acts as a means of transport for ions between the skin and the electrode and its use allows for the control of metal electrolyte interface stability in electrical properties. This is achieved not only by providing an electrically stable, conductive medium, but by also providing a physically stable medium. By keeping the skin-electrode contact area stable and by preventing non-contact areas, drastic changes in the skin-electrode interface are avoided. (Grimnes and Martinsen, 2000)

The electrolyte used in the gelled electrodes can come in many forms: a liquid, conductive paste applied to the electrodes, a gel that is confined in a cup-like design between skin and electrode, a sponge like interface that holds the gel in place, or a solid hydrogel that has high conductivity and may or may not be adhesive. (Grimnes and Martinsen, 2000)

While the easiest and simplest electrolyte to use is a sodium chloride (NaCl) solution, which is also one of the electrolytes better tolerated by the skin, its conductivity at 0.9% concentration, saline, is not as good as electrolytes with more concentrated ions. Another disadvantage is that it is fully liquid, making its containment difficult. (Grimnes and Martinsen, 2000)

The most common used type of gelled electrode is the silver/silver chloride (Ag/AgCl) electrode. The Ag/AgCl electrode is characterized by its low over-potentials, making it to be considered as an almost perfectly non-polarizable electrode. Ag/AgCl electrodes are formed by depositing chloride on a silver surface. In the context of gelled electrodes, the Ag/AgCl metal is galvanically coupled to the skin by an electrolyte and physically attached by an adhesive layer. The electrolyte contains Cl- as the main electrolyte, but it is also saturated with AgCl to prevent the electrode layer from dissolving (Webster, 2009). These electrodes are mostly single use and come in a ready package with the electrode metal, electrolyte, and adhesive, and are used on abraded skin.

The best-known commercial Ag/AgCl electrodes are Red Dot electrodes (3M Inc., St. Paul, Minnesota, USA) and AmbuBlu electrodes (Ambu A/S, Ballerup, Denmark).

In the case of gelled electrodes, the gel and the skin might moisten each other. Hydrogels are occasionally used with dry electrodes, as explained in the next chapter, and allow for ionic conduction and have a well-defined area, even if they have a lower DC (direct current) conductance and higher capacitance than liquid gel. This makes the electrical properties of hydrogels slightly different than those of liquid gel in that their low frequency behavior is not as desirable, while in high frequency applications the use of hydrogel might be preferable to conventional electrode gel. Yet again, the low mobility of ions in the hydrogel might cause problems for specific applications such as plethysmography at 50 kHz. While the hydrogel does not directly wet the skin, it might provide moisture to the skin in long-term use or remove moisture from the skin, depending on skin condition. (Grimnes and Martinsen, 2000)

2.3.2. Dry Electrodes

Textile electrodes can be manufactured in many different ways and some parameters that can be selected are the choice of conductive yarn fiber material and fabric base material, the composition, and the manufacturing method: weaving, knitting, embroidering, and coating. (Rattfält et al., 2007). Different manufacturing methods result in different surface structures and different physical, electrical, and electrochemical properties of the electrodes and directly affect the functionality of the electrodes.

Electrodes placed on completely dry skin will present a large contact resistance, in the range of megaohms, due to the top most layer of the skin that comprises dead and dry skin cells (Kutz, 2003). This high skin-electrode impedance causes deterioration in signal quality (Grimnes and Martinsen, 2000; Webster, 2009).

The term “dry electrodes” is commonly used but it is misappropriate when the dry electrode is applied and the skin starts to perspire and a rapid rise in conductivity occurs, even without strenuous activity. Dry skin humidity depends on the environment humidity and on sweating history (Grimnes and Martinsen, 2000), and on many factors such as the psychological state (Edelberg, 1977), etc. In addition to physiological process, some applications require the user to wet the electrodes with tap water or saline before use and some require the application of hydrogels (Paradiso et al., 2005b; Puurtinen et al., 2006; Scilingo et al., 2005), which were discussed in the previous chapter. The differences between gelled, dry, and capacitive electrodes are presented in simple models in Figure 7.

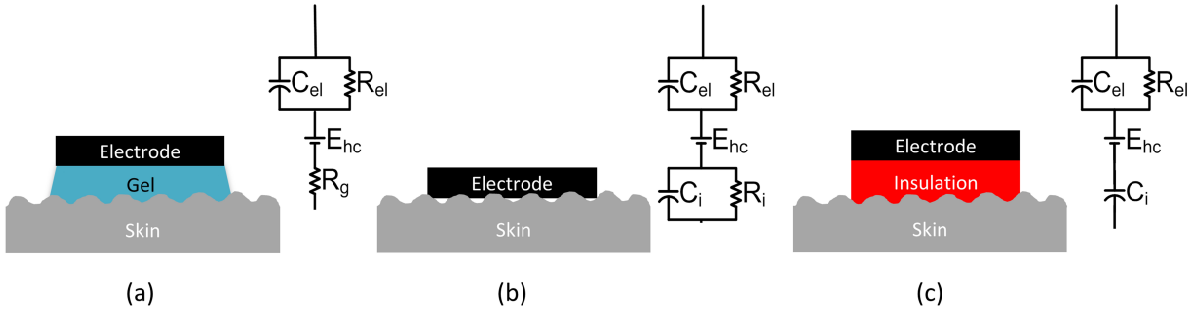

Figure 7. Differences in skin-electrode interface electrical models: (a) gelled electrode, (b) dry electrode, (c) capacitive electrode. The electrical model of the skin is not shown. C_{el} is the capacitance of the electrode and the electrode-electrolyte interface, R_{el} is the resistance of the electrode and the electrode-electrolyte interface, E_{hc} is the half-cell potential, R_g is the resistance of the highly conductive electrode gel, C_i is the capacitance of the skin-electrode interface layer in the absence of gel, and R_i is the resistance of the skin-electrode interface layer in the absence of gel.

2.3.2.1. Dry Electrodes used in Research and Products

Because dry electrodes do not use gel and are intended for use in non-ideal situations such as during patient movement in a non-medical setting, different electrode designs have been tried. Also, due to different textile manufacturing methods, the electrode surface can vary between studies and products. Different materials have been used for manufacturing textile electrodes. In addition to textiles, other materials such as rubber or silicone have been used to construct dry electrodes. Below, the most common manufacturing methods, electrode materials, and various electrode designs are introduced. Because each study uses a different research methodology and different ways of reporting results, a comparison of results between these studies was not made, while some results were reported on their own.

Beckmann et al. studied the difference between knitted electrodes made of different yarns and knitting methods and found impedance and frequency-dependent behavior differences between these electrodes (Beckmann et al., 2010). A similar study undertaken by Rattfält et al. revealed that a difference also existed between the weaving methods used (Rattfält et al., 2007). Pola and Vanhala report on the embroidered electrode working better than their knitted or woven electrodes (Pola and Vanhala, 2007). A similar finding was also reported by Mestrovic et al. who state that sewn electrodes are more resistant against slippage on the skin (Mestrovic et al., 2007).

Not all studies report on the method of textile electrode manufacturing used, yet most are knitted (M. Catrysse, 2003; Mestrovic et al., 2007; Pacelli et al., 2006; Paradiso et al., 2005b), woven (Di Rienzo et al., 2007; M. Catrysse, 2003), sewn onto fabric (Fratini et al., 2009; Marozas et al., 2011), or embroidered (Cho et al., 2009; Puurtinen et al., 2006), if not cut from a ready-made conductive textile sheet (Marquez et al., 2013).

The conductive material used is also not reported in all studies. Most use some form of silver-coated yarn (Cho et al., 2009; Löfhede et al., 2012; Mestrovic et al., 2007; Pola and Vanhala, 2007; Rattfält et al., 2007), pure or partial stainless steel yarn (M. Catrysse, 2003; Noury et al., 2004; Paradiso et al., 2005b; Paradiso and De Rossi, 2006; Rattfält et al., 2007), or partial copper yarn (Noury et al., 2004). In some cases, a hydrogel is used to improve contact (Paradiso et al., 2005b; Paradiso and De Rossi, 2006; Puurtinen et al., 2006; Scilingo et al., 2005).

The surface shapes of textile electrodes did not change much and mostly adhered to simple geometric shapes such as squares, ovals, and circles of different dimensions. Square textile electrodes (Scilingo et al., 2005) with dimensions of 2x2 cm (Fratini et al., 2009; Mestrovic et al., 2007) and 3x3 cm (M. Catrysse, 2003) as well as flat, round electrodes of different diameters from 7 mm to 30 mm (Noury et al., 2004; Pengjun et al., 2011; Puurtinen et al., 2006) can be given as examples.

Among the electrode designs researched to improve the textile-on-skin contact were machine embroidering the conductive yarn onto an inflated shape to improve skin-electrode contact (Cho et al., 2009), covering a foam with conductive textile (Lin et al., 2011; Saone et al., 2014, 2013; Tseng et al., 2013), a textile electrode covering a textile pillow (Löfhede et al., 2012), and knitting the loops of a Velcro type textile with conductive yarn (Marquez et al., 2013).

Novel dry electrodes made of a rubber-like conducting material with small bumps on the electrode surface (Buxi et al., 2012; Laferriere et al., 2011), circular disk electrodes with a diameter of 35 mm and a depth of 2 mm made of a dry polysiloxane material with embedded conductive nanoparticles (Chan and Lemaire, 2010; Garcia et al., 2007; Laferriere et al., 2011), polysiloxane with conductive load (Pylatiuk et al., 2009), oval-shaped carbon-loaded conductive rubber with 7.8 cm^2 contact area (Muhlsteff et al., 2004; Muhlsteff and Such, 2004), dry rubber with silver fillings (Pandian et al., 2008), a foam electrode made of conductive polymer (Gruetzmann et al., 2007), screen printed electrodes made of silver paste (Yoo et al., 2009), and a telescope-like structure extending towards the skin intended as a dry electrode holder (Griebel et al., 2009) can be given as non-textile dry electrode examples.

2.3.3. Capacitive Electrodes

While not studied in this research, another surface electrode type is worth mentioning. Both gelled and dry electrodes have galvanic contact to the skin, with current flowing back and forth between the skin and the electrode. A third type of electrode is the non-contact electrode. This electrode has no conductive coupling to the skin, and capacitively picks up the surface potentials. These electrodes are also called polarizable electrodes because no charge crosses the electrode-electrolyte interface during measurement; the current observed by the capacitive electrode is a displacement current. For their implementation, these types of electrodes require different amplifiers than other contact electrodes.

Even if there are recent projects that successfully use capacitive electrodes for biopotential measurements, their use is not widespread. (Chi et al., 2010; Eilebrecht et al., 2013; Gandhi et al., 2011; Harland et al., 2003, 2002; Ottenbacher et al., 2007; Park et al., 2006; Prance et al., 2000). Harland and Prance managed to measure details of the ECG such as the His bundle to Purkinje discharge and the U

wave with their capacitive electrode placed on the skin. Such details are not usually seen on a conventional ECG. In addition, they could detect the heart rate of a subject when the electrode was placed 1 m away from the fully clothed subject. Park et al. report a 99% correlation of the signal measured by their capacitive electrode to the signal obtained from commercial ECG electrodes (Park et al., 2006). Eilebrecht et al. report that they have also used capacitive electrodes for bioimpedance measurements (Eilebrecht et al., 2013).

2.4. Major Electrode Noise Sources

When measuring a biopotential, the ideal case would be that the biopotential and the electrode are directly connected, and that the measured signal is composed purely of the source signal. In real life, however, especially for surface biopotentials, this is not the case. Between the signal source and the measurement system, there exist many layers of tissue and interfaces each with their own electrical properties, physiological processes, and even environmental factors adding noise to the measurement. Below is a short summary of the most influential noise sources. A discussion on skin-electrode interface impedance has been included as part of motion artifact noise source and described in detail in the following chapter on motion artifact. It is generally accepted that lower electrode impedance results in better signal quality.

2.4.1. Thermal Noise

In the ideal case, electronic circuits would produce no noise of their own. In real electronic circuits, however, an inherent noise is always present. Electrons are at a complete standstill only at absolute zero, and move randomly at temperatures above that. This random movement generates random current, and the randomness, over a short time, cancels itself out. Yet, the randomness can also be detected as high frequency noise and is called thermal agitation noise, thermal noise, or Johnson's noise. (Carr and Brown, 1993)

This noise possesses a white noise characteristic that has an almost Gaussian distribution over a wide frequency band. The noise amplitude increases with increasing temperature, resistance, and the frequency bandwidth, and is independent of frequency (Ananthi, 2006). For example, a 1 MΩ resistor will have 126 nV/√Hz thermal noise. (Carr and Brown, 1993).

Thermal noise exists at all times, even in the absence of current passing through the system. The thermal noise of a system can be reduced by narrowing the frequency band and lowering the system temperature (Ananthi, 2006).

2.4.2. Amplifier Noise

Even if it not directly caused by electrode and skin-electrode interface, it is apt to note here that the amplifier itself possesses two noise components that are frequency dependent: an internal noise present as voltage and an internal current that causes a noise voltage at the load resistance. In modern

devices, this inherent voltage noise is around 10 nV/√Hz and the current noise less than 1 pA/√Hz, and both are inversely correlated to the root square of frequency. (Bronzino, 1995)

The common-mode rejection ratio (CMRR) is the extent to which a signal common to both inputs of a differential amplifier are rejected by the amplifier and is a determinant in the noise susceptibility of the measurement system. Most current systems have a CMRR of 70-100 dB (Perez, 2002). A 70 dB CMRR reduces a 1V common mode signal to approximately 300 µV interference. A CMRR of 100 dB reduces a 1V common mode signal to 10 µV interference. For example, the head movement of a subject can create different potentials in different leads and the CMRR cannot help reduce that. (Ananthi, 2006) The CMRR is also important in that if the skin-electrode interface impedance changes; this voids the CMRR for the amount that the interference seen by the electrodes differs. This difference is then seen as a differential input by the amplifier and results in noise being picked up by the system. (Riistama, 2010)

2.4.3. Half-cell Potential

When an electrode is in contact with an electrolyte, ions from the metal diffuse into the electrolyte, releasing electrons. Positively charged ions are called cations and initially, as the electrolyte is at neutral potential, there will be an equal number of anions, negatively charged ions, in the solution. The initial diffusion of the metal ions depends on the initial concentration of the ions in the solution and the equilibrium conditions for the particular ion's oxidization. As the positively charged ions enter the electrolyte and the electrons remain as free charges in the electrode, an equilibrium forms at the electrode boundary with the layer of the metallic cations attracting a layer of anodes from the electrolyte. This layer, described by Helhmholtz as early as 1879, is called the double layer and acts as a capacitor. As one type of charge is present at the electrode side layer and another type is at the electrolyte side of this double layer, this causes a potential difference between the two sides of the double layer. This potential difference is called the half-cell potential (Webster, 2009). A depiction of this potential is presented in Figure 8.

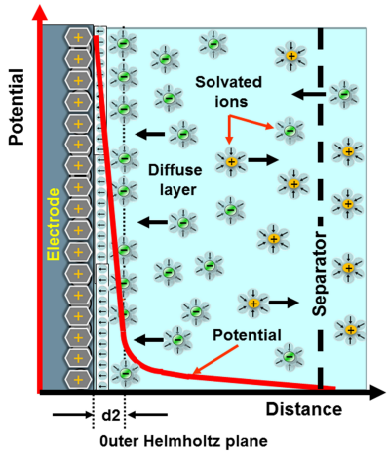

Figure 8. The formation of the double layer and of the half-cell potential. Image retrieved from http://en.wikipedia.org/wiki/Double_layer_(interfacial) on 29.01.2015. The image has no copyright.

The hydrogen electrode has been defined to have a half-cell potential of zero and the half-cell potentials of electrodes are measured in reference to the hydrogen electrode (Webster, 2009). Half-cell potentials of some common metals and compounds are presented in Table 4.

Table 4. Half Cell potentials (Webster, 2009)

Metal And Reaction	Potential
H	0
Al	-1.7
AgCl	0.22
Ag	0.79
Fe	0.41
HgCl	0.27
Au (+3 e-)	1.4
Au (+1 e-)	1.7

This table also shows the effect of using AgCl electrodes instead of pure Ag. The Cl ions provide the interface with a lower half-cell potential, which is also more stable as an already saturated Ag Cl solution is attached to the Ag electrode surface.

The half-cell potentials of electrodes made of the same material will ideally be the same, so in a measurement between these two electrodes, the half-cell potentials will cancel each other out. Any change in in the half-cell potential caused by changes to the double layer of either electrode will be picked up by the electrodes as an unwanted signal (Kutz, 2003). On the other hand, if the electrodes used are made of a different metal, the difference in half-cell potentials can cause a battery effect, generating a DC voltage in the range of hundreds of millivolts. (Grimnes and Martinsen, 2000)

2.4.4. Polarization

The half-cell potential is given for steady state cases, and this is why they are noted as standard potentials. When there is a current flowing through the interface, the half-cell potential changes. The resistance of the electrolyte causes a potential drop when current flows through it, but this drop depends on the electrolyte resistance, which in turn can depend on the current. Thus, this kind of voltage drop might not follow the ohms law. Similar to resistance, the ionic concentrations at equilibrium are disturbed when current is passed through, and this new equilibrium will alter the half-cell potential. (Webster, 2009)

The last kind of polarization effect arises because the oxidation and reduction processes are not entirely reversible for many metals. The activation energy required for the metal might be different for the oxidation and reduction, and this will cause a different resistance of the electrode to be observed, depending on the direction of the current flow. This resistance will cause offset potentials to be generated between the electrodes, and these potentials can easily reach the level of measured biopotentials. (Webster, 2009)

This problem is more prevalent for pure metal electrodes, and it can be overcome by using a combination of a metal and its metallic salt. The metal is covered by its metallic salt and easily oxidizes and reduces with its salt. In turn, the metallic salt readily oxidizes and reduces with electrolyte in contact with skin, subject to changing biopotentials. This two-layered electrical charge transfer has much lower resistance than there would be between the metal and the electrolyte. (Webster, 2009)

It should be noted that a pure silver electrode might initially possess this offset potential. However, after longer contact with skin and the NaCl ions present on the skin and in sweat, it becomes coated with AgCl as the Ag chemically binds to the Cl ions. This could potentially point to an improvement in the signal quality in wearable systems that use silver yarn as an electrode material, after longer periods of use (Kutz, 2003).

2.4.5. Electrolyte Interface Noise

Low level noise exists both at the electrode-electrolyte and the electrolyte-skin interfaces. This noise is uncategorized as its origins are not fully known (Gondran et al., 1996)

Electrode-electrolyte interface noise can be measured by putting two electrodes together. As an example, Red Dot electrodes were found to have a 0.25 µV peak-to-peak noise in the 0.5 – 100 Hz bandwidth. (Gondran et al., 1996).

The electrode-electrolyte interface is reported to have a noise level of 0.3 µV-1 µV, which is negligible. The noise between the electrolyte and skin is found to be dependent on skin impedance at frequencies higher than 100 Hz, and to be in the ranges of 10- 60 µV, with a $1/f^2$ characteristic in the frequencies lower than 100 Hz. It has been suggested that this is due to a process that disturbs the interface equilibrium, or by an inherent property of the ionic nature of the skin. (Gondran et al., 1996)

These results are supported by Huigen et al. who report that the electrode-electrolyte interface noise, which is less than 1 µV, is negligible compared with the electrolyte-skin interface noise which is between 1 and 20 µV RMS (root mean square) and is inversely proportional to the square root of the electrode area (Huigen et al., 2002). Puurtinen et al. report that the skin-electrode interface noise is around 50 µV for wet textile electrodes and textile electrodes with hydrogel. The reported value is given for circular electrodes with a 20 mm diameter. Noise and impedance decreased with increasing electrode area. (Puurtinen et al., 2006)

2.4.6. Residual EMG

Even if it is noise directly stemming from the skin-electrode interface, noise with frequencies below 100 Hz and amplitudes of at most 5 µV that possibly originates from muscle activity at rest have been reported. (Gondran et al., 1996)

2.4.7. 50/60 Hz Power Line Interference

In our environment, we are surrounded by power lines, radio towers, and cell phones that all emit electromagnetic waves that are picked up by the human body acting as an antenna. In the typical home or work setting, this effect can cause voltages of tens of millivolts, even in the order of volts, to be created in the body, with respect to ground.

This signal can also be measured from the skin, and will superimpose itself onto the measured biopotential as a clear 50/60 Hz sinusoidal.

Using differential amplifiers with a high common-mode rejection ratio helps solve this problem. The 50/60 Hz interference is uniformly present throughout the human body and any electrode placed on the body will be subject to this signal. A high common-mode rejection ratio ensures the reduction of this signal present at all electrodes in the measurement system (Kutz, 2003). Another option is to feed the interference signal back to the patient, canceling out any picked up interference (Webster, 1984). This method is commonly used together with the implementation of a high CMRR.

A difference in the skin-electrode interface impedances changes the interference observed by the differential amplifier inputs from a common-mode voltage to a differential voltage and can cause some of the interference to be present in the measured signal. As the dry electrodes are more prone to impedance mismatch between two electrodes, they are also more susceptible to power line interference (Riistama, 2010).

2.4.8. Motion Artifact Noise

A short introduction to motion artifact is presented here. Because motion artifact can be tens of millivolts and occur in the frequencies of the signals of interest, which makes it an important noise source, and because this thesis deals with motion artifact, it is explained in detail in its dedicated chapter 2.5 below.

Motion artifacts can occur when the skin is stretched and are caused by changes in the voltage generated on skin epithelia assumed to be located in the upper layers of skin, half-cell potential changes due to geometrical changes of the electrolyte, changes in skin impedance, skin-electrode contact area, and cable movement. As wearable monitoring is becoming more widely implemented, this type of noise is becoming more of a challenge than when monitoring was mainly done on stationary subjects.

In Figure 9 below, a comparison of these noise sources to the measured biosignals is presented.

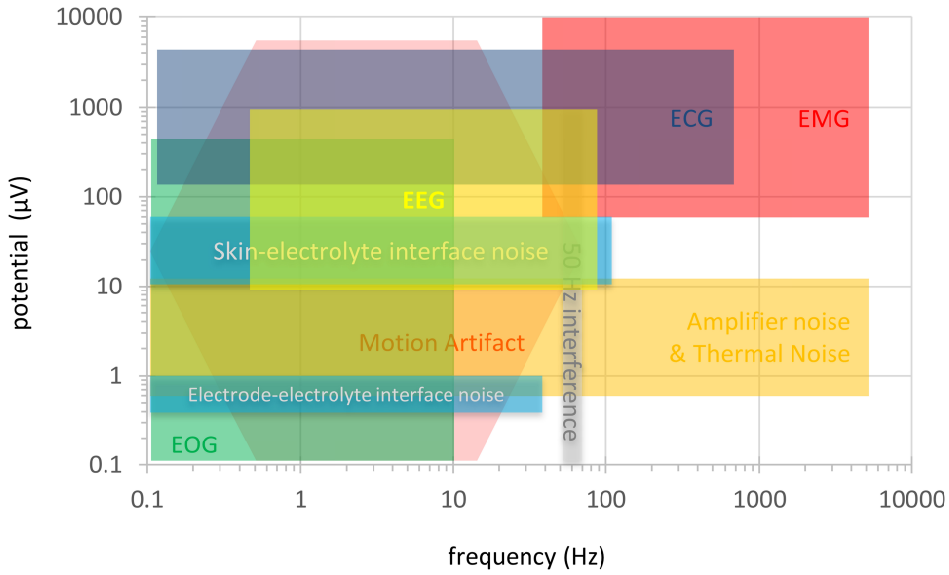

Figure 9. A comparison of major biopotentials to noise sources. The x-axis presents the frequency band of the signals while the y-axis presents the amplitudes. The values have been taken from the publications referenced in this thesis, and thus most of the values are source-dependent.

2.5. Motion Artifact

As previously shown, the skin-electrode interaction is a complex one, and so is motion artifact. Even today, there is no clear agreement on the main cause of motion artifact. In *Medical Instrumentation*, Neuman and Webster give the main cause as the disturbance of the half-cell potentials at the electrode-electrolyte interface, while mentioning the potential difference across the epidermis. In the *Standard Handbook of Biomedical Engineering*, Kutz states that the internal skin potentials are the main cause. Most probably, it is a combination of all these factors. In the case of non-gelled electrodes, the lack of a relatively stable electrolyte gel layer further adds to the challenge.

Below, I will explain the skin-electrode model to give an understanding of the underlying factors, the mechanisms for motion artifact generation, and the methods investigated to reduce motion artifact, focused on wearable systems. Finally, I will provide a short explanation of the mechanical properties of the skin.

2.5.1. Skin-electrode Interface Model

The electrode-skin surface models shown in Figure 7, in chapter 2.3.2 Dry Electrodes, are only part of the picture. To understand motion artifact, we need to look at the whole skin-electrode interface.

As presented in Figure 10, skin comprises multiple layers, with each layer having different mechanical and electrical properties.

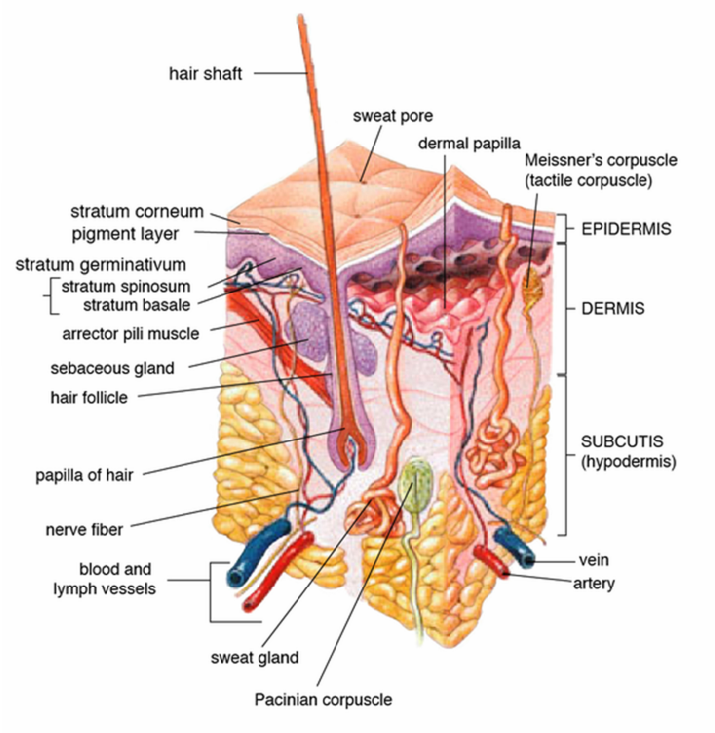

Figure 10. The layers of skin. Image retrieved from http://en.wikipedia.org/wiki/Human_skin on 29.1.2015. The figure holds no copyright.

The top layer of skin is called the epidermis. It is thickest at the palms of the hands and soles of the feet at 0.5 mm. The rest of the body is covered in epidermis that is around 0.1 mm thick. Beneath the epidermis is the dermis, which can have a thickness of 4 mm at the palms and soles and 0.2 mm at the eyelids. (*Anatomy and Physiology* by Kenneth S. Saladin | *eBook on*, n.d.) The epidermis comprises five layers and the topmost layer, the stratum corneum, is of interest for biopotential measurements. The stratum corneum is composed of dead, dehydrated, keratinized cells, and has very large impedance in the ranges of megaohms. The dermis, on the other hand, is fully composed of living tissue and has its own important characteristics in resistance, capacitance, and generated potentials. (Kutz, 2003). How do these factors act in the creation of motion artifact?

The skin-electrode interface model takes into account all the layers of the signal pathway, and gives an overall picture of the biopotential conduction process. The model for gelled electrodes and non-gelled electrodes will differ, so they are presented side by side in Figure 11 for ease of comparison. The model is a combination of the models presented by Neuman and Webster (Neuman, 1997), Kutz (Kutz, 2003), and Beckmann et.al (Beckmann et al., 2010).

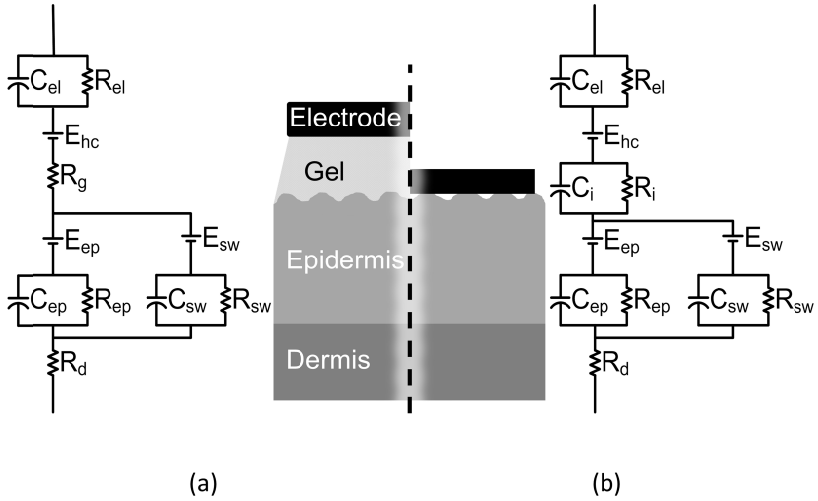

Figure 11. Electrical model of the skin-electrode interface. (a) presents the model for gelled electrodes and (b) presents the model for un-gelled electrodes. The presented image is slightly modified from the original version first published in Paper 1 that was based on (Beckmann et al., 2010; Neuman, 1997).

C_{el} and R_{el} represent the capacitance and the resistance of the electrode and the electrode-electrolyte interface. E_{hc} is the half-cell potential. Electrode gel is a highly conductive medium and is modeled by the simple resistor R_g. The potential across the epidermis due to ionic concentration differences across this semi-permeable membrane layer (Neuman, 1997) and the physiological processes of living tissue (Kutz, 2003), also called “skin battery” (Edelberg, 1973, 1968), are presented as E_{ep}. C_{ep} and R_{ep} and are the capacitance and resistance of the epidermis. The dermis is highly conductive living tissue and can be modeled as a resistor R_d. Because the potentials generated in the dermis are very low in amplitude, they can be ignored (Neuman, 1997). As the skin starts to sweat, the sweat ducts are introduced in parallel with the dry epidermis current pathway. Sweat is an ion rich fluid, and thus has high conductivity. The ion concentration differences between the inside of the sweat ducts and the extracellular fluid cause a potential difference to be generated, shown as E_{sw}. The capacitance and the resistance of the sweat ducts are represented as C_{sw} and R_{sw}.

The gel layer that is modeled as the resistor R_g provides a stable conductive medium that when applied to the skin is absorbed and reduces the skin impedance over time. Un-gelled electrodes, on the other hand, do not have this electrically and physically stable layer and rely on skin moisture or applied water/saline to facilitate conduction. The lack of a gel layer can cause areas of non-contact to occur, further complicating the stability of the contact. This interface layer can be as well modeled as a capacitance in parallel with a resistor, C_i and R_i, where the impedance largely depends on the use of water/saline or the presence of sweat. In the absence of sweat/water/saline, the dry interface resistance R_i is much larger than the gel resistance, R_g. Yet, this seems to be more important in the first minutes of electrode application as it has been reported that perspiration occurs under the electrode a few minutes after application (Grimnes and Martinsen, 2000; Gruetzmann et al., 2007). Perspiration increases the conductivity between the electrode and the skin, while at the same time adding the more conductive sweat glands in parallel to the dry skin.

The skin-electrode impedance has a frequency dependent behavior, having higher magnitude in lower frequencies and lower magnitude in higher frequencies. (Rosell et al., 1988) The high impedance observed in the lower frequencies is mainly due to the high resistance of the epidermis R_{ep}. At 10 Hz, 98% of the overall skin impedance can be attributed to the stratum corneum, while at 100 kHz this contribution of R_{ep} is reduced to 10% of the skin impedance. (Martinsen et al., 1999). An earlier study on skin impedance is presented in Figure 12.

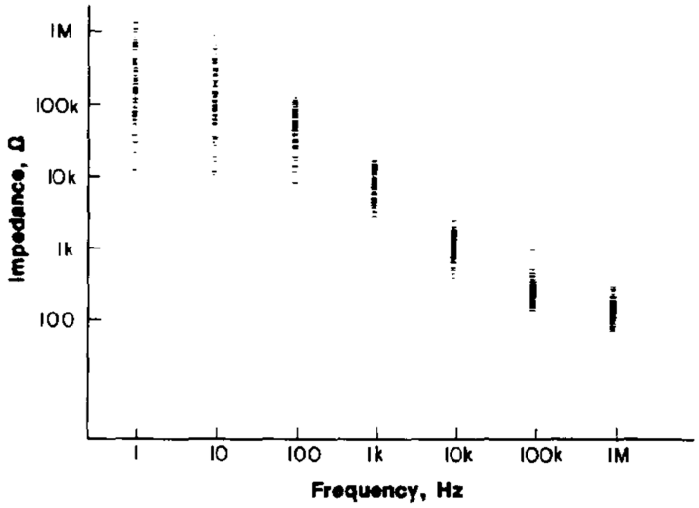

Figure 12. Skin impedance from 1 Hz to 1MHz. Image used with the kind permission of IEEE, from (Rosell et al., 1988), © 1988 IEEE.

2.5.2. Sources of Motion Artifact

Motion artifact can be generated at various levels in the presented skin model. Yet, the most commonly accepted artifact origin is the change of the skin potential (Ödman and Öberg, 1982; Tam and Webster, 1977). The potential change can normally be as high as 5-10 mV (Neuman, 1997), 16 mV in response to stretch by a 1 kg hanging weight (Talhouet and Webster, 1996), and 17 mV changes for 6% skin strain have been reported (Burbank and Webster, 1978). Originally, the outer layer of the epidermis is 30 mV more negative than the layer bordering the dermis. This potential difference is attributed to the so-called injury currents that are caused by the metabolic activity difference between the dead cells of the topmost skin layer and the living cells in the lower levels. (Talhouet and Webster, 1996) Any kind of skin deformation will cause changes in the skin potential reducing the magnitude to around 25 mV (Webster, 1984). Therefore, vertical forces (Ödman, 1989), lateral forces (Edelberg, 1973), as well as rotational forces (a form of lateral stretching) can be identified as causes of motion artifact. Another factor that causes motion artifact are changes in the impedance of the skin as the deformation causes changes in the current pathways, as presented in Figure 13. This is, however, assumed to be of minor importance, when compared with the above-mentioned causes. The impedance change in the skin is independent of the potential changes as these potential changes are not found to be caused by the change in skin impedance (Ödman, 1981; Ödman and Öberg, 1982). Ödman also reported that the changes in skin potential are not linearly related to skin deformation. The skin potential rise was faster than 1 mV/s in

response to stretch, while the recovery speed was much slower in response to the skin being released from stretch (Ödman, 1981).

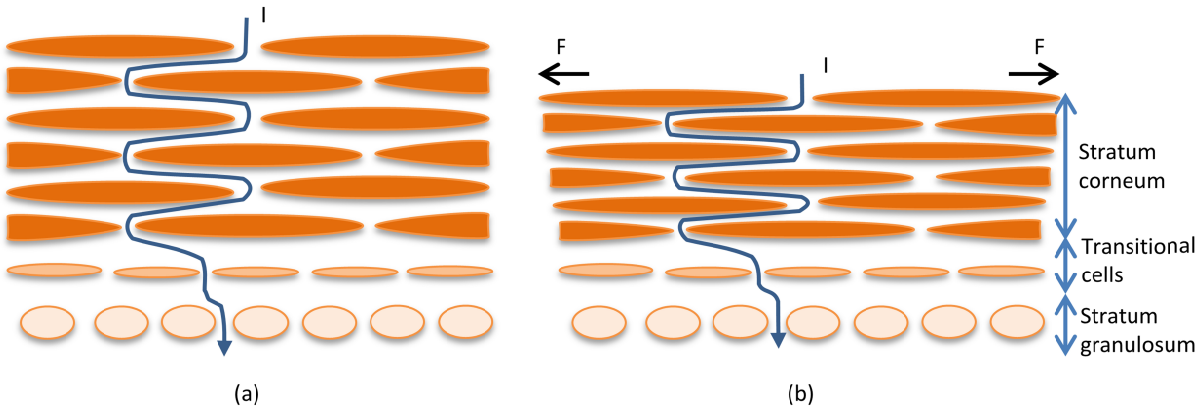

Figure 13. Effect of skin stretch on current pathway. (a) Depicts relaxed skin and (b) depicts skin stretched by laterally applied forces. Image modified and simplified from (Talhouet and Webster, 1996)

The explanations given above are for gelled electrodes. The electrical properties of the gel layer are relatively stable against physical deformation. For un-gelled electrodes, this layer is absent and the skin-electrode contact is achieved by a thin layer of moisture that has electrical properties that are sensitive to the physical forces acting on them. Thus, the above explanations might be insufficient for un-gelled electrodes.

For un-gelled electrodes, the thin layer of skin moisture that forms the basis of skin-electrode contact does not provide a continuous, uniform contact. Furthermore, the contact area might change considerably in size and shape when vertical or lateral forces, likely due to motion, posture changes, clothing effects, or any other factor are applied, and this change effectively alters the electrical properties of the skin-electrode interface (Medrano et al., 2007).

Because the skin-electrode contact layer is a thin film of moisture, any geometrical changes to the skin-electrode contact, even by small forces acting on the electrode and causing slight movements, can result in large changes in the ionic concentration gradient in this layer, changing the half-cell potential by noticeable amounts. This factor, not so much present for gelled electrodes, needs to be taken into account when investigating the motion artifacts of un-gelled electrodes. (Neuman, 1997)

An interesting side note is that this potential difference across the epidermis will also show slow changes in the absence of skin deformation. The processes that generate this potential difference are partially regulated by the sympathetic nervous system. Fast and sudden changes in the emotional state of the person such as excitement, fear, and joy can cause changes in the skin battery (physiological processes) in the order of millivolts, which will be superimposed onto the biopotential of interest.(Kutz, 2003)

2.5.3. Generation of Motion Artifact for electrode testing

In previous studies, various methods have been used to generate motion artifact. Most commonly, a subject is asked to perform a predetermined movement pattern such as walking or running on a treadmill (Di Rienzo et al., 2007; Kang et al., 2008; Lee et al., 2008, 2010; Merritt et al., 2009; Jorg Ottenbacher et al., 2008), jumping (Laferriere et al., 2011), various multi-joint or single-joint movements (Cho et al., 2009; Kearney et al., 2007; Lee et al., 2010; Muhlsteff et al., 2004; Pengjun et al., 2011; Pola and Vanhala, 2007; Sweeney et al., 2010), or hardware-restricted and guided movements (Roy et al., 2007) such as the elliptical trainer (Marozas et al., 2011) and the stationary bicycle (Raya and Sison, 2002). Random movement has been investigated (Romero et al., 2012, 2011). There have been studies where the movement-causing force was created by the pressing and moving of the electrode (Buxi et al., 2012; Hamilton et al., 2000; Tong et al., 2002), manually pulling on the skin around the electrode (Hamilton and Curley, 1997; Liu, 2007), and a pulse-like increase in the force acting on the electrode (Beckmann et al., 2010). In other studies, the force was created by a stepwise increase of the pressure applied to the electrode (Vos et al., 2003), hanging a weight from the skin to stretch it in a step function (Talhouet and Webster, 1996), a vibration-generating system generating vertical vibration under the foot of the subject at 10-50 Hz with the electrodes located on the upper leg which was bent in a 100 degree flexion (almost parallel to the ground) (Fratini et al., 2009), and a solenoid that oscillated parallel to the skin at 5 Hz (Searle and Kirkup, 2000). Three studies mechanically generated the motion at the electrode using a motorized system. Two studies used back-and-forth generated motion of a gelled electrode on skin while monitoring the skin-electrode interface impedance and the surface potential (Hokajärvi, 2012) and visually tracked the electrode movement using a stroboscope-aided camera (Ödman and Öberg, 1982). One study was on the movement of un-gelled electrodes on a skin-simulating membrane and then on actual skin using motorized motion. Pressure and temperature were monitored and the skin-membrane impedance and the generated potentials were measured (Liu et al., 2013).

In motion artifact studies, it is also important to note that motion artifact can be generated by forces acting directly on the electrode, or by deformations and elastic changes of the garment of a complete wearable system undergoing a motion artifact test. For example, in studies involving garments and human movement, the movements more resemble daily life and thus are applicable to questions relating to daily life. However, motion artifact also depends a lot on garment design and not just the design of the electrode. Garment tightness, elasticity patterns, material type, and user anatomical properties can all affect the resulting motion artifact.

2.5.3.1. Mechanical aspects of skin deformation in response to applied force

Skin deformation in response to applied vertical or lateral forces has been studied for medical and cosmetic purposes. These studies looked at the mechanical structure and behavior of skin. Unfortunately, the studies that formed the background of this thesis revealed that most of the skin deformation studies were done using indentation (Boyer et al., 2007; Delalleau et al., 2006; Pailler-Mattei et al., 2008; Tran et al., 2007) or suction (Hendriks et al., 2006, 2003). Earlier, skin response to applied torsion was studied (Sanders, 1973). Even if it is said that motion artifact is created from both

vertical and lateral skin deformation, a model relating the potential and impedance changes to mechanical skin deformation could not be found.

Further, most of the studies bundle the epidermis and dermis together in experimentation (Boyer et al., 2007; Delalleau et al., 2006; Pailler-Mattei et al., 2008; Sanders, 1973) and modeling (Delalleau et al., 2012; Wu et al., 2003). This unfortunately does not help reduce the lack in the understanding of the different electrical and mechanical properties of these two separate skin layers.

Indeed, studies that used suction methods (Hendriks et al., 2006) and indentation methods (Tran et al., 2007) to separate the epidermis and the dermis found these two layers have different mechanical properties.

An understanding of the mechanical behavior of the dermis and epidermis when force is applied to the skin would be immensely helpful in understanding motion artifact and the physical events that underlie the creation of motion artifact. This would considerably improve motion artifact reduction methods aimed at the origin of this phenomena.

2.5.4. Reduction of Motion Artifact

2.5.4.1. Basic guidelines in skin preparation

As mentioned in the skin model, given ample time, the skin can moisturize with the use of gel. Soaking the skin in alcohol or saline before electrode application can also produce the same effect.

Common ways to remove the effect of the stratum corneum, and thus removing the effect of E_{ep}, R_{ep} and C_{ep}, are rubbing the skin with a pad soaked in acetone or rubbing the skin with sandpaper (Burbank and Webster, 1978; Tam and Webster, 1977), stripping the top-most skin with tape (Talhouet and Webster, 1996), or even puncturing the skin (Burbank and Webster, 1978). Abrasion effectively shortens the pathway across the epidermis and reduces the skin impedance as well as lowering the potential difference in response to skin stretch to 0.1 mV (Tam and Webster, 1977). In a similar fashion, ten 0.5 mm skin punctures reduce this change to below 0.2 mV (Burbank and Webster, 1978). Skin stripping also reduces the impedance and the potential change in response to skin stretch (Talhouet and Webster, 1996).

These procedures can cause skin irritation, allergic reactions (Tam and Webster, 1977), and the removal of the protective layer of skin can increase the risk of infection. Also, it needs to be noted that the skin regenerates itself and the stratum corneum layer can be regenerated in as little as 24 hours, negating the effect of abrasion for long-term monitoring. (Neuman, 1997)

2.5.4.2. Motion Artifact Reduction Methods

2.5.4.2.1. Skin-electrode impedance studies in motion artifact research

A number of studies have investigated the skin-electrode impedance in relation to electrode motion and motion artifact more directly. These studies look at the behavior of skin-electrode impedance during electrode motion, its shape, the effect of applied force, the effect of electrode pressure, and its relation

to electrode motion and motion artifact. (Albulbul and Chan, 2012; Beckmann et al., 2010; Buxi et al., 2012; Ödman, 1981; Ödman and Öberg, 1982; Talhouet and Webster, 1996)

When talking about the relationship between skin-electrode impedance and motion artifact, causation and correlation are the two relationships of importance. Earlier, Ödman and Öberg stated that the skin potentials are not caused by impedance changes (Ödman, 1981; Ödman and Öberg, 1982), and the same conclusion was later given by Ottenbacher (J. Ottenbacher et al., 2008). Yet, Talhouet and Webster stated that skin-electrode impedance had partly been found to be the cause of motion artifact (Talhouet and Webster, 1996). While the causality between skin-electrode impedance and motion artifact remains a matter of debate, it is generally accepted that skin deformation and electrode movement cause motion artifacts and also cause changes in skin-electrode impedance. Thus, it is safe to think that there must be some correlation.

2.5.4.2.2. Detection and Adaptive Filtering Methods Summary

Adaptive filtering is the most common method used for the reduction of motion artifact, followed by the detection of motion artifact to mark the affected signal portion for further analysis or omission. These methods usually employ a second input signal to detect the parameters to be used as adaptive filter factors. Measured and successfully implemented signals are motion at the electrode by accelerometers (Di Rienzo et al., 2007; Kim et al., 2008; Lee et al., 2010; Luprano et al., 2013; Raya and Sison, 2002; Romero et al., 2012; Sweeney et al., 2010; Tong et al., 2002) and anisotropic magneto resistive sensors (Tong et al., 2002), skin deformation detection by optical sensors (Hamilton et al., 2000; Liu, 2007; Pengjun et al., 2011) and by strain gauges (Hamilton and Curley, 1997; Lee et al., 2010), skin-electrode contact pressure changes (Kim et al., 2008; Pengjun et al., 2011), biopotential changes on other body parts also affected by motion but not containing the biosignal of interest (Kearney et al., 2007), voltage differences from two adjacent electrodes (Luo and Tompkins, 1995), and skin-electrode impedance (Hamilton et al., 2000; Laferriere et al., 2011; Luprano et al., 2013; J. Ottenbacher et al., 2008; Romero et al., 2012, 2011).

Many of the studies use these measured signals as input parameters for adaptive filtering. Two studies use the additional input signals to detect motion artifact and to label the corresponding sequences in the original signal as artifact (Kearney et al., 2007; J. Ottenbacher et al., 2008). Active electrodes pick up the biopotential to be measured while at the same time transform the electrode impedance, as seen from the measurement system, from high to low. This reduces the effect of noise acting on the electrode, reduces the detrimental effect of the electrode impedance mismatch on CMRR, and improves signal quality. Active electrodes have been investigated to successfully reduce motion artifact (Kang et al., 2008; Merritt et al., 2009). Investigating a number of adaptive filtering methods such as independent component analysis, canonical correlation analysis, morphological component analysis, and dynamical embedding single spectrum analysis, Sweeney et al. concluded that the method selection is dependent on which reference signals are available, and that all the methods work to some degree, yet a single robust and reliable method for a wide range of conditions and applications was not present (Sweeney et al., 2012). Nevertheless, out of the mentioned methods, skin-electrode impedance is the most interesting due to its ability to also measure skin-electrode quality over time and skin conditions such as perspiration.

2.5.4.2.3. Non-uniform selection of impedance frequencies

The studies incorporating skin-electrode impedance are not standardized in the impedance measurement frequencies they use. Moreover, some studies use single impedance measurement frequencies while some use multi-frequency measurements. Nevertheless, no study has used simultaneous multi-frequency impedance measurements to investigate skin-electrode impedance in the presence of electrode motion. Ödman came to the conclusion that skin-electrode interface impedance is not the cause of the motion artifact, first using a 2 kHz sine wave (Ödman, 1981) and then, together with Öberg, using a 2 kHz sine wave and a 200 Hz sine wave (Ödman and Öberg, 1982), Later, Ottenbacher supported this conclusion using a 400 Hz sine wave as impedance current (J. Ottenbacher et al., 2008). While Ödman also stated that the relationship between motion artifact and the deformation is non-linear (Ödman, 1981), Ottenbacher found that skin-electrode impedance was suitable for recognizing the occurrence of motion artifact and used it to label corresponding segments of the ECG as being affected with the artifact. Talhouet and Webster used a 13 Hz current frequency when coming to the conclusion that impedance changes partly cause motion artifact (Talhouet and Webster, 1996). Hamilton used seven frequencies between 120 Hz and 1.8 kHz, and found that the skin-electrode impedance at 120 Hz functions as well as the output of a skin stretch sensor as an adaptive filter input and recommends the use of impedance instead of the optical sensor (Hamilton et al., 2000). Using a 2 kHz square wave impedance measurement, Romero reported a successful implementation of adaptive filtering of motion artifact (Romero et al., 2011), and later reported, albeit without reporting the impedance frequency, that the skin-electrode impedance functioned better than accelerometer output as an adaptive filter input parameter (Romero et al., 2012). Monitoring the skin impedance at 20 Hz, Hokajärvi reported that reducing the skin-electrode impedance reduced motion artifact (Hokajärvi, 2012).

Buxi reported skin-electrode impedance to have good correlation with motion artifact at an impedance current of 2.2 kHz (Buxi et al., 2012). Using a standardized measurement setup for exerting force on the electrode, Beckmann reported that the skin-electrode impedance at 5 kHz, tested on an agar-agar dummy, decreased with increasing forces of 2.14 N, 4.65 N, 9.73 N, and 23.54 N. Albulbul and Chan, when measuring on skin, found a similar yet not fully consistent effect for impedance measurements between 1 Hz and 1 MHz for forces of 0.8 N, 8.2 N, and 22.8 N acting on the electrode. The inconsistency arose at 22.8 N force where one subject showed a continuing decrease in impedance while another subject showed an increase (Albulbul and Chan, 2012). Skin-electrode impedance was seen to be lower under increasing pressure by Laferriere et al., but neither the applied pressure magnitude nor the impedance measurement is discussed (Laferriere et al., 2011). The measured impedance changes were reduced the further the electrode was located from the stretch area (Ödman, 1982). These are good examples of those factors that affect motion artifact and what means can be used to test them. Yet, as has been seen, the results are various and a measurement protocol that simultaneously controls or measures a number of factors and measures multiple impedance frequencies has been missing.

2.5.4.2.4. Other Interesting Research Results

Besides the successful reduction of motion artifact to various degrees by the aforementioned research using supplementary input signals as the reduction or detection method, there are some other

interesting results reported by the researchers. Pengjun et al. report that the pressure measured between the electrode and the garment showed good correlation with motion artifact and is a suitable input parameter for an adaptive filter (Pengjun et al., 2011). Regarding pressure, Kim et al. report that gradually increasing pressure from 0.3 kPa to 6 kPa also increased the signal-to-noise ratio (SNR), but a lowering of the SNR is observed at the highest pressure. This increase in SNR was less than the improvement obtained by moistening the dry textile electrodes (Kim et al., 2008). Pola et al. reported that simply moistening the skin provided better results than skin preparation by cleaning and abrasion (Pola and Vanhala, 2007). Tong et al. report they had better results with a three-axes accelerometer than a two-axes anisotropic magneto resistive motion sensor with two measuring axes set up parallel to the skin (Tong et al., 2002). Using accelerometers on both electrodes, Sweeney et al. conclude that the movement difference between two electrodes is better for quantifying motion artifact than is body movement (Sweeney et al., 2010).

2.5.4.2.5. Additional related studies

Skin potential changes when pressure is applied to the electrode is also reported by Vos et al., and they add that these potentials were not observed from the skin of a dead subject (Vos et al., 2003).

Skin impedance and skin-electrode impedance have also been investigated in the steady state case when no motion or force was applied. Using different frequency bands such as 1 Hz to 1 MHz (Rosell et al., 1988), 0.5 Hz to 10 kHz (Lin et al., 2011), 30 Hz to 100 kHz (Gruetzmann et al., 2007), and 0.1 Hz to 100 kHz (Hoffmann and Ruff, 2007), these measurements show the trend that skin-electrode impedance is dominated by the skin layer resistance in the lower frequencies and decreases with increasing frequency.

Even with the listed studies, there is a large gap in factors that need research. For example, how initial electrode mounting pressure in the absence of motion affects the changes in the pressure exerted by the electrode to the skin when the subject or the electrode moves. How this is affected by electrode location, garment design, electrode design, or subject body type, and how this affects the skin electrode interface and the generated motion artifact are topics that have not been comprehensively researched.

3. Methods

In this chapter, an overview of the used methods is presented. The details of the methods can be found in the published papers that are part of this thesis and referenced in the relevant locations.

To investigate motion artifact and its relation to electrode movement, reliable and repeatable movement of the electrode needs to be achieved. When talking about electrode movement, it is important to note that the electrode movement that is discussed in this thesis is of magnitudes that ensure the electrode does not slide on the skin, but moves in relation to its initial position and deforms the skin when the top most layer of skin in contact with the electrode moves together with the electrode. When electrode movement is too large, the electrode will slide on the skin and the measurement becomes useless. In the initial stages of the study, the electrode was attached to the upper arm of the subject with garment-mimicking elastic bands and the subject moved the forearm using elbow flexion. This generated motion artifact but was tiring on the subject and was not completely repeatable as the subject might twitch, move too slow or too fast, or get tired and lose focus. For this reason, a system that mechanically generated programmable movement at the electrode was conceptualized, designed, built, and tested. This device was used for the latter part of the research. During the studies, motion artifact was measured as a surface potential. The ECG and the skin-electrode impedance at single frequency or in a frequency spectrum were used as reference and comparison signals. In all studies, the motion artifact and an ECG channel containing the motion artifact were measured simultaneously. The electrode setup varied, but the idea behind the measurement method remained the same. When measured at a single frequency, the impedance was measured simultaneously with the aforementioned surface biopotentials (Paper 2 and Paper 4), or consecutively using a switching mechanism (Paper 1). The impedance spectroscopy was measured separately from the surface biopotentials, switching the lead connectors, without changing the basic measurement setup (Paper 3). The effect of various electrode motion parameters such as motion magnitude and speed were investigated, as well as electrode mounting parameters such as applied force and electrode location. The use of padding between garment and electrode was researched, and following this study, the impact of different electrode support structure designs was investigated. In this chapter, these aspects of the research are explained in more detail.

3.1. Generating Motion Artifact

In Paper 1, the movement of the subject generated motion artifact. The shortcomings of subject-generated movement were observed in this study, and in Paper 2 a device to mechanically generate electrode motion was introduced. The studies for Paper 3 and 4 were done using this system. These motion artifact generation methods are introduced below.

3.1.1. Using Subject Movement to Generate Motion Artifact

To test the effect of using padding between the garment and the electrode for Paper 1, an experiment was designed where the electrodes were attached to the skin with elastic ribbons and motion artifact was created by the subject's own movement.

The elastic ribbons act in the same way as a tight elastic garment will, and the movement used mimicked a very simple and common daily motion that affects the electrodes at the selected location. The electrode subject to motion artifact was located on the outside of the upper arm in the area falling between the biceps and the triceps muscles. It was found that this area is the one least affected by the EMGs coming from the muscles and would therefore be a suitable location for a limb electrode in actual monitoring systems. (Paper 1)

Two channels of ECG were measured with a measurement setup designed for this experiment and later adopted for other experiments. The measurement setup is presented in Figure 14. By designing the lead setup so that the common electrode for the two biopotential leads was the electrode subject to motion, the exact same motion artifact was superimposed on the measurements from both channels. This allowed for the measurement of a channel with ECG affected by motion artifact, a channel consisting mostly of motion artifact, and an undisturbed ECG channel derived from the former two. Using a switching setup designed specifically for this experiment, the skin-electrode impedance was measured between the arm and the right chest electrodes, after the surface potential measurements, without touching or otherwise affecting the electrodes. (Paper 1)

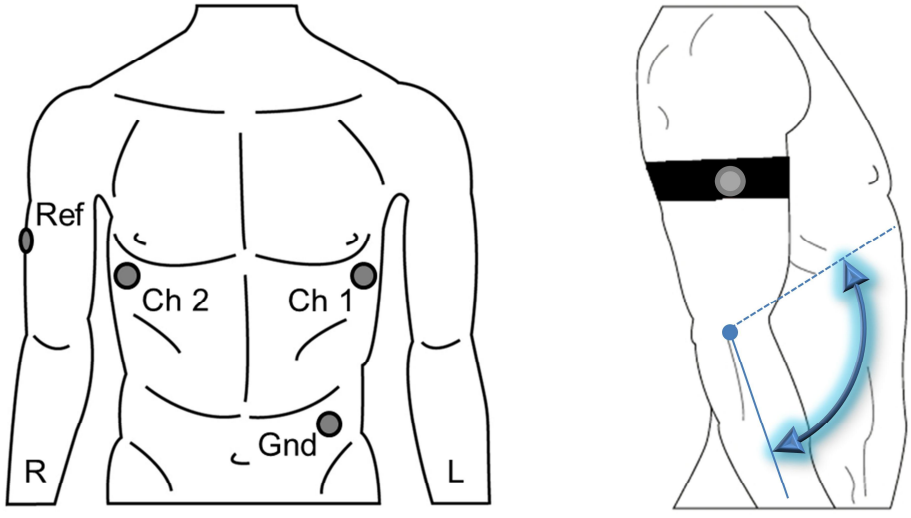

(a) (b)

Figure 14. The electrode locations and subject-generated motion used in Paper 1. (a) Shows the electrode locations. (b) Shows the motion of the arm generated by the flexion and extension of the forearm from the elbow. Modified from the image originals published in Paper 1.

The motion used was a single-joint motion where the only moving part was the forearm via biceps contraction and relaxation, as presented in Figure 14. The only load on the arm was its own weight and care was taken not to flex the biceps extensively at the upper end of the motion nor the triceps at the lower end of the motion, and the shoulder joint was kept stiff. The movement was synchronized to a metronome. (Paper 1)

Throughout the experiment, the pressure acting on the electrode was adjusted between 5 and 25 mmHg (0.66 kPa and 3.33 kPa) by the tightening of the elastic ribbon, while a hand-held pressure monitor monitored the pressure. (Paper 1)

3.1.2. The Motion Artifact Generation and Assessment System

To be able to isolate the forces acting on the electrode that are causing electrode movement and to be able to separate the effects of garment design and the effects of electrode design on motion artifact, a prototype Motion Artifact Generation and Assessment System was developed and presented in Paper 2.

The aim of this system is to generate known and programmable motion of the electrode. The system monitors the electrode mounting force and informs the operator of the applied force levels. During electrode movement, the pressure under the electrode will inevitable change, but the electrode mounting module should be vertically and horizontally stable.

Such a system allows for repeatable experiments between subjects and between experiments for the same subject by keeping the force applied to the electrode. Thus, the pressure applied by the electrode to the skin and the movement of the electrode are in the same ranges.

The system presented in Figure 15 is introduced in Paper 2, and is used for the research leading to Papers 3 and 4.

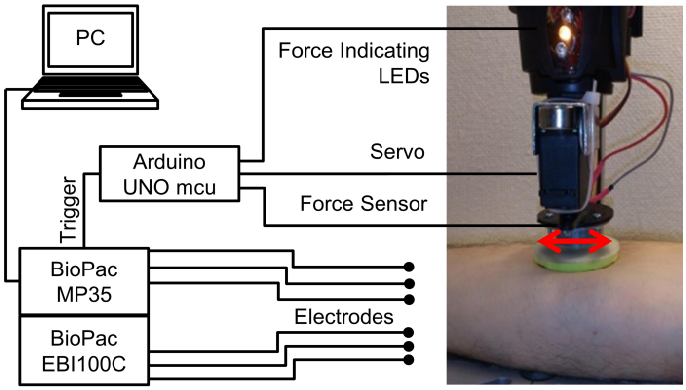

Figure 15. Motion artifact generation and assessment system overview and the motion generation module. Image modified from the original image published in Paper 4.

An Arduino UNO microcontroller board (SmartProjects, Turin, Italy) is the controlling unit for this system and is programmed by compiler installed on a PC. The UNO has three tasks: to monitor the applied force; to provide feedback to the user on the applied force, and to control the motion.

The mechanical backbone of the setup is a modified Dremel 220 workstation (Robert Bosch Tool Corp., Illinois, USA). The platform, originally intended to secure Dremel work tools, was modified to hold the movement generation module of the system, and was used to mount the electrode onto the skin at varying forces. The large lever-arm-to- vertical-platform-movement ratio and a little give in the lever arm before the vertical movement of the platform ensure that the force can be controlled in small steps and then remains stable provided the user pays attention to the lever.

The servo and the force sensor are positioned between the electrode itself and the vertically moving platform.

The UNO board controls the servo, and in this design the rotational movement of the servo is translated into lateral movement of the electrode, as presented in Figure 16 (a). In our used servo rotation angles, the movement of the servo stays mainly in the x-direction, while some movement is also caused in the y-direction, and these displacements in different axes are presented in Figure 16 (b).

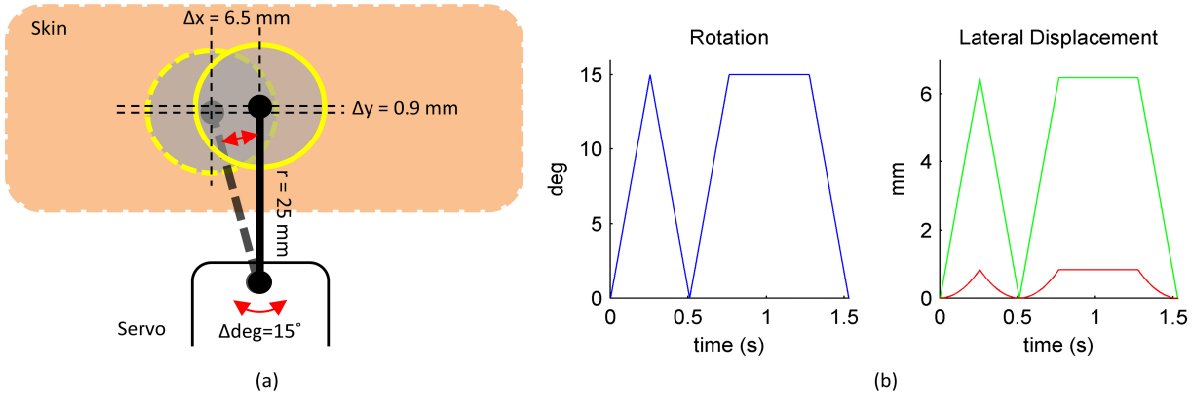

Figure 16. Electrode movement generated by servo rotation. (a) Shows the principle how rotational servo movement is translated into lateral electrode movement. (b) Shows how the rotation angle translates into x- and y-axis displacement of the electrode. The displacement in the x-axis is shown in green and the displacement in the y-axis is shown in red. Image modified from the original image published in Paper 3.

The force sensor is located in a custom-made sensor housing that is positioned between the servo arm and the electrode, as shown in Figure 17. This housing ensures that there are no lateral forces acting on the sensor, and enables the measurement of only the vertical forces acting on the sensor. The output of the sensor is read by the UNO, and in turn, the UNO lights up LEDs corresponding to the applied force.

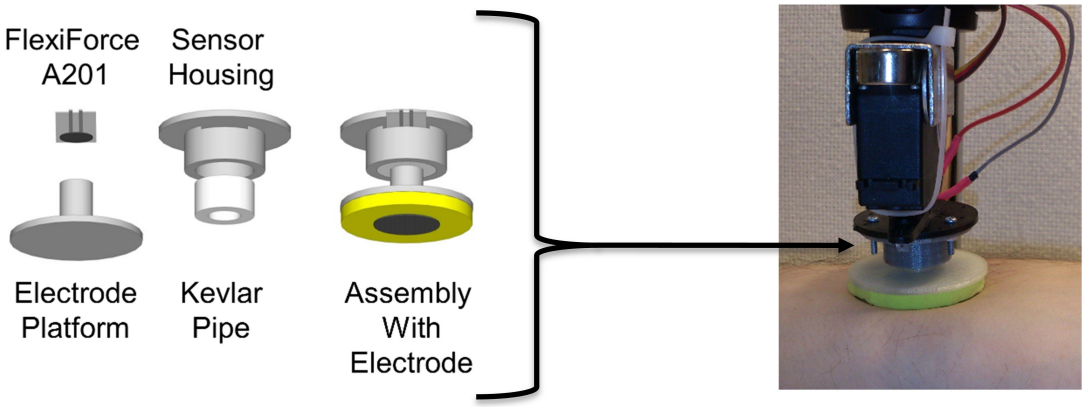

Figure 17. Construction of the force sensor housing. The FlexiForce sensor (Tekscan Inc., South Boston, USA) is inserted in the dedicated slot in the sensor housing part and the Kevlar pipe is inserted vertically to the sensor. When the electrode platform is inserted into this device, the platform column sits perfectly on the sensor. Vertically the platform moves freely, yet the lateral movement of the platform and thus the lateral forces acting on the sensor are minimized. A more detailed explanation of this system can be found In Paper 2.

3.1.3. Using Mechanically Induced Electrode Movement to Generate Motion Artifact

In the introductory Paper 2, electrode motion was generated by the Motion Artifact Generation and Assessments system to demonstrate system functionality. This system was then used in Paper 3 in order to generate the motion of the electrode to investigate the skin-electrode impedance spectroscopy during electrode motion. The electrode motion used in Paper 4 to investigate the isolated effect of electrode structure and the isolated effect of applied pressure, without being affected by the influences of the mounting system such as the garment or straps, was also generated by this system.

Because it provides testing opportunities on different tissue thicknesses under the skin, the forearm was used in all experiments. Close to the wrist, the hard structures such as the ulna and radius bones and the tendons of the forearm muscles, especially flexor carpi radialis and palmaris longus, are directly under the electrode area with little soft tissue to act as a buffer. Close to the elbow, on the other hand, thick muscle tissue, which is relatively soft when relaxed, provides a natural buffer between skin and hair tissue, and the electrode effectively rests on soft tissue when pressed on the skin.

The applied back-and-forth motion was programmed to have a triangular wave pattern of servo rotation and various parameters such as rotation step magnitude and rotation step frequency to vary the rotation speed, rotation end range, or both. Increasing the rotation range while keeping speed constant reduced movement frequency, whereas increasing the speed for constant end range increased movement frequency, and increasing both parameters did not affect movement frequency. In Paper 3, a one-second pause was added to the beginning and the end of rotations to observe the effect of short pauses in motion. Force or pressure applied to the electrode was measured in all experiments. The force was measured as an initial condition before the movement was initiated. The pressure was seen to change upon movement, both in the body movement experiments and the mechanically applied

electrode movement cases, but these were not synchronized to the electrical measurements, and thus were not reported as results but merely as observations. The applied forces differed for the experiments, ranging from barely holding the electrode in place to the physically uncomfortable: between 250 grams and 3000 grams (2.45 N and 29.42 N).

3.2. Measurement Setup

In all studies, two channels of surface biopotentials were measured. One channel was set up so that it contained mostly motion artifact; the other channel was set up so that it measured an ECG lead subject to motion artifact. This was achieved by using the electrode subject to motion as a common electrode for the two channels while using a separate electrode for the other end of the biopotential measurement channel, thus making the motion artifact common to both channels. The biopotentials were measured by the BioPac Data Acquisition System Unit (BioPac Systems Inc., Goleta, California, USA).

For Paper 1, 2, and 4, the skin-electrode impedance was measured simultaneously to the surface biopotential measurements, again using the electrode subject to motion as the common electrode. To measure this single frequency impedance at 100 kHz, the electrobioimpedance module EBI 100C of the BioPac Data Acquisition System Unit was used. For Paper 3, the Zurich Instruments HF2IS Impedance Spectrometer (Zurich Instruments AG, Zurich, Switzerland) was used. Twenty-four frequencies spaced logarithmically between 25 Hz and 1 MHz were divided into three groups of eight frequencies. These groups were designed so that the frequencies they contained were interwoven. For this experiment, the 3 groups of impedance and the surface biopotential measurements were taken in sequence.

For Paper 1, 2 and 4, a two-point impedance measurement was used. For Paper 3, a three-point impedance measurement with a slightly different sensitivity field was used. However, due to the high conductive nature of inner tissue, the measurement remains most sensitive to changes in the skin-electrode interface for both setups.

Details of the individual experimental protocols can be found from Papers 1, 2, 3, and 4.

3.2.1. Measurement Systems

3.2.1.1. BioPac Data Acquisition System

To measure the surface biopontentials, the BioPac MP35 Data Acquisition Unit module was used throughout the studies. The MP35 has a high input impedance of 2 MΩ and a resolution of 3 μV

In Paper 1, Paper 2, and Paper 4, the EBI 100C Electrobioimpedance Amplifier measured simultaneously skin-electrode impedance and the surface potentials. This amplifier has a resolution of 1.5 mΩ and can measure single frequency, real-time impedance at four frequencies between 12.5 kHz and 100 kHz by injecting a 100 μA current. The BioPac Data Acquisition System is presented in Figure 18.

Figure 18. The BioPac Data Acquisition System

3.2.1.2. Zurich Instruments HF2IS Impedance Spectrometer

For the real time impedance spectrum measurement research done for Paper 3, the HF2IS impedance spectrometer, presented in Figure 19, was used. This system can simultaneously measure the real-time potentiostatic impedance at eight different impedance frequencies. The voltage input level of a sine wave at a given frequency can be specified and the resulting impedance, phase, resistance, or reactance can be directly observed from the system's software user interface, or the data can be saved for use in other data processing software such as Matlab (MathWorks, Natick, Massachusetts, USA). In this case, the device output was saved as the measured real current and the measured imaginary current.

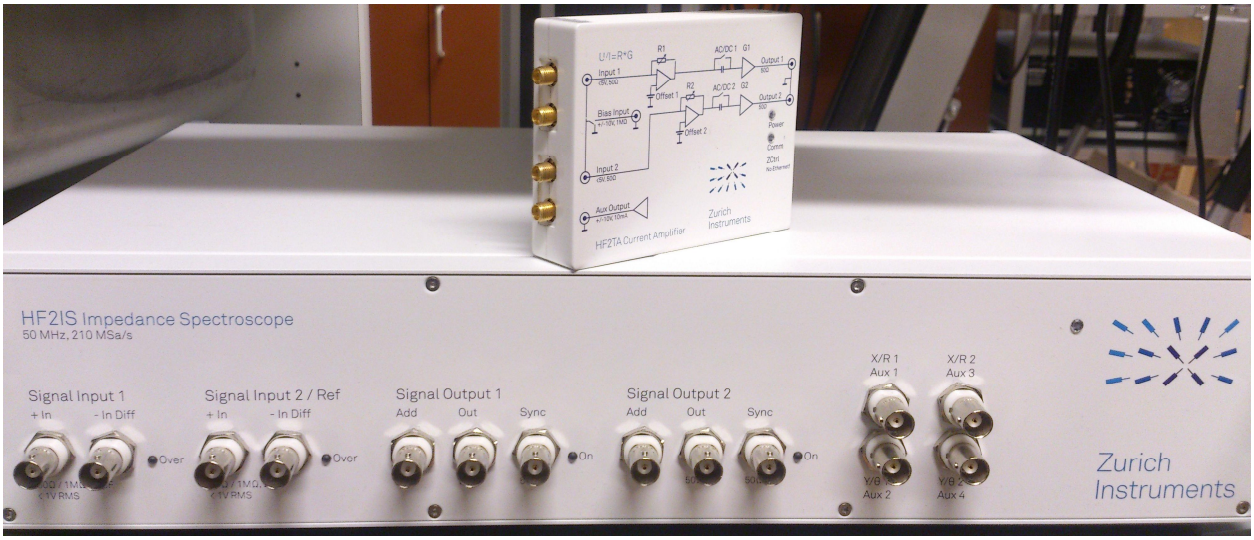

Figure 19. The Zurich Instruments HF2IS Impedance Spectrometer and the HF2TA Current Amplifier.

3.3. Electrodes and Cables

The research was done with textile electrodes, and commercial AmbuBlu electrodes were used as a reference point.

In the initial stages of the research, conductive 234 dtex silver plated high grade multifilament nylon yarn was embroidered onto elastic and non-elastic fabrics in various patterns (Cömert et al., 2009, 2008). Some examples of used electrode designs are presented in Figure 20.

Figure 20. A sample of electrode surface structures used in the experiments. The electrode squares used in the studies leading up to Papers 2, 3, and 4 were cut from the textile sheet shown in the bottom right hand corner. For size comparison, the elastic ribbons used for the embroideries had a width of 3 to 4 cm.

In the later stages of research that are presented in this thesis, Papers 1, 2, 3 and 4, the electrodes were cut out from a MedTex P180 (Statex productions & Vertriebs GmbH, Bremen, Germany) warp knitted textile made of silver coated yarn. Having high conductivity, elasticity in two dimensions, and being antibacterial, this textile was found to be suitable, and initial tests that compared the embroidered electrodes TechTex 130 and 180 (Statex productions & Vertriebs GmbH, Bremen, Germany) and MedTex P130 and P180 showed the MedTex P180 textile electrode to be the one with the best skin-electrode impedance and biopotential measurement results.

The electrodes were moistened with drops of water to improve the conductivity of the skin-electrode interface.

For the research in Paper 1, the electrodes were connected to the measurement system using unshielded textile cables (Finn-Nauha, Haapamaki, Finland). The conductive yarn used in these cables was a 234 dtex silver-plated, high-grade multifilament 6.6 polyamide yarn with a 10% stretch tolerance.

For Paper 2, 3, 4, we used the default cables provided by the used measurement systems, and the electrodes were connected to the cables via snap connectors. In the case where more than one lead was attached to the electrode, an adapter was constructed that combined male snap connectors for the connections to the leads with one female snap connector for the connection to the electrode.

3.4. Electrode Support Structures

Initially, the embroidered electrodes were used directly embedded into the garment fabric without the use of a support structure between the fabric and the electrode (Cömert et al., 2009, 2008). In this type of structure, the embroidered yarn causes a small indent in the skin. This indent improves the physical contact area and lateral stability when compared with a woven structure where the yarn is in the supportive textile structure (Mestrovic et al., 2007; Pola and Vanhala, 2007).

For Paper 1, it was hypothesized that this type of structure, however, might not be stable against vertical forces acting on the electrode because the vertical forces acting on the electrode are transferred directly to the skin-electrode interface.

3.4.1. Padding Between Garment and Electrode

In Paper 1, various paddings were tested as electrode supports. These paddings were made of different materials: Pudgee (Dynamic Systems, Inc., Leicester, USA), an open-celled viscoelastic gel-like foam, Poron XRD foam (Rogers Corporation, Rogers, USA), impact protection cushion, SunMate Memory Foam (Dynamic Systems, Inc., Leicester, USA), and an elastomeric open-celled viscoelastic polyurethane foam and are presented in Figure 21. These materials have differing physical properties with regard to elasticity. The green Pudgee foam had gel-like properties in a foam structure, while the yellow Poron foams were high-impact memory foams, resistant to impact effects but changing shape for slower applied forces. The Poron cushions were softer on the skin when warmed by the body than at room temperature. The blue SunMate foams were simple foams of a different hardness. The height of the cushions differed and the diameter was on average 38 mm. The circular textile electrodes made of MedTex P180 conductive fabric, supported by these cushions, had a diameter of 25 mm.

Figure 21. The paddings used between garment and electrode in Paper 1. The radii of the paddings are between 16 and 19 cm, and the thickness from 6 to 16 mm.

For Paper 2, a 50x4 mm and a 20x4 mm Poron XRD cushion were used to test the functionality of the Motion Artifact Generation and Assessment system and to see if the system showed a difference in behavior between these two electrode designs. The same 50 mm diameter cushion was used in Paper 3

for the testing of various impedance current frequencies in their ability to relate to motion. Resulting from the experience gained from these published studies and other experiments and the knowledge that the origins of motion artifact are at the thin upper layer of skin, an idea on how motion artifact could be reduced by restricting epidermis deformation was formed.

3.4.2. Restricting Epidermis Deformation to Reduce Motion Artifact

One can say that the epidermis generates large potentials for its thickness. Being only a fraction of the dermis underneath it, its deformation generates much higher voltages than dermis deformation. Following the reasoning that it could be possible to trap the epidermis under the electrode and transfer the skin deformation resulting from electrode motion primarily to the dermis, a hypothesis was defined.

The hypothesis states that an electrode design that constricts the epidermis under the electrode area will cause the epidermis deformation to be restricted and transfer the overall skin deformation, which is unavoidably caused by electrode movement, to the dermis. This would prevent the trans-epidermis voltages to change in response to electrode movement and, since the electrical contribution of the dermis to motion artifact is small, motion artifact would be reduced.

Figure 22 depicts the process presented in the hypothesis where the epidermis-constricting electrode design is presented as electrode B. The black dots drawn for electrode B represent a cross section of an outer ring of the electrode that digs itself into the skin and is designed to trap the epidermis.

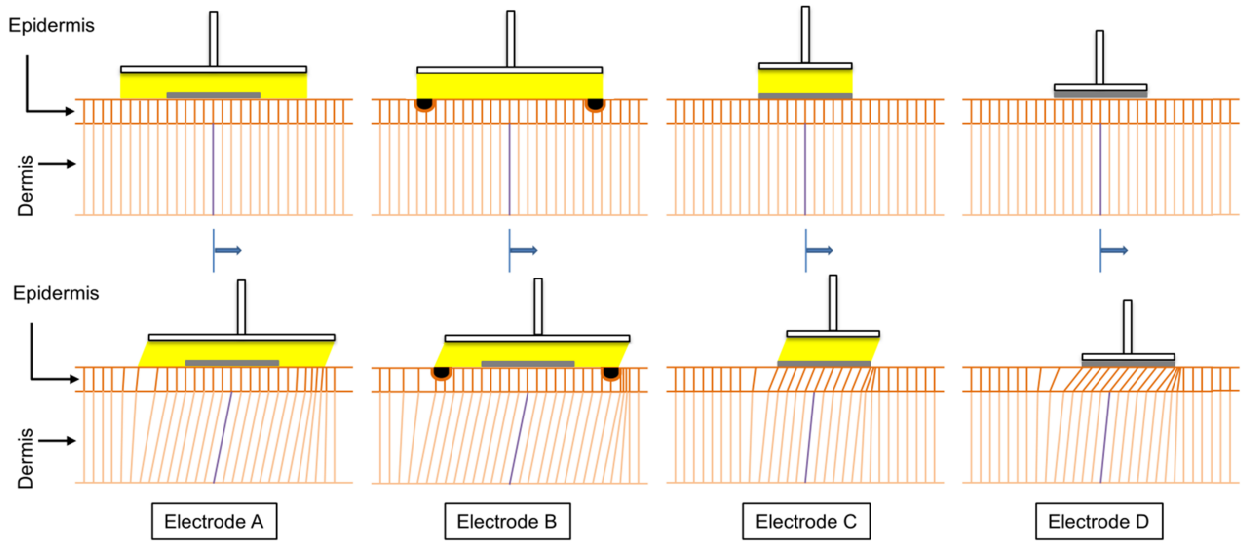

Figure 22. Depiction of the proposed functionality of epidermis restricting electrodes. Electrode A is designed to distribute electrode movement over an area larger than the electrode. Electrode B is designed to additionally restrict epidermis deformation. Electrode C shows the proposed effect of padding between the movement generated and the electrode. Electrode D shows the effect of the applied force being directly translated into electrode movement. Image originally published in Paper 4.

3.4.3. Electrode Support Structure Design

For the testing of the hypothesis presented in Chapter 3.4.2, a novel electrode structure was introduced in Paper 4 that aimed to restrict epidermis deformation. This new structure also had a diameter of 40 mm and was compared with the previously designed electrodes and medical electrodes. In all experiments, the textile electrode was of a circular nature with a diameter of 20 mm. The ring on the outer border of electrode B is made of silicone and is postulated to constrict the epidermis under the electrode by acting together with the indent in the electrode structure between the electrode surface area and the border ring. The electrodes used to test the hypothesis presented in the previous chapter are presented in Figure 23.

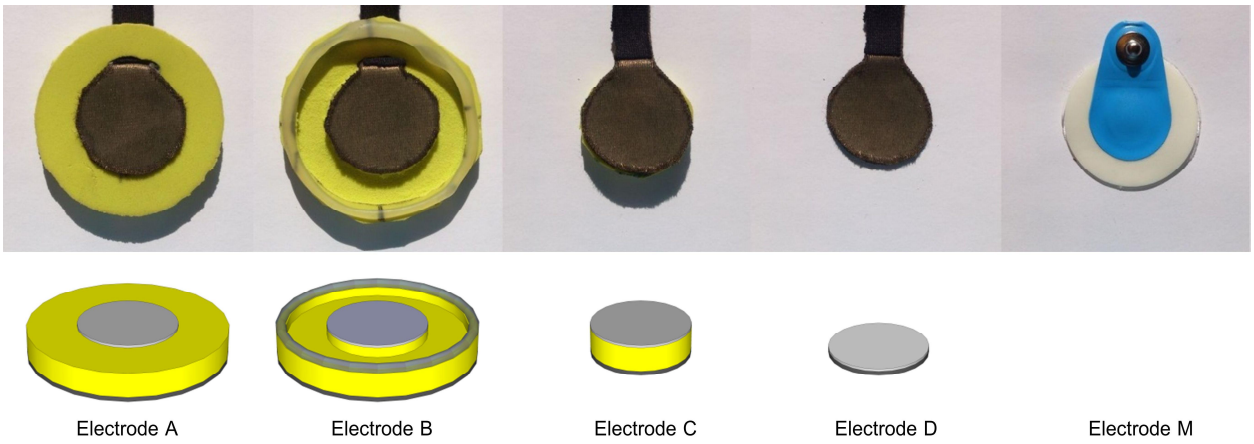

Figure 23. Electrodes used in the investigation of the effects of epidermis restriction. Upper row presents the actual electrodes and the lower row presents the 3D models. Electrode M is not modeled as it was not designed by the author. Image originally published in Paper 4.

3.5. Subjects

For the studies leading to Papers 1 and 2, the thesis author was the sole subject. Subject was aged 35 years old during the studies for Paper 1 and 36 years old for Paper 2 with a body mass index (BMI) of 28 and an athletic build.

Paper 3 had 10 male volunteers aged between 26 and 45 years old with body mass indexes (BMI) between 20.2 and 30.1.

The first experiment for Paper 4 had 5 male volunteers aged between 25 and 36 years old with BMIs of 20.7 to 28.2.

The second experiment for Paper 2 had 5 male volunteers aged between 30 and 36 years old with BMIs of 20.7 to 31.

Here the author would like to note that the BMI is not a perfect measure as it tends to overestimate the body fat content in athletically built individuals and tends to underestimate the fat content in individuals with little muscle mass. In these experiments, the subjects ranged from athletic to overweight, with most of them falling into the average body type category.

3.6. Data Analysis

Using the motion artifact generation device, the applied motion to the electrode was accurately known and could be used to assess the relationship of the created surface potentials –motion artifact – and the skin-electrode interface impedance changes to the electrode movement.

For all the experiments, Matlab was used for the data analysis. The data was analyzed visually and quantitatively in time domain and frequency domain.

The data was band pass filtered to remove the baseline wander not related to the applied motion, without affecting motion artifact, and to remove high-frequency components not in the frequencies covered by the applied motion or its harmonics.

For Paper 1, the R-peaks of the noisy and clean ECG were detected and used to calculate a score for different paddings and different applied pressures. Because the ECG measured by textile electrodes had a too low signal-to-noise ratio (custom-defined) for reliably detecting and quantifying the lower amplitude components of the ECG such as the P-wave and the T-wave, this analysis was limited to the R-peaks. The signals were visually analyzed and compared in the time domain, and the signal peak amplitudes and median amplitudes were used for quantitative analysis. For this research, the frequency domain analysis was done to find the frequency band of the noise signals related to the applied motion and to limit time domain analysis in this 1-7 Hz bandwidth.

In the later research, the surface potential, the skin-electrode impedance, and motion patterns were visually compared. Further, their linear relationships were analyzed via correlation calculations, and the peak-to-peak amplitudes or the root mean square values were used for quantitative comparison. Power spectrum densities of the signals were calculated. These frequency domain representations of the signals were visually compared and their correlations were analyzed for a quantitative analysis.

A summary of the main aspects of each paper is presented in Table 5.

Table 5. Summary of the Papers

Paper	Subjects	Motion Generation Method	Electrodes Used	Measured Signals	Applied Force/ pressure	Main Aim
1	1	Subject generated	Uncategorized Paddings	Motion Artifact, ECG, Impedance	5 mmHg (0.66 kPa) 10 mmHg (1.33 kPa) 15 mmHg (1.99 kPa) 20 mmHg (2.66 kPa)	Investigate effect of padding on motion

				@ 100 kHz	25 mmHg (3.33 kPa) (Overall Garment Pressure)	artifact
2	1	Mechanically Generated	Electrode A, C, & M	Motion Artifact, ECG, Imp @ 100 kHz	250 gr (2.45 N) 500 gr (4.90 N) 750 gr (7.35 N) 1000 gr (9.80 N) 1250 gr (12.26 N) +/- 100 gr (0.98 N) (force applied to electrode)	Investigate the ability of the system to generate motion artifact
3	10	Mechanically Generated	Electrode A	Motion Artifact, Impedance Spectrum 25 Hz -1 MHz	750 +/- 100 gr (7.35 +/- 0.98 N) (force applied to electrode) Approx. 28 mmHg (3.73 kPa) (pressure under electrode)	Investigate the skin-electrode impedance response to impedance measurement frequency
4	5 for stage 1 5 for stage 2	Mechanically Generated	Electrode A, B, C, D, M	Motion Artifact, ECG, Imp @ 100 kHz	250 gr (2.45 N) 500 gr (4.90 N) 750 gr (7.35 N) 1000 gr (9.80 N) 2000 gr (19.61 N) 3000 gr (29.42 N) +/- 100 gr (0.98 N) (force applied to electrode)	Investigate the effect of padding structure on the motion artifact

4. Results

First, the results of Paper 1 on the functionality of the motion artifact generation methods by subject are presented. Then, the functioning of the Motion Artifact Generation and Assessment System is presented, followed by the findings of the impedance spectroscopy study about how impedance measurements at different impedance frequencies relate to the electrode motion and motion artifact. Then, the relationship between the skin-electrode impedance and motion artifact, investigated in all papers, are presented. How the amplitude and speed parameters of the electrode motion affect motion artifact is then presented. Then, the effects of garment pressure and the force applied to the electrode on the susceptibility of the electrode to motion artifact are presented. Results that point to the importance of correct electrode location are then presented. The differences between subjects were not studied, but the tissue differences between the studied electrode locations can be used as a pointer for this purpose. The research provided answers to the effects of padding use between garment and electrode. Finally, the results from these studies and the results obtained from the studies regarding the effect of structural electrode design on motion artifact are presented.

4.1. Motion Artifact Generation

The use of the subject-generated motion used in Paper 1 resulted in motion that was adequately repeatable over the long term, and motion artifact that was in the frequency ranges covered by the subject movement. The impedance change was also closely related to the subject movement, yet with less noise than the surface potentials. However, because the exact electrode motion is not known as a measured signal or a control parameter, the generated motion artifact and impedance change cannot be directly compared to the movement.

Presented in Paper 2 and used for Papers 3 and 4, the system generates electrode motion and this can be clearly observed as motion artifact and impedance change. The system functions outstandingly as the impedance change and the applied motion are very similar in shape and are highly linearly correlated. Three movement patterns are experimented with. For Pattern 1, the servo rotation angle is gradually increased, keeping the rotation speed constant. For Pattern 2, the servo rotation speed is gradually increased, keeping the rotation angle relatively constant. For Pattern 3, the servo rotation speed and angle are gradually increased. The frequency of the back and forth rotation decreases for Pattern 1, increases for Pattern 2 and stays same for Pattern 3. As seen from Figure 24, the electrode motion, via the impedance as proxy, can be seen to be accurately programmed and repeatable, therefore succeeding in the intended functionality. Motion artifact, on the other hand, possesses the frequency components that are very similar to the applied motion but, as expected from previous studies(Ödman, 1981), the linear correlation to applied motion and impedance is not as high. The similarities between motion artifact, impedance, and applied motion using impedance as proxy are presented in Figures 24 and 25.

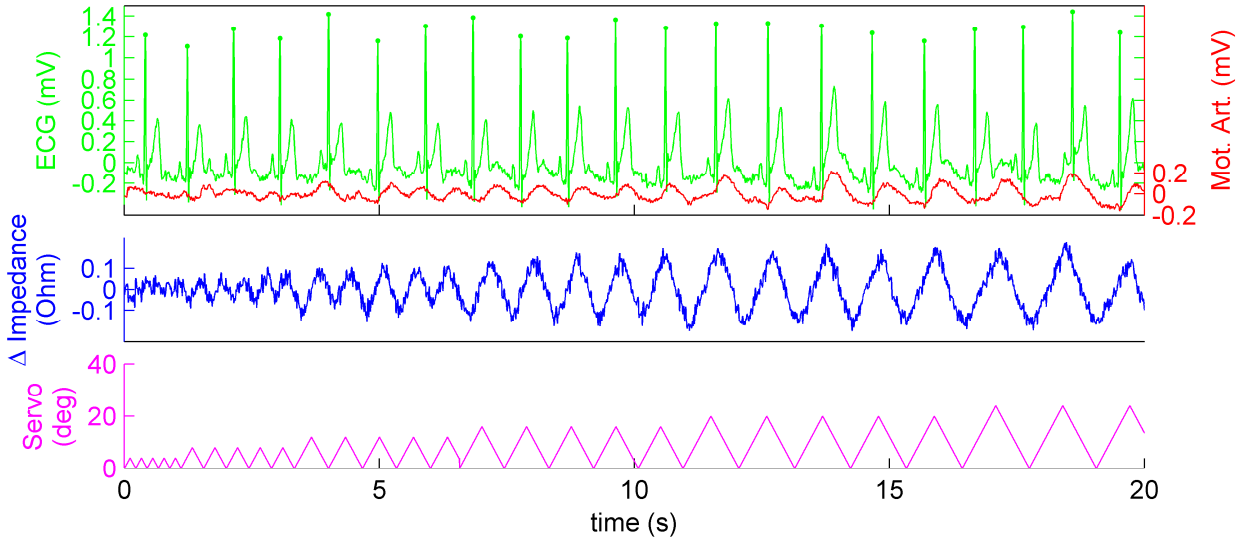

Figure 24. The ECG, motion artifact, impedance, and servo rotation pattern. ECG is shown in green, motion artifact in red, the change in impedance in blue, and the servo rotation pattern in pink. The graphs correspond to servo rotation Pattern 1 for which the speed of the servo is kept constant while the rotation magnitude is increased after every fifth rotation. All four graphs have the same time axis.

In frequency domain, the similarity between the signals and the pattern as shown in Figure 25, also points to the successful functionality of the system, and that the applied motion creates motion artifact and the impedance change, and that the main components of the signals and the motion are related.

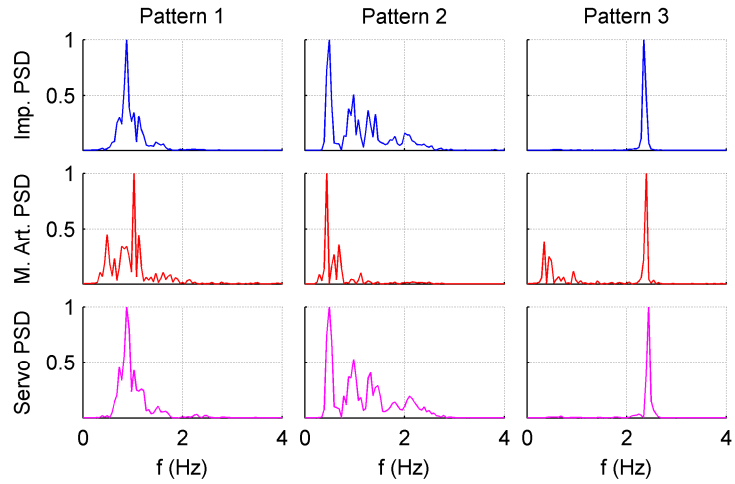

Figure 25. The power spectrum densities (PSD) of impedance, motion artifact, and the electrode movement pattern for each movement pattern investigated in Paper 2. The PSD's are normalized between 0 and 1 for better comparison. The image was originally published in Paper 2.

4.2. Motion Magnitude, Motion Speed, and Motion Artifact

Increasing the motion magnitude caused an increase in motion artifact, yet in the larger displacements this increase was seen to be out of proportion to the increase in the motion magnitude. Figure 26 presents these findings using data obtained for Paper 4. Each boxplot is drawn for the data from an electrode at a given location for all subjects. The electrodes are presented from left to right while the top boxplot represents a given electrode at the distal location and the lower boxplot represents the same electrode at the proximal location. The x-axis data columns represent the rotation magnitudes.

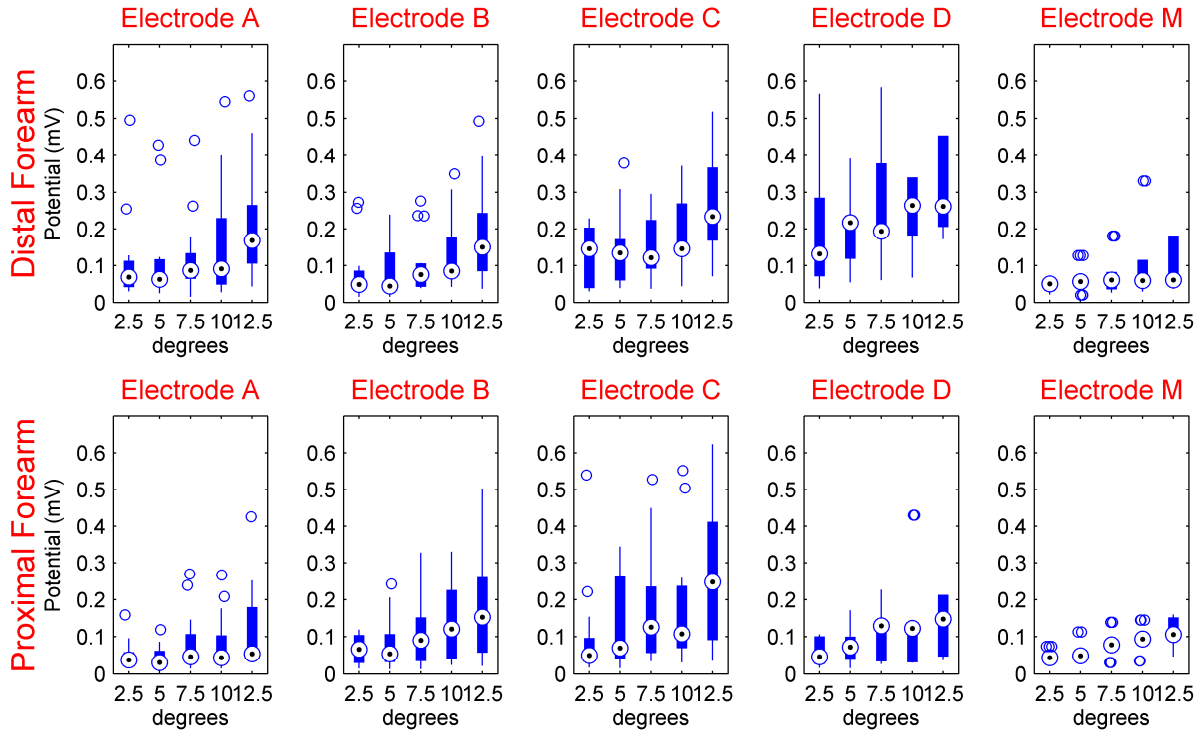

Figure 26. Effect of movement magnitude on motion artifact RMS value. Each row in the boxplots corresponds to a specific movement magnitude at the same speed. The applied force to the electrode is equivalent to 500 gr (4.90 N).

Not published in Paper 4 but observed in the data, motion artifact is not affected or is slightly reduced by increasing the speed of the electrode movement. Figure 27 presents this behavior and the x-axis columns inside the boxplots represent servo rotational speeds.

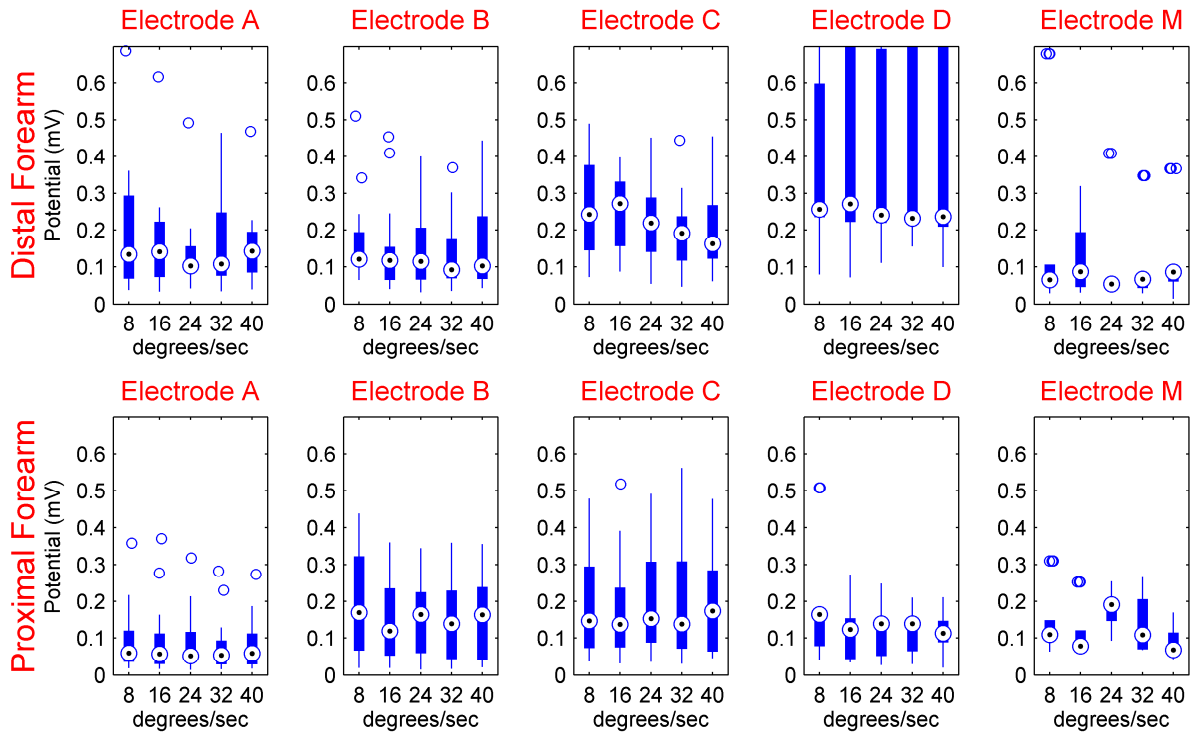

Figure 27. Effect of movement speed on motion artifact RMS value. Each row in the boxplots corresponds to a specific movement speed at relatively steady magnitude. The magnitude of the movement at the presented speeds stays within 5% of the median movement magnitude. The applied force to the electrode is equivalent to 500 gr.

Due to experiment design, a clear distinction between electrode motion speed and electrode back-and-forth motion frequency was not made. Thus, the results presented in Chapters 4.2 and 4.5 related to the effect of motion speed to the measured signals, motion artifact, and skin-electrode interface impedance can be regarded as the effect of the back-and-forth motion frequency. Among the motion patterns used in the research of Paper 4, two patterns have changing frequency, one is decreasing and one is increasing. In the pattern that has decreasing frequency, the main effect can be seen to be from the increase in the motion magnitude, as the speed stays constant. The presented pattern in the context of this chapter is so that the motion speed increases while the amplitude stays almost constant. Thus, speed and frequency have been used interchangeably for these results.

4.3. Impedance Current Frequency and Electrode Motion

The results of the impedance spectroscopy study done in Paper 3 that looked at the best possible impedance current frequencies to be used in motion artifact and/or electrode motion studies are presented in Figure 28. The impedance spectroscopy results are presented for 25-second motion duration and the impedance current frequencies are sorted in an ascending order from top to bottom. The resistance and reactance are presented in the top row, and impedance and phase are presented in

the second row. The vertical spacing between consecutive frequency traces is 1% of impedance change relative to the impedance baseline at the respective frequencies. Motion artifact and the ECG affected by motion artifact are presented in the third row. As a reference point to all these signals, the programmed pattern of the applied motion is presented in the bottom row in the form of servo rotation. It can be seen that the applied motion is detectable in all current frequencies. While impedance at higher frequencies matches perfectly (correlation >0.9) with the pattern of the applied motion, impedance at lower frequencies has a low frequency drift and low frequency noise.

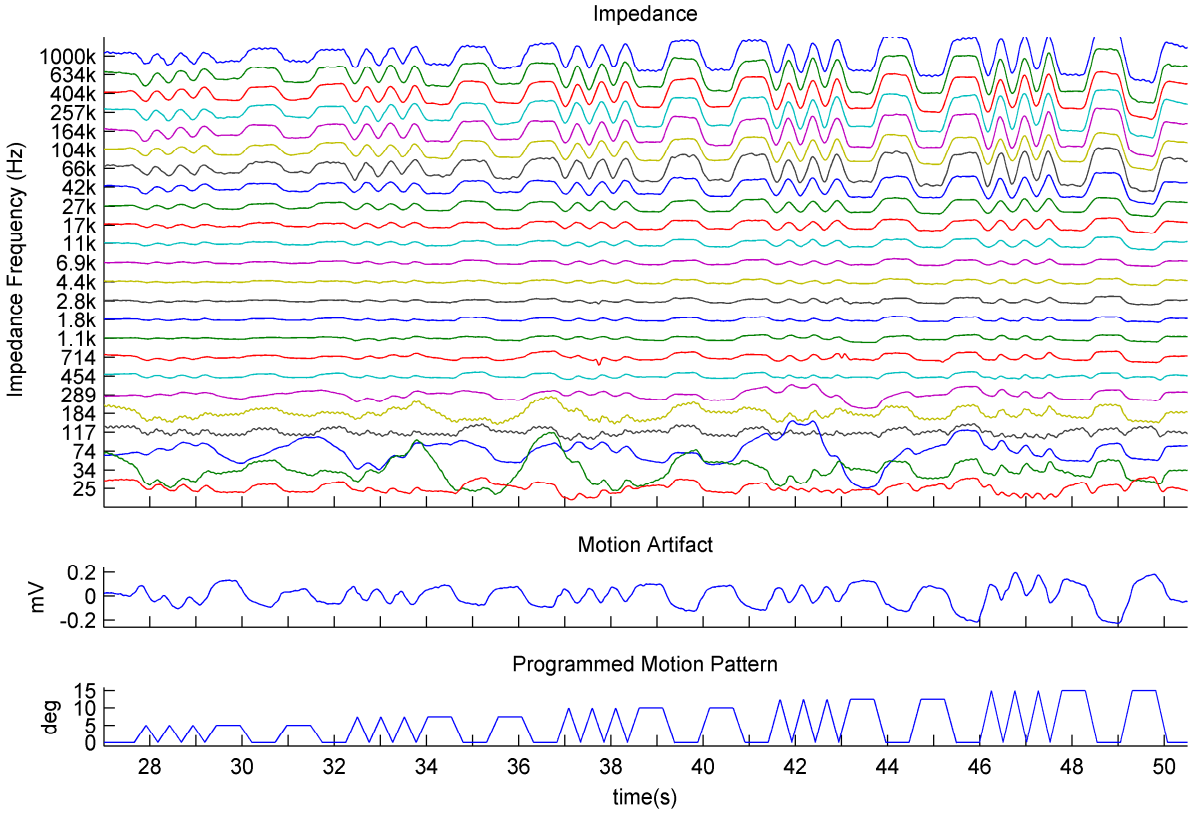

Figure 28. The effect of impedance current frequency on the percentage impedance change caused by electrode movement. The impedance change is presented in percentage relative to the baseline impedance amplitude. The separation between consecutive current frequencies represents a 1% change. Image modified from the original first published in Paper 3.

The linear relationship between skin-electrode impedance and motion artifact is lower than the relationship between skin-electrode interface impedance and the electrode motion pattern. In the same light, the relationship between the electrode motion pattern and motion artifact is also lower than the relationship between motion artifact and impedance.

4.4. Impedance and Motion Artifact

In Figures 24, 25 and 28, it can be observed that motion artifact, while clearly related, differs slightly from the impedance changes and the motion pattern. This difference can also be observed in the correlation analysis which analyzes how linearly related two signals are.

This does not mean that there is no relationship; only that the relationship is not linear. There is a clear, visually-detectable relationship between the applied motion and motion artifact and between the skin-electrode impedance and motion artifact. A similar relationship can be seen from the frequency analysis of these signals and the pattern, where the main frequency components of the pattern and the impedance change can be detected in the frequency domain representation of motion artifact.

4.5. Motion Magnitude and Speed and Skin-electrode Interface Impedance

Electrode motion magnitude and speed also affect the impedance change, and this effect is different for different tissue properties under the skin at the electrode location. When the tissue under the electrode was thin, as in the distal forearm electrode location close to the wrist, increasing the electrode motion magnitude increased the skin-electrode impedance change. Unlike motion artifact, this change appeared to increase in proportion to the increase in the motion magnitude. On the other hand, when the tissue under the electrode was thicker, as in the proximal forearm electrode location, increasing the electrode motion magnitude tended to increase the skin-electrode interface impedance change, but this increase was not consistent. Figure 29 presents these findings using the data obtained for Paper 4. Each boxplot is drawn for the data from an electrode at a given location for all subjects. The electrodes are presented from left to right while the top boxplot represents a given electrode at the distal location and the lower boxplot represents the same electrode at the proximal location. The x-axis data columns represent the rotation magnitudes.

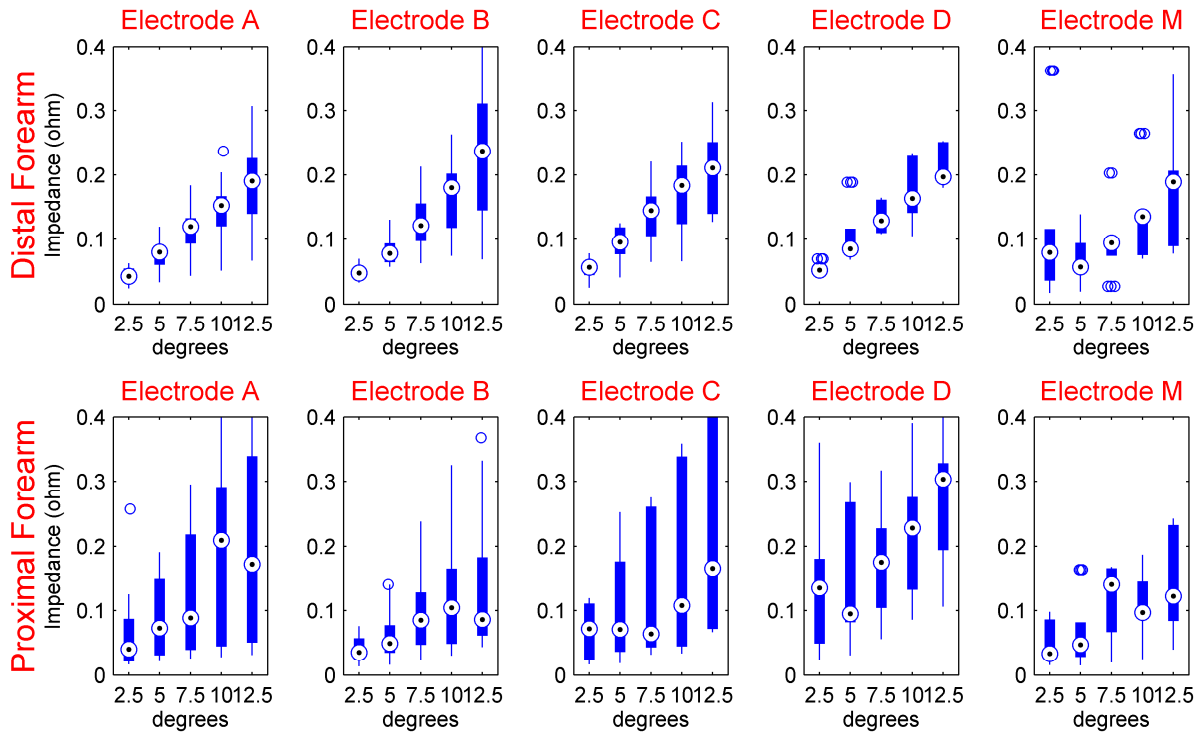

Figure 29. Effect of movement magnitude on the RMS value of the change in the skin-electrode interface impedance. Each row in the boxplots corresponds to a specific movement magnitude at the same speed. The applied force to the electrode is equivalent to 500 gr (4.90 N).

Not published in Paper 4 but reanalyzed from the data, the impedance change shows the tendency to decrease with increasing electrode movement speed, but as was seen in the relationship between impedance and motion magnitude, this trend is not consistent. Figure 30 present this behavior and the x-axis columns inside the boxplots represent servo rotational speeds.

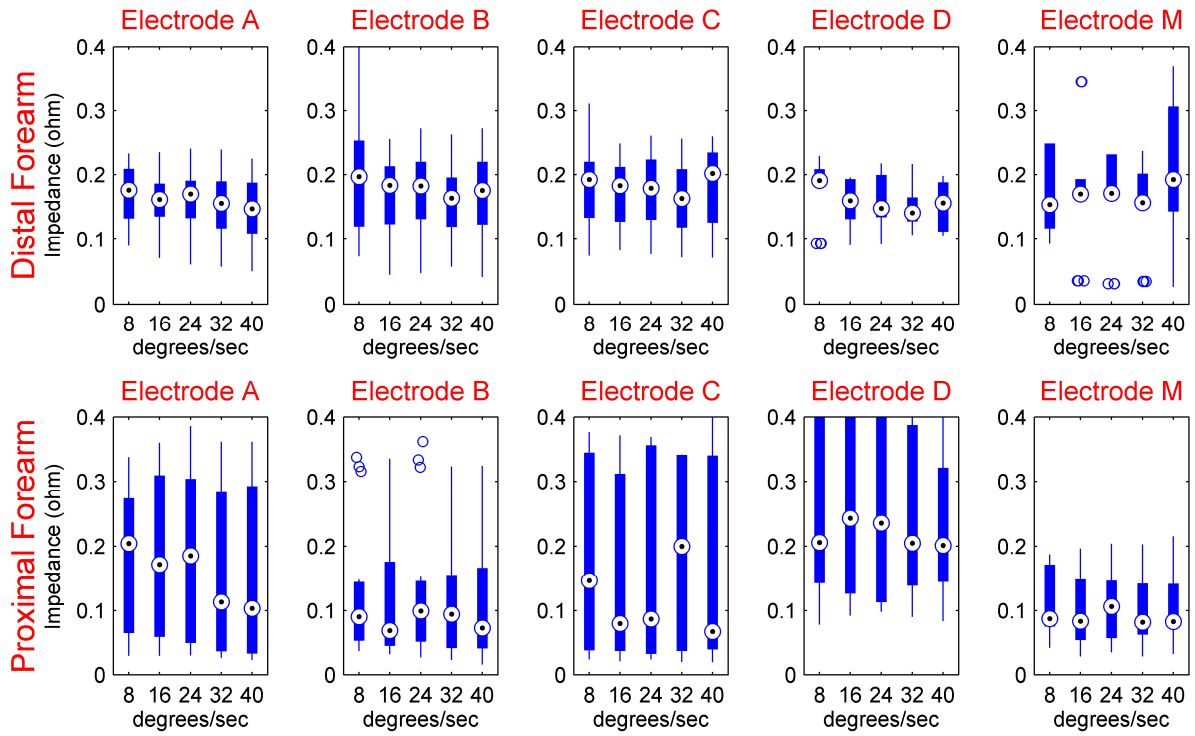

Figure 30. Effect of movement speed on the RMS value of the change in the skin-electrode interface impedance. Each row in the boxplots corresponds to a specific movement speed at relatively steady magnitude. The magnitude of the movement at the presented speeds stays within 5% of the median movement magnitude. The applied force to the electrode is equivalent to 500 gr.

4.6. Effect of Applied Force and Location Effect on Motion Artifact

In the studies done for Paper 2 and Paper 4, the mechanically applied force was seen to have an effect on the creation of motion artifact. Figure 31 presents these findings using data from Paper 4. Each electrode is presented in one row of boxplots. The two left columns present data from the distal forearm location and the two right columns present data from the proximal forearm location. Starting from a light pressing force equivalent to 250 grams (2.45 N) to higher pressing forces, the reduction in motion artifact can be observed. The trend continues up to 1000 grams (9.80 N), after which motion artifact might increase slightly. Here, it is important to note that in the presented graph the forces applied to Electrodes C and D create pressures under the electrodes that are four times higher than the pressures created under Electrodes A and B for the same applied force. This difference arises because pressure under an area is the force applied to that area divided by the area, so for the same applied force the smaller electrodes exert more pressure on the skin. For this reason, Figure 32 shows the selected results that can be compared by the pressure the electrodes exert on the skin, and the difference in electrode structure in the generation of motion artifact can be observed. How this is observed in the time domain signals of motion artifact and the skin-electrode interface impedance is presented in Figure 35.

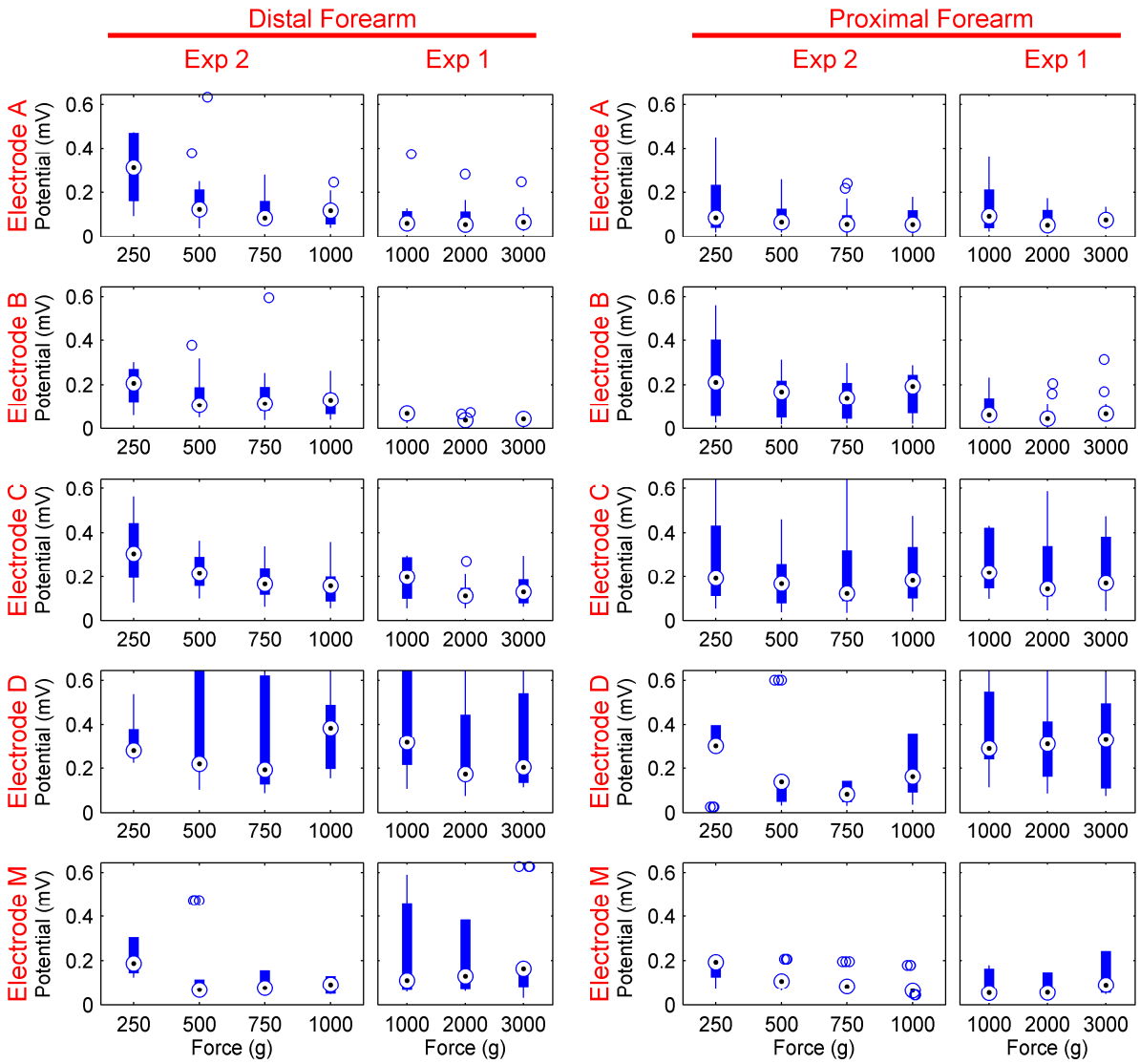

Figure 31. The effect of force on the motion artifact, compared for both locations. This figure serves to present the effect of force applied to the electrodes on the RMS of the motion artifact, and the effect of location on the RMS of the motion artifact.

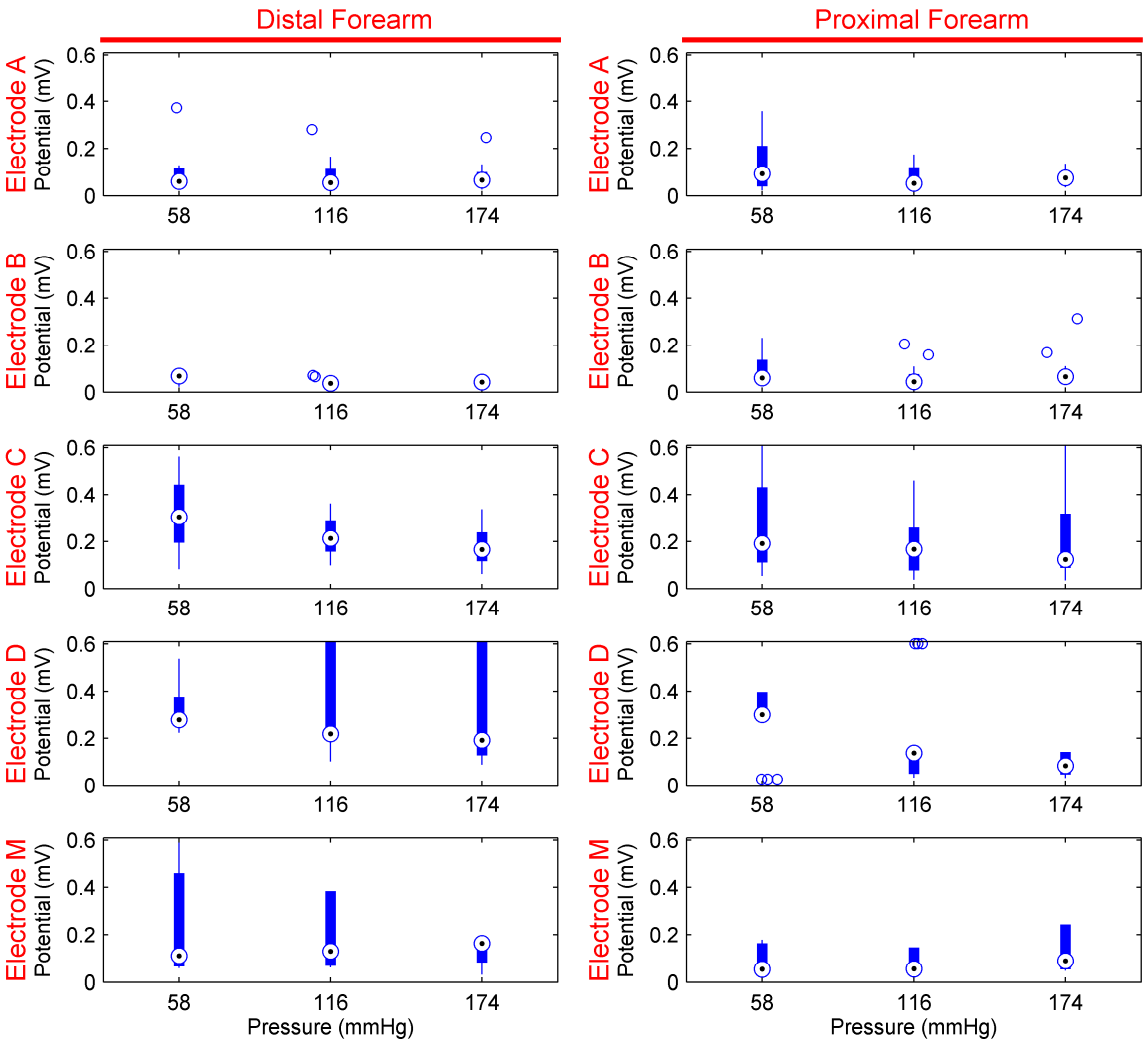

Figure 32. The effect of pressure on motion artifact RMS value for different electrodes compared. The data is presented for 58, 116, and 174 mmHg (7.73, 15.47, and 23.20 kPa) pressure under the electrode, which is the equivalent of 1000, 2000, and 3000 grams (9.80, 19.61 and 29.42 N) of mounting force for the large electrodes (Electrode A, Electrode B and Electrode M), and is the equivalent of 250, 500, and 750 grams (2.45, 4.90, and 7.35 N) of mounting force for the small electrodes (Electrode C and D). As a reference, atmospheric pressure at sea level is 750 mmHg (99.99 kPa) and in water at the depth of about 1 meter, the increase in pressure is 75 mmHg (10.00 kPa).

Electrode location determines the properties of the tissue beneath the electrode location and the closeness to muscles which generate EMG when active. In the mechanically applied motion experiments presented in this thesis, the muscles around the electrode location were relaxed, and thus the EMG is not a large contributor in the presented results. The difference between the two left columns and the two right columns in Figure 31 can be attributed to the differing tissue under the two electrode locations. The two large paddings function well in both locations, while there are differences in the effect of applied force at these locations. The failure of the hard support structure of Electrode D to

adapt the electrode shape to the underlying anatomy in the case of thin tissue between the electrode and the rigid anatomical structures can also be seen in Figures 31 and 32.

4.7. Garment Pressure Effect

When the electrode was tested integrated into a garment for Paper 1, changing the garment pressure resulted in the change of some parameters, while seemingly not affecting others. While the R-Peak detection algorithm is seen to improve in performance with increasing garment tightness up to 25 mmHg, performance is seen to worsen at 25 mmHg. As the garment pressure was measured on a location separate from the electrode location and the paddings used had different heights and elastic properties, the exact force exerted by the garment on the electrode and the exact pressure under the electrode cannot be known. Nevertheless, the force exerted by the garment to the skin on an area the size of the paddings was approximately 400 grams equivalent of force, or 3.9 N, at 25 mmHg garment tightness.

This effect is not seen in the skin-electrode interface baseline impedance that decreases with increasing pressure. Out of the measured parameters, Figure 33 shows these results

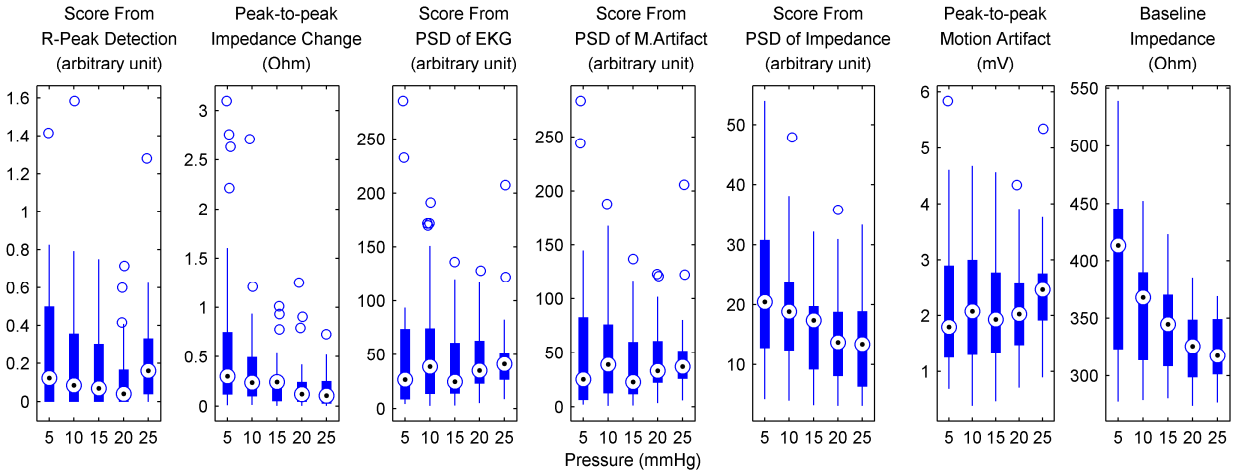

Figure 33. Changes in various parameters with the increase of garment tightness. For the scores from R-Peak detection, a smaller score is better. Peak-to-peak changes in impedance are presented. Scores from the PSDs of EKG, motion artifact, and impedance change are calculated as the energies of these signals in the frequency band 1 -7 Hz. Peak-to-peak motion artifact is presented as well as the baseline values of the impedance. The image is modified from the original published in Paper 1.

4.8. Padding Use in Wearable Garments

The use of padding between garment and electrode shows that the padding helps to reduce motion artifact. In the studied paddings of Paper 1, all paddings showed this result, but no definite conclusion between padding material or dimensions could be made with regard to their effectiveness. However,

considering that there is a difference in their effectiveness, padding material and design can be said to be important factors to consider. In general, the paddings were made of soft material and were between 6 and 16 mm in height with radii between 16 and 19 mm. These results from Paper 1 are presented in Figure 34

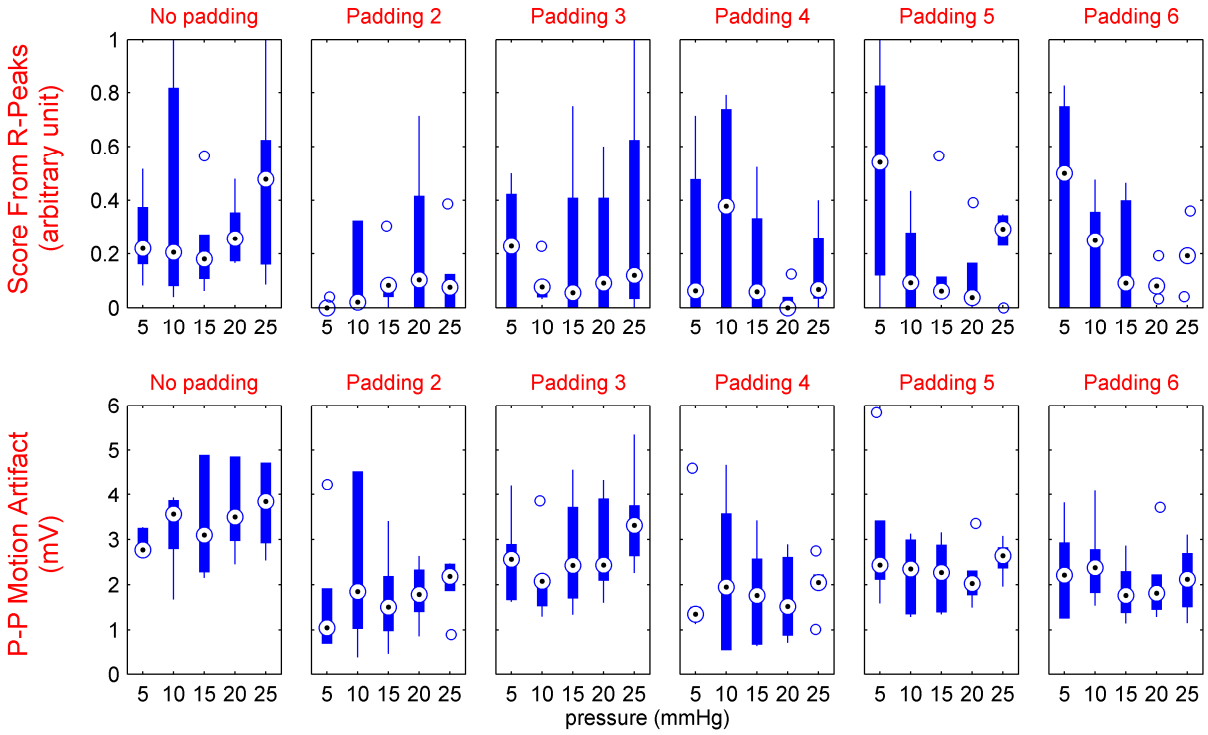

Figure 34. Effect of padding use between garment and electrode. Score from R-peaks is based on the detection error rate, and the lower the better. The second row presents the median peak-to-peak values of the motion artifact. It can be seen that while paddings differ in their effect of improving the detection rate, overall they behave in a similar way when compared to when no padding is used. The padding numbering follows Paper 2 annotation, where the “no padding” case was “Padding 1”.

4.9. The Padding Design Effect with Regard to Motion Artifact

When tested with mechanically induced motion in Paper 4, different padding structures showed differences in the susceptibility of the electrode to motion artifact. Electrodes A and B, with a larger padding area and the latter with the novel design, showed the best results for textile electrodes and were comparable to the medical electrodes. The performance of electrodes C and D depended largely on location, and overall fared worse than electrodes A and B. The visual representation of this behavior is shown in Figure 35 where a 51-second data window from Paper 4 data of the time domain signals for each electrode at different forces is presented. Further examples of the effect of structure design can be seen in Figures 26, 27, 29, and 30, where the structure-dependent differences can be observed in relation to the effect of motion speed and magnitude on motion artifact and skin-electrode interface

impedance. Further representations of how these electrodes behaved can be seen in Figures 31 and 32.

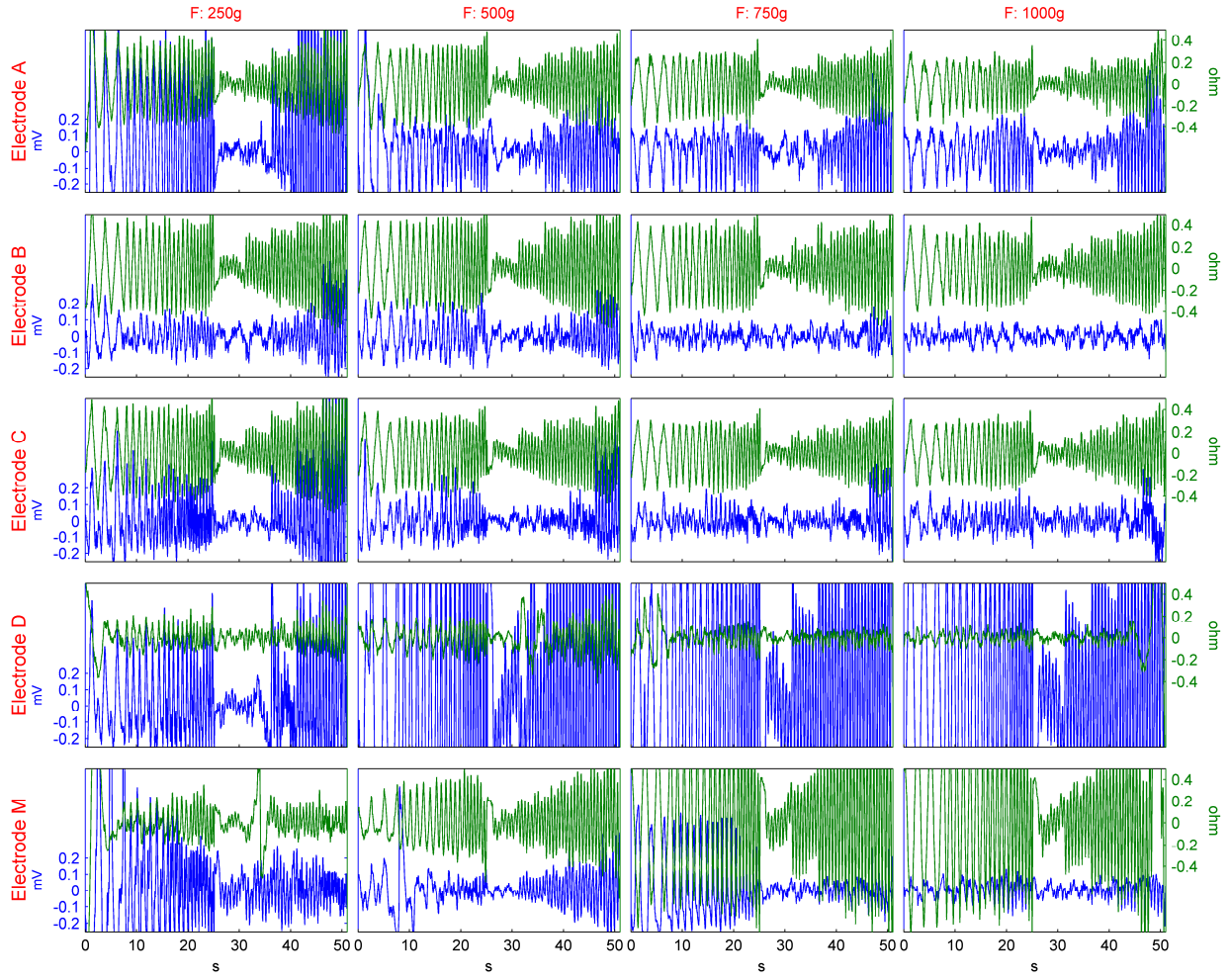

Figure 35. The filtered data obtained from the different electrodes under different applied forces. The data is filtered between 0.2 and 10 Hz. Motion artifact is depicted in blue, skin-electrode interface impedance is depicted in green. Image was originally published in Paper 4.

To summarize, the structural design of the electrode changes the susceptibility of the electrode to motion artifact and also the sensitivity of the electrode to applied motion for changes in the location and applied force.

5. Discussions

In this thesis, the motion artifact of un-gelled electrodes intended for wearable biosignal monitoring has been investigated. For the reliable and repeatable generation of motion under controlled mounting conditions, a user-based motion system was used, and also a Motion Artifact Generation and Assessment System was designed and built. Using this system, motion artifact was studied with mechanically generated motion together with subject-generated motion by measuring motion artifact from electrodes secured onto the upper arm with elastic bands. Using these systems, various aspects that affect either motion artifact or the measurements were assessed. The effect of using padding between clothing and skin was investigated and this research was expanded into a study of the effect of different padding structures. The influence of force applied to the electrode was studied both on subject-generated motion and on mechanically-generated motion by measuring the force or pressure applied to the electrode. The effect of the properties of the tissue underneath the electrode was investigated by the mechanical generation of motion on two different forearm locations each with vastly different tissue underneath the electrode. The impact of body composition on motion artifact was also studied by having subjects with differing BMIs. To answer the concerns about which impedance measurement frequencies are best suited for motion artifact studies, impedance spectroscopy was measured from an electrode subject to motion and the skin-electrode impedance most related to electrode motion and motion artifact was determined. In all the studies, the data was visually, qualitatively, and quantitatively analyzed both in time and frequency domain.

The three main questions regarding the design of motion artifact studies for un-gelled electrodes are as follows: what signals and parameters should be measured, how should the electrode be mounted on the skin, and how should the motion artifact be generated. The obvious answer to the first question is the surface potential change at the moving electrode, which is by definition motion artifact. To this measurement, an ECG channel was added to have a well-known signal as a reference for assessing how disruptive motion artifact is in shape, magnitude, and frequency. Additionally, the skin-electrode impedance, which has been found to be correlated in different degrees to electrode motion and motion artifact (Albulbul and Chan, 2012; Beckmann et al., 2010; Buxi et al., 2012; Hamilton et al., 2000; Laferriere et al., 2011; Luprano et al., 2013; Ödman, 1981; Ödman and Öberg, 1982; Jorg Ottenbacher et al., 2008; Romero et al., 2012, 2011; Talhouet and Webster, 1996), was measured. We used two electrode-mounting methods. One electrode-mounting method used elastic bands, tightened around the arm, to keep the electrode in place. This simulated the use of tight clothing, a common method in electrode attachment for wearable systems, and the tightness of the band was monitored as the pressure exerted by the band to the skin. The other method used the introduced Motion Artifact Generation and Assessment System as a mechanical mounting platform with integrated sensors for applied force monitoring. With the first mounting method, the motion was generated by the subject flexing and extending the lower arm, causing anatomical changes in the upper arm, and thus motion

artifact. For the mechanical mounting method, motion artifact was created by the Motion Artifact Generation module by applying programmable and repeatable motion to the electrode.

5.1. Motion Artifact Generation and Assessment System

In the studies leading up to Paper 1, it was observed that the subject movement in the form of elbow flexion was made repeatable over many repetitions by the careful attention of the subjects to their movement and by guiding the movement with a metronome. Nevertheless, there were still issues with the repeatability of the individual movements. Furthermore, the motion of the electrode or in this case also the changes to the garment were not clearly known except for the main movement frequency, and therefore could not be used in the analysis of motion artifact or skin-electrode impedance. To overcome the shortcomings in on-subject testing, a new method for creating repeatable and known, and thus usable in analysis, motion of the electrode was found to be necessary.

The motion artifact generation and assessment tool designed for the testing of the electrode motion artifact's response to the forces applied to it functioned as intended by mechanically generating the motion artifact. The motion of the electrode can be programmed and is repeatable with different subjects and experiments. Because the exact motion is known, it is possible to quantitatively, qualitatively, and pattern-wise compare the movement of the electrode and the resulting surface potentials of the changes in skin-electrode interface impedance. The rotation used is the angular change following a simple triangular pattern but, depending on the needs of the experiment and the movement parameters to be tested, this movement pattern can be controlled. The mounting force can be measured accurately. As a result, different mounting forces can be tested and the resulting knowledge can be translated into garment tightness parameters.

As the system is a prototype (the presented system is the second generation, a big step forward from the first prototype), there are of course drawbacks in system design and a variety of improvements can be made to improve system use and reliability. As presented, the lowering of the servo-electrode platform is done manually. This can be motorized using step motors controlled by the microcontroller, making use of the feedback from the force sensor. Currently, the force is measured as initial mounting force and the vertical force changes that occur during electrode motion due to skin stretch causing vertical dimension changes in the skin, and the non-uniform nature of human anatomy is not monitored. Changes to the software and triggering setups could allow the use of the changes in force as synchronized to either the movement pattern or the measured biosignals, making non-tedious analysis possible. The rotational movement of the servo is not translated into linear x or y movement of the electrode. Instead, the rotational movement of the servo causes circular movement of the electrode. Within the practical ranges of electrode movement, meaning movement magnitudes that do not cause electrode slippage, these movements are relatively close to being linear in the x dimension and almost negligible in the y dimension. A custom-made servo arm design or the use of a linear actuator instead of a servo could make the movement of the electrode as similar as possible to the programmed actuator movement.

Hokajarvi also used a servo-motor to move the gelled electrode and generate motion artifact on the skin of a subject. The resulting artifact noise was used to assess the effect of electrode skin impedance on motion artifact. As Hokajarvi reports only the use of a servo in a back-and-forth rotation pattern, no more is known about the system setup, except that electrode-mounting force is not measured (Hokajärvi, 2012). Ödman and Öberg created electrode movement by translating the rotational movement of a stepper movement into lateral electrode movement with mechanical junction elements. They measured gelled electrodes on skin dummies and actual skin and found that the main cause of motion artifact are the changes in skin potentials (Ödman and Öberg, 1982). They investigated various electrode movement speeds and found that for lateral movement, motion artifact reduced with increasing speed up to the last speed they investigated, and then increased slightly. For vertical movement, the increase of speed consistently reduced the resulting potential changes. Even though this study was done three decades ago, without monitoring the mounting force, the results they present about using a camera and stroboscope are promising and warrant further visual research into skin deformation with high-quality and high-speed cameras aided by digital image processing techniques for the automated analysis of skin deformation. Liu et al. presented a system that generated rotational movement of a dry electrode on a skin model and actual skin, which measured the pressure exerted to the electrode at the same time. The pressure adjustment in this system is manual and they reported that controlling the pressure of the electrode on the skin was difficult. However, they report that pressure and movement distance correlated with the generated motion artifact magnitude. In their results, it is also shown that motion speed has no effect on motion artifact magnitude (Liu et al., 2013)

Our results show that by using a system that mechanically generates electrode motion, motion artifact can be studied in direct relation to the known electrode motion. This enables the detailed investigation of the effect of electrode structure in translating applied motion to the motion artifact. An electrode that is improved in this way will also have improved resilience to motion artifact when integrated into a garment worn on a subject when the movement cannot be fully known. On the other hand, this device does not remove the need for on-garment testing, as the garment's resilience to motion artifact needs to be tested together with the electrodes. The way this device can help is that it can aid in the determination of the optimal parameters that can be used to guide garment design such as the pressure to be exerted on the electrode, the acceptable ranges of this pressure as garment tightness changes during motion, the tolerance ranges for motion applied to the electrode, and electrode location.

5.2. Impedance Spectroscopy

In the studies leading up to Papers 1 and 2 and in the background research, it was not clear what was the best impedance frequency to use for motion artifact studies, and this question was not researched extensively. Earlier studies show that a relationship between skin-electrode impedance and motion artifact existed, yet a causal relationship could not be drawn (Ödman, 1981; Ödman and Öberg, 1982), first for a 200 Hz sinusoidal impedance measurement then for a 2 kHz sine wave. Later on, Ottenbacher came to the same conclusion that the relationship exists but it is not causal. Using a 400 Hz sine wave, Ottenbacher successfully used impedance change to detect the existence of motion artifact (Jorg

Ottenbacher et al., 2008). On the other hand, using a 13 Hz impedance current, Talhouet and Webster stated that the skin-electrode impedance change was partly caused by motion artifact (Talhouet and Webster, 1996). One study that looked at multiple frequency was done by Hamilton et al. in which they non-simultaneously measured the impedance at seven frequencies between 120 Hz and 1.8 KHz, and found that the impedance at 120 Hz functioned best as an adaptive filter input because, compared with higher frequency currents, less current was needed at this frequency to induce a specific level of change in the impedance (Hamilton et al., 2000). Among impedance current frequencies successfully used for the adaptive filtering of motion artifact were 2 kHz square wave (Romero et al., 2011) and 2.2 kHz sine wave (Buxi et al., 2012).

In Paper 3 of this thesis, a study that simultaneously investigates the changes of the skin-electrode interface impedance at multiple current frequencies caused by electrode motion, and in relation to motion artifact, is presented for the first time. The simultaneous measurement of eight impedance frequencies in three non-simultaneous but overlapping groupings providing a 24-point spectrograph that allows us to investigate the effect a selected impedance frequency has on the relationship identified by the studies. This study was done for impedance frequencies between 25 Hz and 1 MHz. Using three groups of eight frequencies is not as ideal as using 24 frequencies simultaneously in one experiment, but the overlapping selection of the frequency groups allowed impedance frequencies to be measured from the low end to the high end of the measurement spectrum for each group.

Impedance currents between 17 kHz and 1 MHz showed the best relationship to the applied motion, both in signal shape and contained frequency components. The time domain correlations between applied motion pattern and the skin-electrode interface impedance in this frequency range were higher than 0.8. The correlations of the frequency domain representations between the motion pattern and the skin-electrode impedance were higher than 0.9 in this frequency range.

On the other hand, the relationship between skin electrode and impedance and motion artifact was lower for all frequencies, and the correlations varied largely between subjects. The reason for this is partly that motion artifact is nonlinearly related to the impedance and, by proxy, applied motion. This non-linearity might also be affected by the anatomy and skin properties of the subject. Even with the lower time domain relationship, the main frequencies contained in the motion artifact were overlapping with the frequencies in the impedance change, yet a clear correlation could not be drawn, even if the correlation tended to be higher in the higher frequencies.

This study shows that, contrary to the commonly held belief that impedance should be measured at the frequencies of the biosignal of interest, the use of lower frequencies has no apparent advantage over the use of these higher frequencies when using impedance to investigate motion artifact.

5.3. Skin-electrode Interface Impedance in Relation to Electrode Motion and Motion Artifact.

The skin-electrode impedance measured during electrode motion shows that the impedance change is very closely related to the applied motion in shape, and thus also in the frequency domain. For this reason, impedance could be used to predict the pattern of the electrode motion and the frequency components of the electrode motion. As previous studies show, the impedance seems to be more linearly related to electrode motion than it is to motion artifact (Ödman, 1981; Ödman and Öberg, 1982). On the other hand as also shown in Papers 2, 3, and 4, motion artifact is not as linearly related to the applied motion as impedance is. For this reason, impedance is not very suitable for predicting either the exact shape or the amplitude of motion artifact. Nevertheless, the main frequency components of the impedance change can be used to predict the main frequency components of motion artifact. Thus, impedance change can be an excellent input parameter for the detection of the presence of motion artifact or as the input for an adaptive filter for the reduction of motion artifact, supporting previous findings (Hamilton et al., 2000; Kearney et al., 2007; Laferriere et al., 2011; Luprano et al., 2013; Jorg Ottenbacher et al., 2008; J. Ottenbacher et al., 2008; Romero et al., 2012, 2011).

5.4. Pressure

The investigation into the forces applied to the electrode revealed that electrode function improves up to a point after the electrode is pressed with adequate force to secure and prevent sliding on the skin. After a specific force level is reached, the electrode becomes uncomfortable on the skin, becoming less user-friendly, while the signal quality also deteriorates in the form of an increasing motion artifact. The electrode pressure range providing both good signal quality, lowered motion artifact, and user comfort was found to be between 15 and 20 mmHg (1.99 and 2.66 kPa) for pressure under garments in Paper 1, and between approximately 5 -10 N force exerted on an electrode with an area of close to 20 cm^2 in Paper 2, which is between approximately 18 and 36 mmHg (2.40 and 4.80 kPa) pressure under the electrode. Similar results were obtained in studies leading to Paper 4, with electrodes of different sizes for forces of between 5 N and 10 N, presented in Figure 31. Thus, it needs to be noted that these magnitudes largely depend on the padding design and a padding design that functions well with less applied force will therefore improve system comfort. In addition to these quantitative descriptions, an easier to understand and use measure can be given as follows: garment needs to be tight, but not too tight.

Kim et al. make a similar observation. They report that increasing the pressure from 0.3 kPa to 6 kPa (2.3 mmHg to 45 mmHg) increases the SNR, but in the graphs they report a lowering of the SNR can also be observed at the highest pressure (Kim et al., 2008). Pengjun reported that pressure measured under the electrode showed good correlation with motion artifact (Pengjun et al., 2011). Increasing the force lowered impedance in the research of Albulbul and Chan (Albulbul and Chan, 2012). In an earlier study done with forces up to 13.7 N, Ödman reported that the skin potentials generated when electrodes

were pressed onto the skin were higher for higher pressing forces (Ödman, 1989). More recently, similar results have been reported by Vos (Vos et al., 2003)

The studies of this thesis added to the findings of previous researchers show that while the applied force affects motion artifact, there might be a motion artifact "sweet spot" between the force range that is necessary to secure the electrode and the force range that does not exceed comfort levels. In this range, the changes in vertically acting forces might not be too important, possibly due to the epidermis already being compressed to a large extent by the force necessary to secure the electrode. These levels might depend on subject, electrode location, garment design, and electrode structure. Thus, electrode and garment-specific investigation might be necessary for accurate assessment.

It is important to note that while garment design affects the pattern of the change of the force acting on the electrode in the presence of movement, this might be less important than the lateral forces exerted on the electrode by the garment. This finding further increases the importance of garment design.

5.5. Electrode Location

An important part of garment design is the electrode location selection. The main criteria for this are of course the biosignals to be measured. If ECG is to be measured, measuring it from two electrodes located on the same forearm makes as much sense as measuring the EMG of the leg muscles from the shoulders. Once the suitable electrode locations are known, a more accurate placement of the electrode may need to be developed to minimize motion artifact. The approach taken by most of the studies is that priority is given to the requirements of the biosignals in question, and a detailed analysis of the effect of electrode location on motion artifact is not made.

In the research of Paper 2 and Paper 4, it was revealed that location of the electrode is an important factor in motion artifact reduction, the functioning of different structures of electrodes, and the effect and comfort of various mounting forces. Motion artifact was found to be lower at locations with more soft tissue underneath the skin than at electrode locations with less tissue between the skin and the harder anatomical structures such as bone and tendons. At the time of writing this thesis, the author knew of no comparable research. The referenced research either selected only one location or did not report on the differences in locations.

Therefore, especially in electrode locations with only a thin layer of soft tissue between the skin and the harder tissue, electrode placement becomes a crucial factor. Small location changes of even a few millimeters can change the severity of motion artifact because of the closeness of more rigid tissue to the skin and the lack of soft tissue such as fat and muscle that would provide a buffer area between these rigid structures and the skin.

The results of Paper 2 and 4 also indicate the importance of using some kind of soft, flexible padding when the harder and more rigid tissue at the electrode location is close to the skin.

5.6. Subject-to-subject Variability

A similar effect to location selection could be seen in the inter-subject differences in motion artifact, where the differences in skin thickness, softness, and elasticity, and the different properties under the tissue affected the results. For Paper 3 for the two subjects with higher BMI than other subjects, a larger ECG component was detected between the electrodes on the forearm and wrist, which points to a difference in overall volume conductor effects as well. These observations show that it might be necessary to consider the target population, especially when designing electrodes with a medical grade signal-to-noise ratio and very low susceptibility to motion artifact. In the studies of this thesis, the subject effect was not studied. Therefore, conclusions cannot be drawn except that the differences were present and clear. The subject effect was not studied in any detail in any of the other studies in the context of motion artifact either. If wearable systems are to be designed for use across a population of varying body shapes and compositions, further research is required in this area.

5.7. Use of Padding in Garments

During the initial stages of the study, it became clear that the use of padding between the garment and the electrode in contact with skin had a beneficial effect. This finding is in line with other studies that have reported promising results for electrode designs that use textile or other conductive material to create a three-dimensional cushion layer between the electrode and the clothing (Buxi et al., 2012; Chan and Lemaire, 2010; Cho et al., 2009; Garcia et al., 2007; Gruetzmann et al., 2007; Laferriere et al., 2011; Lin et al., 2011; Löfhede et al., 2012; Muhlsteff et al., 2004; Muhlsteff and Such, 2004; Pandian et al., 2008; Pylatiuk et al., 2009; Seoane et al., 2014, 2013; Tseng et al., 2013). In Paper 1, for an electrode integrated into a monitoring garment and tested on the subject with subject-generated motion, padding was seen to improve the resilience of the electrode to motion artifact. In Papers 2 and 4, the same effect was seen for electrodes mechanically mounted on the skin with mechanically-generated motion applied to them, without the mechanical behavior of the garment interfering with the translation of the applied motion into electrode motion. There may be a number of reasons for the reduction in motion artifact with the use of padding. One is that the soft padding acts as a suspension between the garment and the electrode, absorbing many of the changes in the vertical forces acting upon the electrode caused by the movement of the garment and anatomical expansion due to muscle activity. A similar task undertaken by the padding is to act as a buffer in lateral movement applied to the electrode in which the padding stretches, bends, and twists and, in this way, absorbs some of the lateral forces. Padding might help the dry electrode to better adapt to the shape of the underlying anatomy, and thereby increase contact quality. Last but not least, by causing a bump between the garment and the electrode, padding increases the pressure exerted by the garment to the electrode to levels higher than the general garment pressure. These ideas are summarized in Figure 36. The effect seen in Figure 36 (c) is especially important for electrode locations such as under or above the clavicle or between the left and right scapula, where a tight garment will still have low contact pressure or even loss of contact due to body anatomy. A padding used for this location must enable the transfer of clothing pressure onto the electrode, instead of the electrode being loose on the skin or even not in contact with the skin.

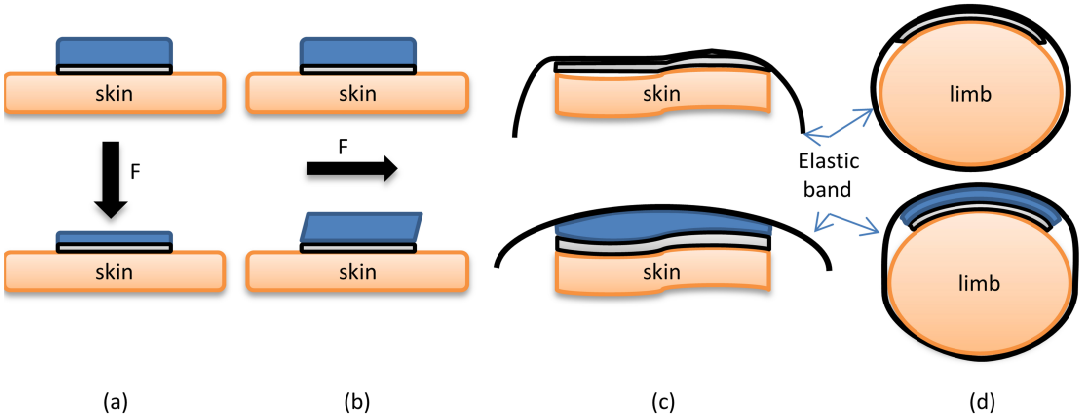

Figure 36. Proposed functionality of padding. (a) The padding compresses upon the application of vertical force and buffers the vertical force the electrode exerts on the skin. (b) The padding adapts to the lateral forces, reducing the lateral movement of the electrode in response to applied force. (c) An elastic band holding the skin in place might not be sufficient for the electrode to be fully in contact with skin due to anatomical structures beneath the skin. The padding will conform to the shape of the structures as well as the elastic band and allow the electrode to be fully in contact. (d) The use of padding might increase the contact pressure under the electrode without necessitating increased garment pressure.

In general, the use of padding between garment and electrode is advised to reduce motion artifact and to improve garment comfort by reducing the necessary garment tightness needed for adequate skin-electrode contact pressure.

5.8. Effect of the Advanced Padding Design

In the research for the Paper 1, the differences between padding structure and material were not clear because there were too many variables between paddings that changed. In the following research and during testing with different paddings, a hypothesis formed that padding structure might considerably affect the performance of the padding in two possible functions, as depicted in Figure 22. Two electrodes were designed for the testing of this hypothesis and presented in Paper 4. The first function is that an electrode support structure that is larger than the electrode area might move the boundaries of motion so that skin deformation is strongest away from the electrode surface and causes less epidermis deformation under the electrode. Also, because the material we used, Poron foam, does not slide on the skin, it might act in a similar way to conventional electrode sticky gel in the context of lateral motion while still being an un-gelled electrode. Another effect of this might be that some of the epidermis deformation is taken over by dermis deformation due to the larger electrode movement area. Electrode A, with the simple padding structure that is larger than the electrode area exemplifies this function in Figure 22.

The second function is also presented in Figure 22, where Electrode B has hollow padding and a silicone ring around its edges. Electrode B was designed to lock-in the epidermis under the electrode area, restrict epidermis deformation, and transfer most of the skin deformation to the dermis where deformation does not cause drastic electrical events or property changes.

The larger padding and the advance padding functioned much better than the smaller padding or the hard support structure, but the effect of the constricting design, Electrode B, compared with the same sized simple support structure, Electrode A, was not clear (Paper 4). This might have been due to Electrode A already being successful in restricting epidermis deformation by transferring a large portion of the deformation to the dermis without the need for a skin trapping ring. As a result, the additional effect of the constricting design was not observed. One disadvantage of Electrode B over Electrode A is that the former leaves a clear mark on the subject's skin and this might be an issue for a commercial product. A related idea has been implemented in a rubber-like electrode that has been designed with small bumps on the electrode (Orbital Research Inc., Cleveland, USA) and tested successfully (Buxi et al., 2012; Laferriere et al., 2011). These electrodes differ from the electrodes tested in this thesis in the way that they constrict the epidermis by acting on it directly at the area under the electrode and the design of the electrode surface that is not smooth. Electrode B aims to restrict the epidermis by acting on an area further away from conductive contact area and had a smooth surface.

Since only one padding material was tested for the electrode structure studies, it is unclear at this point how these designs would function with different materials with different viscoelastic properties, different skin friction properties, and other physical properties. A material that is too soft compresses too much under applied pressure and loses its elastic properties, and thus the motion dampening effect. A material that is too hard, on the other hand, will not provide a dampening effect from the applied forces. This points to the importance of material selection.

Overall, the hypothesis shows promise and further research and development could lead to an electrode that successfully reduces motion artifact by manipulating the skin's response to the movement that is applied to the electrode, is user friendly, and is suitable for long-term use.

As the background research showed, the electrical behavior of various skin layers such as the epidermis and the dermis in response to motion is fairly well understood. It is not clear, however, how the various skin layers respond to lateral and vertical forces and how this mechanical behavior relates to the electrical behavior of these layers. Further studies in this area will improve the understanding of how an electrode can mechanically affect the skin layers and reduce the electrical changes in the skin caused by electrode motion.

5.9. Garment Design

A well-designed garment will be more resilient against subject movement and anatomical changes due to activity, and will result in reduced amplitudes of the fluctuations in the forces it applies to the electrode. This garment design effect was shown by Cho et al., when they tested different arrangements

of tight band harnesses and found clear differences between the harness designs during subject motion (Cho et al., 2009).

Garment design and electrode design can be independently undertaken, with the improvement of each system component combining to produce a well-functioning system. This could even be in the form that the combined improvements are stronger than the improvements made to each component.

5.10. Benefits of Isolated Electrode Testing

The benefit of testing the function of the electrode with regard to the movement applied directly to the electrode is that it allows the assessment of the resilience of the electrode to motion artifact regardless of garment design. This would be the first level of investigation and improvement made to the electrode. This kind of study would translate itself into design recommendations for improving the motion artifact response of the whole garment. Indeed, the investigations carried out for this study show that electrode structures have different properties with regard to motion artifact and guidelines for electrode design can be drawn up that would improve the overall signal quality of wearable systems when the design guidelines are implemented.

By definition, motion artifact is created by electrode motion. That electrode motion can be generated by mechanical means and that this motion correlates well with the generated motion artifact was reported earlier by Ödman and Öberg (Ödman and Öberg, 1982). A few recent studies have successfully adopted this approach to generate motion artifact using motorized systems (Hokajärvi, 2012; Liu et al., 2013). Motion artifact generated by the mechanical vibration of the electrode can also be mentioned here (Searle and Kirkup, 2000). In these studies, the motion shape and frequency is known and this allows for the accurate study of motion artifact.

With the device presented in this thesis, for example, it was seen that motion magnitude has a larger effect than motion speed on motion artifact magnitude in that motion artifact increased in magnitude with increasing electrode motion distance, but not with electrode motion speed. Thus, if faster movement does not also mean larger movement, faster movement cannot be said to generally cause worse motion artifact. Yet, if the movement is in the frequencies of the biopotentials that are of interest, motion artifact in these frequencies will be more detrimental.

6. Conclusion

In this thesis, I introduce a Motion Artifact Generation and Assessment Device that I designed and built. The need for such a device arose when I noticed that the motion artifact generated by the experiment subject had repeatability and accuracy issues and that the motion could not be quantized for detailed analysis. The presented device is the second prototype that I improved, based on the lessons from the first prototype. With this device, the motion applied to the electrode is isolated from human effects, mechanically generating repeatable motion and the effects that garment design has on the motion. The ability to program motion makes it possible to study various scenarios, settings, and parameters. Knowing exactly the cause of motion makes the comparison of motion to the created signals more accurate. Being able to control the applied force makes it possible to test electrodes against various force levels and to investigate the optimal force ranges to be used for a given electrode. The device can also be used to investigate the design parameters of a garment that will house the electrodes. While a number of systems that mechanically generate the motion of the electrode have been introduced by other researchers, the device presented here is a lightweight and portable system and, to the best of my knowledge, this is the first time such a device has been used for the extensive research of motion artifact in relation to electrode type, location, applied force, movement range, and movement speed over multiple subjects.

I show that that the electrode-skin impedance at high frequencies is a reliable indicator of electrode motion, closely matches the pattern of the applied motion, and is suitable for the detection and prediction of electrode movement. In a similar light, I argue that the frequency components of the skin-electrode impedance are closely related to the frequency components of motion artifact. Thus, even though the linear relationship between these two signals is low, impedance can be used as an input to an adaptive filter for the reduction of motion artifact. Conventional thinking is that the impedance measurements at low frequencies, usually under a few hundred Hertz, are better for the study of motion artifact in physiological signals. I demonstrate that impedance at lower frequencies, under a few kilohertz, does not have an overall better correlation to motion artifact than impedance at higher frequencies. This leads to the conclusion that the higher impedance frequencies such as 100 kHz are suitable for motion artifact research.

From the research I have done with the electrodes that were attached to the subject by elastic bands, it is clear that padding between the garment and the electrode reduces motion artifact when compared with electrodes directly stitched, knitted, sewn, or embroidered on the garment. Furthermore, the design of the padding is an important factor in the reduction of motion artifact.

I propose the idea of mechanically restricting the deformation of the epidermis by electrode design and report promising results even if they are not conclusive. Leading up to this research and following it, I have proposed a hypothesis on how epidermis restriction might function mechanically, but the hypothesis needs to be further refined and revised to make it more accurate. A study to understand the

mechanical behavior of different skin layers under vertical or lateral load would help with this issue. Further development of the hypothesis could lead to the point where it would be possible to predict electrode susceptibility to motion artifact from the shape of the electrode. These findings might guide further research into creating motion-resistant electrodes that are easy and cheap to produce and could be widely used in different settings.

Related to garment design, I present the findings that motion artifact is dependent on the underlying tissue for the same amount of motion applied under the same pressure. These findings are also related to the findings that applied force affects motion artifact. Therefore, these two factors need to be considered when designing a garment intended for wearable monitoring of physiological signals.

This thesis presents one of the most comprehensive works on the motion artifact of un-gelled electrodes intended for wearable systems. I hope that the research questions answered in this thesis will further help researchers to advance this important area, and that the questions that have arisen in this thesis will be tackled in future research. Making wearable physiological monitoring systems more reliable in signal quality and more comfortable for long-term use will benefit many people and possibly open up new markets for wearable monitoring garments. This thesis lights the way in that it presents possible solutions to motion artifact and research methodology to tackle electrode design. The thesis presents a functioning Motion Artifact Generation and Assessment System, the importance of electrode mounting choices such as pressure and location, and the possibility of reducing motion artifact by using structural electrode design to physically minimize the deformation of upper layers of the skin.

References

Albulbul, A., Chan, A.D.C., 2012. Electrode-skin impedance changes due to an externally applied force, in: 2012 IEEE International Symposium on Medical Measurements and Applications Proceedings (MeMeA). Presented at the 2012 IEEE International Symposium on Medical Measurements and Applications Proceedings (MeMeA), IEEE, New York City, USA, Budapest, pp. 1–4. doi:10.1109/MeMeA.2012.6226628

Alive Bluetooth Heart & Activity Monitor — Alive Technologies [WWW Document], n.d. URL http://www.alivetec.com/alive-bluetooth-heart-activity-monitor/ (accessed 1.9.15).

Ananthi, S., 2006. A Textbook of Medical Instruments. New Age International Pvt Ltd Publishers, New Delhi.

Anatomy and Physiology by Kenneth S. Saladin | eBook on, n.d.

Anliker, U., Ward, J.A., Lukowicz, P., Tröster, G., Dolveck, F., Baer, M., Keita, F., Schenker, E.B., Catarsi, F., Coluccini, L., Belardinelli, A., Shklarski, D., Alon, M., Hirt, E., Schmid, R., Vuskovic, M., 2004. AMON: a wearable multiparameter medical monitoring and alert system. IEEE Trans. Inf. Technol. Biomed. Publ. IEEE Eng. Med. Biol. Soc. 8, 415–427.

Bailey, J.J., Berson, A.S., Garson, A., Horan, L.G., Macfarlane, P.W., Mortara, D.W., Zywietz, C., 1990. Recommendations for standardization and specifications in automated electrocardiography: bandwidth and digital signal processing. A report for health professionals by an ad hoc writing group of the Committee on Electrocardiography and Cardiac Electrophysiology of the Council on Clinical Cardiology, American Heart Association. Circulation 81, 730–739. doi:10.1161/01.CIR.81.2.730

Beckmann, L., Neuhaus, C., Medrano, G., Jungbecker, N., Walter, M., Gries, T., Leonhardt, S., 2010. Characterization of textile electrodes and conductors using standardized measurement setups. Physiol. Meas. 31, 233. doi:10.1088/0967-3334/31/2/009

BioHarness 3 - Wireless Professional Heart Rate Monitor & Physiological Monitor with Bluetooth - Zephyr Technology Corporation [WWW Document], n.d. URL http://zephyranywhere.com/products/bioharness-3/ (accessed 1.9.15).

Biometric shirts for performance improvement and sleep tracking [WWW Document], n.d. URL http://www.hexoskin.com/ (accessed 1.9.15).

Boyer, G., Zahouani, H., Le Bot, A., Laquieze, L., 2007. In vivo characterization of viscoelastic properties of human skin using dynamic micro-indentation, in: 29th Annual International Conference of the IEEE Engineering in Medicine and Biology Society, 2007. EMBS 2007. Presented at the 29th Annual International Conference of the IEEE Engineering in Medicine and Biology Society, 2007. EMBS 2007, pp. 4584–4587. doi:10.1109/IEMBS.2007.4353360

Bronzino, J.D., 1995. The biomedical engineering handbook. CRC Press.

Burbank, D.P., Webster, J.G., 1978. Reducing skin potential motion artefact by skin abrasion. Med. Biol. Eng. Comput. 16, 31–38. doi:10.1007/BF02442929

Buxi, D., Kim, S., van Helleputte, N., Altini, M., Wijsman, J., Yazicioglu, R.F., Penders, J., Van Hoof, C., 2012. Correlation Between Electrode-Tissue Impedance and Motion Artifact in Biopotential Recordings. IEEE Sens. J. 12, 3373–3383. doi:10.1109/JSEN.2012.2221163

Carr, J.J., Brown, J.M., 1993. Introduction to biomedical equipment technology. Prentice Hall Career & Technology.

Chan, A.D.C., Lemaire, E.D., 2010. Flexible dry electrode for recording surface electromyogram, in: 2010 IEEE Instrumentation and Measurement Technology Conference (I2MTC). Presented at the 2010

IEEE Instrumentation and Measurement Technology Conference (I2MTC), pp. 1234–1237. doi:10.1109/IMTC.2010.5488293

Chi, Y.M., Jung, T.-P., Cauwenberghs, G., 2010. Dry-Contact and Noncontact Biopotential Electrodes: Methodological Review. Biomed. Eng. IEEE Rev. In 3, 106 –119. doi:10.1109/RBME.2010.2084078

Cho, H.-S., Koo, S.-M., Lee, J., Cho, H., Kang, D.-H., Song, H.-Y., Lee, J.-W., Lee, K.-H., Lee, Y.-J., 2009. Heart Monitoring Garments Using Textile Electrodes for Healthcare Applications. J. Med. Syst. 35, 189–201. doi:10.1007/s10916-009-9356-8

Cömert, A., Honkala, M., Aydogan, B., Vehkaoja, A., Verho, J., Hyttinen, J., 2009. Comparison of Different Structures of Silver Yarn Electrodes for Mobile Monitoring, in: Sloten, J.V., Verdonck, P., Nyssen, M., Haueisen, J. (Eds.), 4th European Conference of the International Federation for Medical and Biological Engineering, IFMBE Proceedings. Springer Berlin Heidelberg, pp. 1204–1207.

Cömert, A., Honkala, M., Puurtinen, M., Perhonen, M., 2008. The Suitability of Silver Yarn Electrodes for Mobile EKG Monitoring, in: Katashev, A., Dekhtyar, Y., Spigulis, J. (Eds.), 14th Nordic-Baltic Conference on Biomedical Engineering and Medical Physics, IFMBE Proceedings. Springer Berlin Heidelberg, pp. 198–201.

Corusfit - Invest the health of your heart [WWW Document], n.d. URL http://www.corusfit.com/ (accessed 1.9.15).

Cuckler, G.A., Sisko, A.M., Keehan, S.P., Smith, S.D., Madison, A.J., Poisal, J.A., Wolfe, C.J., Lizonitz, J.M., Stone, D.A., 2013. National Health Expenditure Projections, 2012–22: Slow Growth Until Coverage Expands And Economy Improves. Health Aff. (Millwood) 10.1377/hlthaff.2013.0721. doi:10.1377/hlthaff.2013.0721

Delalleau, A., Josse, G., Lagarde, J.M., 2012. Dual-parameter optimisation of the elastic properties of skin. Comput. Methods Biomech. Biomed. Engin. 15, 83–92. doi:10.1080/10255842.2011.633904

Delalleau, A., Josse, G., Lagarde, J.-M., Zahouani, H., Bergheau, J.-M., 2006. Characterization of the mechanical properties of skin by inverse analysis combined with the indentation test. J. Biomech. 39, 1603–1610. doi:10.1016/j.jbiomech.2005.05.001

Di Rienzo, M., Rizzo, F., Meriggi, P., Bordoni, B., Brambilla, G., Ferratini, M., Castiglioni, P., 2006. Applications of a textile-based wearable system for vital signs monitoring. Conf. Proc. Annu. Int. Conf. IEEE Eng. Med. Biol. Soc. IEEE Eng. Med. Biol. Soc. Conf. 1, 2223–2226. doi:10.1109/IEMBS.2006.260173

Di Rienzo, M., Rizzo, F., Meriggi, P., Castiglioni, P., Mazzoleni, P., Ferrarin, M., Ferratini, M., 2007. MagIC: a Textile System for Vital Signs Monitoring. Advancement in Design and Embedded Intelligence for Daily Life Applications. pp. 3958 –3961. doi:10.1109/IEMBS.2007.4353200

Di Rienzo, M., Rizzo, F., Parati, G., Ferratini, M., Brambilla, G., Castiglioni, P., 2005. A textile-based wearable system for vital sign monitoring: applicability in cardiac patients. pp. 699 –701. doi:10.1109/CIC.2005.1588199

Edelberg, R., 1977. Relation of electrical properties of skin to structure and physiologic state. J. Invest. Dermatol. 69, 324–327.

Edelberg, R., 1973. Local electrical response of the skin to deformation. J. Appl. Physiol. 34, 334–340.

Edelberg, R., 1968. Biopotentials from the skin surface: the hydration effect. Ann. N. Y. Acad. Sci. 148, 252–262.

Eilebrecht, B., Willkomm, J., Pohl, A., Wartzek, T., Leonhardt, S., 2013. Impedance measurement system for determination of capacitive electrode coupling. IEEE Trans. Biomed. Circuits Syst. 7, 682–689. doi:10.1109/TBCAS.2013.2237905

Fratini, A., Cesarelli, M., Bifulco, P., Romano, M., 2009. Relevance of motion artifact in electromyography recordings during vibration treatment. J. Electromyogr. Kinesiol. Off. J. Int. Soc. Electrophysiol. Kinesiol. 19, 710–718. doi:10.1016/j.jelekin.2008.04.005

Gandhi, N., Khe, C., Chung, D., Chi, Y.M., Cauwenberghs, G., 2011. Properties of Dry and Non-contact Electrodes for Wearable Physiological Sensors, in: 2011 International Conference on Body Sensor Networks (BSN). Presented at the 2011 International Conference on Body Sensor Networks (BSN), pp. 107–112. doi:10.1109/BSN.2011.39

Garcia, G.A., Zaccone, F., Ruff, R., Micera, S., Hoffmann, K.-P., Dario, P., 2007. Characterization of a New Type of Dry Electrodes for Long-Term Recordings of Surface-Electromyogram, in: IEEE 10th International Conference on Rehabilitation Robotics, 2007. ICORR 2007. Presented at the IEEE 10th International Conference on Rehabilitation Robotics, 2007. ICORR 2007, pp. 849–853. doi:10.1109/ICORR.2007.4428523

Georgia Tech Wearable Motherboard [WWW Document], n.d. URL http://www.gtwm.gatech.edu/ (accessed 1.9.15).

Geselowitz, D.B., 1971. An Application of Electrocardiographic Lead Theory to Impedance Plethysmography. IEEE Trans. Biomed. Eng. BME-18, 38–41. doi:10.1109/TBME.1971.4502787

Gondran, C., Siebert, E., Yacoub, S., Novakov, E., 1996. Noise of surface bio-potential electrodes based on NASICON ceramic and Ag-AgCl. Med. Biol. Eng. Comput. 34, 460–466.

Griebel, S., Zentner, L., Böhm, V., Haueisen, J., 2009. Sensor placement with a telescoping compliant mechanism, in: Sloten, J.V., Verdonck, P., Nyssen, M., Haueisen, J. (Eds.), 4th European Conference of the International Federation for Medical and Biological Engineering, IFMBE Proceedings. Springer Berlin Heidelberg, pp. 1987–1989.

Grimnes, S., Martinsen, Ø.G., 2006. Bioimpedance, in: Wiley Encyclopedia of Biomedical Engineering. John Wiley & Sons, Inc.

Grimnes, S., Martinsen, Ø.G., 2000. Bioimpedance and Bioelectricity Basics. Academic Press.

Gruetzmann, A., Hansen, S., Müller, J., 2007. Novel dry electrodes for ECG monitoring. Physiol. Meas. 28, 1375. doi:10.1088/0967-3334/28/11/005

Hamilton, P.S., Curley, M.G., 1997. Adaptive Removal of Motion Artifact, in: Proceedings of the 19th Annual International Conference of the IEEE Engineering in Medicine and Biology Society, 1997. Presented at the Proceedings of the 19th Annual International Conference of the IEEE Engineering in Medicine and Biology Society, 1997, IEEE, New York City, USA, Chicago, IL,USA, pp. 297–299. doi:10.1109/IEMBS.1997.754531

Hamilton, P.S., Curley, M.G., Aimi, R.M., Sae-Hau, C., 2000. Comparison of methods for adaptive removal of motion artifact, in: Computers in Cardiology 2000. Presented at the Computers in Cardiology 2000, IEEE, New York City, USA, Cambridge, Massachusetts, USA, pp. 383–386. doi:10.1109/CIC.2000.898537

Harland, C.J., Clark, T.D., Prance, R.J., 2003. High resolution ambulatory electrocardiographic monitoring using wrist-mounted electric potential sensors. Meas. Sci. Technol. 14, 923. doi:10.1088/0957-0233/14/7/305

Harland, C.J., Clark, T.D., Prance, R.J., 2002. Electric potential probes - new directions in the remote sensing of the human body. Meas. Sci. Technol. 13, 163. doi:10.1088/0957-0233/13/2/304

Harris, M., Habetha, J., 2007. The MyHeart project: A framework for personal health care applications. pp. 137 –140. doi:10.1109/CIC.2007.4745440

Heart Rate Monitors, Workout Clothes and Fitness Gear - NuMetrex [WWW Document], n.d. URL http://www.numetrex.com/ (accessed 1.9.15).

He, B., 2010. Modeling & Imaging of Bioelectrical Activity: Principles and Applications. Springer Science & Business Media.

Hendriks, F.M., Brokken, D., Oomens, C.W.J., Bader, D.L., Baaijens, F.P.T., 2006. The relative contributions of different skin layers to the mechanical behavior of human skin in vivo using suction experiments. Med. Eng. Phys. 28, 259–266. doi:10.1016/j.medengphy.2005.07.001

Hendriks, F.M., Brokken, D., van Eemeren, J.T.W.M., Oomens, C.W.J., Baaijens, F.P.T., Horsten, J.B. a. M., 2003. A numerical-experimental method to characterize the non-linear mechanical behaviour of human skin. Skin Res. Technol. Off. J. Int. Soc. Bioeng. Skin ISBS Int. Soc. Digit. Imaging Skin ISDIS Int. Soc. Skin Imaging ISSI 9, 274–283.

Hoffmann, K.-P., Ruff, R., 2007. Flexible dry surface-electrodes for ECG long-term monitoring. Conf. Proc. Annu. Int. Conf. IEEE Eng. Med. Biol. Soc. IEEE Eng. Med. Biol. Soc. Annu. Conf. 2007, 5740–5743. doi:10.1109/IEMBS.2007.4353650

Hokajärvi, I.A., 2012. Electrode Contact Impedance and Biopotential Signal Quality. Tampere Universtiy of Technology, Tampere, Finland.

Huigen, E., Peper, A., Grimbergen, C., 2002. Investigation into the origin of the noise of surface electrodes. Med. Biol. Eng. Comput. 40, 332–338. doi:10.1007/BF02344216

Intelesens | Responsive Healthcare - zensor [WWW Document], n.d. URL http://www.intelesens.com/inhomemonitoring/zensor.html (accessed 1.9.15).

Intelligent training with a Fitness Shirt and an E-bike [WWW Document], n.d. URL http://www.fraunhofer.de/en/press/research-news/2013/november/intelligent-training.html (accessed 1.9.15).

Kang, T.-H., Merritt, C.R., Grant, E., Pourdeyhimi, B., Nagle, H.T., 2008. Nonwoven Fabric Active Electrodes for Biopotential Measurement During Normal Daily Activity. Biomed. Eng. IEEE Trans. On 55, 188 –195. doi:10.1109/TBME.2007.910678

Katsis, C.D., Ganiatsas, G., Fotiadis, D.I., 2006. An integrated telemedicine platform for the assessment of affective physiological states. Diagn. Pathol. 1, 16. doi:10.1186/1746-1596-1-16

Kauppinen, P., Hyttinen, J., Malmivuo, J., 2006. Sensitivity Distribution Visualizations of Impedance Tomography Measurement Strategies. Int. J. Bioelectromagn. 8, VII/1–VII/9.

Kearney, K., Thomas, C., McAdams, E., 2007. Quantification of Motion Artifact in ECG Electrode Design, in: Conference Proceedings: Annual International Conference of the IEEE Engineering in Medicine and Biology Society. IEEE Engineering in Medicine and Biology Society. pp. 1533 –1536. doi:10.1109/IEMBS.2007.4352594

Kim, S., Leonhardt, S., Zimmermann, N., Kranen, P., Kensche, D., Muller, E., Quix, C., 2008. Influence of contact pressure and moisture on the signal quality of a newly developed textile ECG sensor shirt. IEEE, pp. 256–259. doi:10.1109/ISSMDBS.2008.4575068

Kligfield, P., Gettes, L.S., Bailey, J.J., Childers, R., Deal, B.J., Hancock, E.W., Herpen, G. van, Kors, J.A., Macfarlane, P., Mirvis, D.M., Pahlm, O., Rautaharju, P., Wagner, G.S., 2007. Recommendations for the Standardization and Interpretation of the Electrocardiogram Part I: The Electrocardiogram and Its Technology: A Scientific Statement From the American Heart Association Electrocardiography and Arrhythmias Committee, Council on Clinical Cardiology; the American College of Cardiology Foundation; and the Heart Rhythm Society Endorsed by the International Society for Computerized Electrocardiology. Circulation 115, 1306–1324. doi:10.1161/CIRCULATIONAHA.106.180200

Kutz, M., 2003. Standard handbook of biomedical engineering and design. McGraw-Hill, New York.

Laferriere, P., Lemaire, E.D., Chan, A.D.C., 2011. Surface Electromyographic Signals Using Dry Electrodes. IEEE Trans. Instrum. Meas. 60, 3259–3268. doi:10.1109/TIM.2011.2164279

Langenhove, L. van, 2007. Smart textiles for medicine and healthcare: materials, systems and applications. CRC Press.

Lee, I.B., Shin, S.C., Jang, Y.W., Song, Y.S., Jeong, J.W., Kim, S., 2008. Comparison of conductive fabric sensor and Ag-AgCl sensor under motion artifacts. Conf. Proc. Annu. Int. Conf. IEEE Eng. Med. Biol. Soc. IEEE Eng. Med. Biol. Soc. Conf. 2008, 1300–1303. doi:10.1109/IEMBS.2008.4649402

Lee, W.-C., Yang, Y.-S.O., Ke, T.-C., Wei, C.-S., Lee, H.-C., 2010. Adaptive reduction of motion artifact in a portable ECG system, in: 2010 IEEE Sensors. Presented at the 2010 IEEE Sensors, IEEE, New York City, USA, Kona, Hawaii, USA, pp. 704–707. doi:10.1109/ICSENS.2010.5690058

LifeShirt - Vivonoetics [WWW Document], n.d. URL http://vivonoetics.com/products/sensors/lifeshirt/ (accessed 1.9.15).

Lin, C.-T., Liao, L.-D., Liu, Y.-H., Wang, I.-J., Lin, B.-S., Chang, J.-Y., 2011. Novel Dry Polymer Foam Electrodes for Long-Term EEG Measurement. IEEE Trans. Biomed. Eng. 58, 1200–1207. doi:10.1109/TBME.2010.2102353

Liu, H., Tao, X., Xu, P., Zhang, H., Bai, Z., 2013. A dynamic measurement system for evaluating dry bio-potential surface electrodes. Measurement 46, 1904–1913. doi:10.1016/j.measurement.2013.01.002

Liu, Y., 2007. Reduction of skin stretch induced motion artifacts in electrocardiogram monitoring using adaptive filtering (PhD thesis). University of Maryland, Department of Mechanical Engineering, College Park, Maryland, USA.

Löfhede, J., Seoane, F., Thordstein, M., 2012. Textile Electrodes for EEG Recording — A Pilot Study. Sensors 12, 16907–16919. doi:10.3390/s121216907

Luo, S., Tompkins, W.J., 1995. Experimental study: brachial motion artifact reduction in the ECG, in: Computers in Cardiology 1995. Presented at the Computers in Cardiology 1995, pp. 33 –36. doi:10.1109/CIC.1995.482564

Luprano, J., de Carvalho, P., Eilebrecht, B., Kortelainen, J., Muehlsteff, J., Sipila, A., Solà, J., Teichmann, D., Ulbrich, M., 2013. HeartCycle: advanced sensors for telehealth applications. Conf. Proc. Annu. Int. Conf. IEEE Eng. Med. Biol. Soc. IEEE Eng. Med. Biol. Soc. Annu. Conf. 2013, 6984–6987. doi:10.1109/EMBC.2013.6611165

Luprano, J., Sola, J., Dasen, S., Koller, J.M., Chetelat, O., 2006. Combination of Body Sensor Networks and On-Body Signal Processing Algorithms: the practical case of MyHeart project, in: Wearable and Implantable Body Sensor Networks, International Workshop on. IEEE Computer Society, Los Alamitos, CA, USA, pp. 76–79. doi:10.1109/BSN.2006.15

Lymberis, A., Paradiso, R., 2008. Smart fabrics and interactive textile enabling wearable personal applications: R #x00026;D state of the art and future challenges, in: 30th Annual International Conference of the IEEE Engineering in Medicine and Biology Society, 2008. EMBS 2008. Presented at the 30th Annual International Conference of the IEEE Engineering in Medicine and Biology Society, 2008. EMBS 2008, pp. 5270–5273. doi:10.1109/IEMBS.2008.4650403

Malmivuo, J., Plonsey, R., 1995. Bioelectromagnetism. Oxford University Press, New York.

Marozas, V., Petrenas, A., Daukantas, S., Lukosevicius, A., 2011. A comparison of conductive textile-based and silver/silver chloride gel electrodes in exercise electrocardiogram recordings. J. Electrocardiol. 44, 189–194. doi:10.1016/j.jelectrocard.2010.12.004

Marquez, J.C., Rempfler, M., Seoane, F., Lindecrantz, K., 2013. Textrode-enabled transthoracic electrical bioimpedance measurements - towards wearable applications of impedance cardiography. J. Electr. Bioimpedance 4, 45–50. doi:10.5617/jeb.542

Martinsen, Øs.G., Grimnes, S., Haug, E., 1999. Measuring depth depends on frequency in electrical skin impedance measurements. Skin Res. Technol. 5, 179–181. doi:10.1111/j.1600-0846.1999.tb00128.x

McAdams, E.T., Jossinet, J., Lackermeier, A., Risacher, F., 1996. Factors affecting electrode-gel-skin interface impedance in electrical impedance tomography. Med. Biol. Eng. Comput. 34, 397–408. doi:10.1007/BF02523842

M. Catrysse, R.P., 2003. Fabric sensors for the measurement of physiological parameters 1758 – 1761 vol.2. doi:10.1109/SENSOR.2003.1217126
Medrano, G., Ubl, A., Zimmermann, N., Gries, T., Leonhardt, S., 2007. Skin Electrode Impedance of Textile Electrodes for Bioimpedance Spectroscopy, in: 13th International Conference on Electrical Bioimpedance and the 8th Conference on Electrical Impedance Tomography, IFMBE Proceedings. Graz, Austria, pp. 260–263.
Merletti, R., Botter, A., Troiano, A., Merlo, E., Minetto, M.A., 2009. Technology and instrumentation for detection and conditioning of the surface electromyographic signal: state of the art. Clin. Biomech. Bristol Avon 24, 122–134. doi:10.1016/j.clinbiomech.2008.08.006
Merritt, C.R., Nagle, H.T., Grant, E., 2009. Fabric-based active electrode design and fabrication for health monitoring clothing. IEEE Trans. Inf. Technol. Biomed. Publ. IEEE Eng. Med. Biol. Soc. 13, 274–280. doi:10.1109/TITB.2009.2012408
Mestrovic, M.A., Helmer, R.J.N., Kyratzis, L., Kumar, D., 2007. Preliminary study of dry knitted fabric electrodes for physiological monitoring. IEEE, pp. 601–606. doi:10.1109/ISSNIP.2007.4496911
Muhlsteff, J., Such, O., 2004. Dry electrodes for monitoring of vital signs in functional textiles. Presented at the 26th Annual International Conference of the IEEE Engineering in Medicine and Biology Society, 2004. IEMBS '04, IEEE, pp. 2212–2215. doi:10.1109/IEMBS.2004.1403645
Muhlsteff, J., Such, O., Schmidt, R., Perkuhn, M., Reiter, H., Lauter, J., Thijs, J., Musch, G., Harris, M., 2004. Wearable approach for continuous ECG--and activity patient-monitoring, in: Conference Proceedings: ... Annual International Conference of the IEEE Engineering in Medicine and Biology Society. IEEE Engineering in Medicine and Biology Society. Conference. pp. 2184–7. doi:10.1109/IEMBS.2004.1403638
Mundt, C.W., Montgomery, K.N., Udoh, U.E., Barker, V.N., Thonier, G.C., Tellier, A.M., Ricks, R.D., Darling, R.B., Cagle, Y.D., Cabrol, N.A., Ruoss, S.J., Swain, J.L., Hines, J.W., Kovacs, G.T.A., 2005. A multiparameter wearable physiologic monitoring system for space and terrestrial applications. IEEE Trans. Inf. Technol. Biomed. Publ. IEEE Eng. Med. Biol. Soc. 9, 382–391.
Myontec | Know Your Muscles [WWW Document], n.d. URL http://www.myontec.com/en/ (accessed 1.9.15).
Neuman, M.R., 1997. Biopotential Electrodes, in: Webster, J.G. (Ed.), Medical Instrumentation: Application and Design. John Wiley & Sons Inc., pp. 183–232.
Noury, N., Dittmar, A., Corroy, C., Baghai, R., Weber, J.L., Blanc, D., Klefstat, F., Blinovska, A., Vaysse, S., Comet, B., 2004. A smart cloth for ambulatory telemonitoring of physiological parameters and activity: the VTAMN project. pp. 155 – 160. doi:10.1109/HEALTH.2004.1324507
Ödman, S., 1989. Changes in skin potentials induced by skin compression. Med. Biol. Eng. Comput. 27, 390–3.
Ödman, S., 1982. On the spread of deformation potentials in the skin. Med. Biol. Eng. Comput. 20, 451–456. doi:10.1007/BF02442405
Ödman, S., 1981. Potential and impedance variations following skin deformation. Med. Biol. Eng. Comput. 19, 271–278. doi:10.1007/BF02442544
Ödman, S., Öberg, P.Å., 1982. Movement-induced potentials in surface electrodes. Med. Biol. Eng. Comput. 20, 159–166. doi:10.1007/BF02441351
Ottenbacher, J., Jatoba, L., Großmann, U., Stork, W., Müller-Glaser, K., 2007. ECG electrodes for a context-aware cardiac permanent monitoring system, in: Magjarevic, R., Nagel, J.H. (Eds.), World Congress on Medical Physics and Biomedical Engineering 2006, IFMBE Proceedings. Springer Berlin Heidelberg, pp. 672–675.
Ottenbacher, J., Kirst, M., Jatobá, L., Großmann, U., Stork, W., 2008. An approach to reliable motion artifact detection for mobile long-term ECG monitoring systems using dry electrodes, in: Müller-Karger, C., Wong, S., Cruz, A.L. (Eds.), IV Latin American Congress on Biomedical Engineering

2007, Bioengineering Solutions for Latin America Health, IFMBE Proceedings. Springer Berlin Heidelberg, Margarita Island, Venezuela, pp. 440–443.
Ottenbacher, J., Kirst, M., Jatoba, L., Huflejt, M., Grossmann, U., Stork, W., 2008. Reliable motion artifact detection for ECG monitoring systems with dry electrodes. pp. 1695 –1698. doi:10.1109/IEMBS.2008.4649502
Pacelli, M., Loriga, G., Taccini, N., Paradiso, R., 2006. Sensing Fabrics for Monitoring Physiological and Biomechanical Variables: E-textile solutions, in: 3rd IEEE/EMBS International Summer School on Medical Devices and Biosensors, 2006. Presented at the 3rd IEEE/EMBS International Summer School on Medical Devices and Biosensors, 2006, pp. 1–4. doi:10.1109/ISSMDBS.2006.360082
Pailler-Mattei, C., Bec, S., Zahouani, H., 2008. In vivo measurements of the elastic mechanical properties of human skin by indentation tests. Med. Eng. Phys. 30, 599–606. doi:10.1016/j.medengphy.2007.06.011
Pandian, P.S., Mohanavelu, K., Safeer, K.P., Kotresh, T.M., Shakunthala, D.T., Gopal, P., Padaki, V.C., 2008. Smart Vest: Wearable multi-parameter remote physiological monitoring system. Med. Eng. Phys. 30, 466–477. doi:10.1016/j.medengphy.2007.05.014
Paradiso, R., Belloc, C., Loriga, G., Taccini, N., 2005a. Wearable healthcare systems, new frontiers of e-textile. Stud. Health Technol. Inform. 117, 9–16.
Paradiso, R., De Rossi, D., 2006. Advances in textile technologies for unobtrusive monitoring of vital parameters and movements. Conf. Proc. Annu. Int. Conf. IEEE Eng. Med. Biol. Soc. IEEE Eng. Med. Biol. Soc. Conf. 1, 392–395. doi:10.1109/IEMBS.2006.259307
Paradiso, R., Loriga, G., Taccini, N., 2005b. A wearable health care system based on knitted integrated sensors. IEEE Trans. Inf. Technol. Biomed. Publ. IEEE Eng. Med. Biol. Soc. 9, 337–344.
Paradiso, R., Pacelli, M., 2011. Textile electrodes and integrated smart textile for reliable biomonitoring, in: 2011 Annual International Conference of the IEEE Engineering in Medicine and Biology Society,EMBC. Presented at the 2011 Annual International Conference of the IEEE Engineering in Medicine and Biology Society,EMBC, pp. 3274–3277. doi:10.1109/IEMBS.2011.6090889
Park, C., Chou, P.H., Bai, Y., Matthews, R., Hibbs, A., 2006. An ultra-wearable, wireless, low power ECG monitoring system, in: IEEE Biomedical Circuits and Systems Conference, 2006. BioCAS 2006. Presented at the IEEE Biomedical Circuits and Systems Conference, 2006. BioCAS 2006, pp. 241–244. doi:10.1109/BIOCAS.2006.4600353
Pengjun, X., Xiaoming, T., Shanyuan, W., 2011. Measurement of wearable electrode and skin mechanical interaction using displacement and pressure sensors, in: 4th International Conference on Biomedical Engineering and Informatics (BMEI). Shanghai, China, pp. 1131 –1134. doi:10.1109/BMEI.2011.6098433
Perez, R., 2002. Design of Medical Electronic Devices. Academic Press.
Plonsey, R., Barr, R.C., n.d. Bioelectricity - A Quantitative Approach.
Pola, T., Vanhala, J., 2007. Textile Electrodes in ECG Measurement. pp. 635 –639. doi:10.1109/ISSNIP.2007.4496917
Prance, R.J., Debray, A., Clark, T.D., Prance, H., Nock, M., Harland, C.J., Clippingdale, A.J., 2000. An ultra-low-noise electrical-potential probe for human-body scanning. Meas. Sci. Technol. 11, 291. doi:10.1088/0957-0233/11/3/318
PRODUCTS PhysioGlove [WWW Document], n.d. URL http://www.commwellmedical.com/index.php?option=com_content&view=article&id=2&Itemid=6 (accessed 1.9.15).
Przywara, B., 2010. Projecting future health care expenditure at European level: drivers, methodology and main results.
PSM | Quasar USA [WWW Document], n.d. URL http://www.quasarusa.com/products_psm.htm (accessed 1.9.15).

Puurtinen, M.M., Komulainen, S.M., Kauppinen, P.K., Malmivuo, J.A.V., Hyttinen, J.A.K., 2006. Measurement of noise and impedance of dry and wet textile electrodes, and textile electrodes with hydrogel. Conf. Proc. Annu. Int. Conf. IEEE Eng. Med. Biol. Soc. IEEE Eng. Med. Biol. Soc. Conf. 1, 6012–6015. doi:10.1109/IEMBS.2006.260155

Pylatiuk, C., Muller-Riederer, M., Kargov, A., Schulz, S., Schill, O., Reischl, M., Bretthauer, G., 2009. Comparison of surface EMG monitoring electrodes for long-term use in rehabilitation device control, in: IEEE International Conference on Rehabilitation Robotics, 2009. ICORR 2009. Presented at the IEEE International Conference on Rehabilitation Robotics, 2009. ICORR 2009, pp. 300–304. doi:10.1109/ICORR.2009.5209576

Rattfält, L., Lindén, M., Hult, P., Berglin, L., Ask, P., 2007. Electrical characteristics of conductive yarns and textile electrodes for medical applications. Med. Biol. Eng. Comput. 45, 1251–1257. doi:10.1007/s11517-007-0266-y

Raya, M.A., Sison, L.G., 2002. Adaptive noise cancelling of motion artifact in stress ECG signals using accelerometer, in: Engineering in Medicine and Biology, 2002. 24th Annual Conference and the Annual Fall Meeting of the Biomedical Engineering Society EMBS/BMES Conference, 2002. Proceedings of the Second Joint. Presented at the Engineering in Medicine and Biology, 2002. 24th Annual Conference and the Annual Fall Meeting of the Biomedical Engineering Society EMBS/BMES Conference, 2002. Proceedings of the Second Joint, IEEE, New York City, USA, Houston, Texas, USA, pp. 1756–1757 vol.2. doi:10.1109/IEMBS.2002.1106637

Riistama, J., 2010. Characterisation of Wearable and Implantable Physiological Measurement Devices.

Romero, I., Berset, T., Buxi, D., Brown, L., Penders, J., Kim, S., Van Helleputte, N., Kim, H., Van Hoof, C., Yazicioglu, F., 2011. Motion Artifact Reduction in Ambulatory ECG Monitoring: An Integrated System Approach, in: Proceedings of the 2Nd Conference on Wireless Health, WH '11. ACM, New York, NY, USA, pp. 11:1–11:8. doi:10.1145/2077546.2077558

Romero, I., Geng, D., Berset, T., 2012. Adaptive filtering in ECG denoising: A comparative study, in: Computing in Cardiology (CinC), 2012. Presented at the Computing in Cardiology (CinC), 2012, pp. 45–48.

Rosell, J., Colominas, J., Riu, P., Pallas-Areny, R., Webster, J.G., 1988. Skin impedance from 1 Hz to 1 MHz. IEEE Trans. Biomed. Eng. 35, 649–651. doi:10.1109/10.4599

Roy, S.H., De Luca, G., Cheng, M.S., Johansson, A., Gilmore, L.D., De Luca, C.J., 2007. Electro-mechanical stability of surface EMG sensors. Med. Biol. Eng. Comput. 45, 447–457. doi:10.1007/s11517-007-0168-z

Sanders, R., 1973. Torsional elasticity of human skin in vivo. Pflüg. Arch. Eur. J. Physiol. 342, 255–260.

Scilingo, E.P., Gemignani, A., Paradiso, R., Taccini, N., Ghelarducci, B., De Rossi, D., 2005. Performance evaluation of sensing fabrics for monitoring physiological and biomechanical variables. IEEE Trans. Inf. Technol. Biomed. Publ. IEEE Eng. Med. Biol. Soc. 9, 345–52.

Searle, A., Kirkup, L., 2000. A direct comparison of wet, dry and insulating bioelectric recording electrodes. Physiol. Meas. 21, 271–283. doi:10.1088/0967-3334/21/2/307

Seoane, F., Ferreira, J., Alvarez, L., Buendia, R., Ayllón, D., Llerena, C., Gil-Pita, R., 2013. Sensorized Garments and Textrode-Enabled Measurement Instrumentation for Ambulatory Assessment of the Autonomic Nervous System Response in the ATREC Project. Sensors 13, 8997–9015. doi:10.3390/s130708997

Seoane, F., Mohino-Herranz, I., Ferreira, J., Alvarez, L., Buendia, R., Ayllón, D., Llerena, C., Gil-Pita, R., 2014. Wearable biomedical measurement systems for assessment of mental stress of combatants in real time. Sensors 14, 7120–7141. doi:10.3390/s140407120

Smartex WWS - Vivonoetics [WWW Document], n.d. URL http://vivonoetics.com/products/sensors/smartex-wearable-wellness-system/ (accessed 1.9.15).

Sweeney, K., McLoone, S., Ward, T., 2010. A simple bio-signals quality measure for in-home monitoring. Presented at the Biomedical Engineering (Vol. 1 and Vol. 2), Innsbruck, Austria.

Sweeney, K.T., Ward, T.E., McLoone, S.F., 2012. Artifact Removal in Physiological Signals #x2014;Practices and Possibilities. IEEE Trans. Inf. Technol. Biomed. 16, 488–500. doi:10.1109/TITB.2012.2188536

Talhouet, H. de, Webster, J.G., 1996. The origin of skin-stretch-caused motion artifacts under electrodes. Physiol. Meas. 17, 81–93. doi:10.1088/0967-3334/17/2/003

Tam, H., Webster, J.G., 1977. Minimizing Electrode Motion Artifact by Skin Abrasion. Biomed. Eng. IEEE Trans. On BME-24, 134 –139. doi:10.1109/TBME.1977.326117

Tavernier, A., Dierickx, M., Hinsenkamp, M., 1993. Tensors of dielectric permittivity and conductivity of in vitro human dermis and epidermis. Bioelectrochem. Bioenerg. 30, 65–72. doi:10.1016/0302-4598(93)80063-Z

The Future Of Healthcare In Europe, 2011. . The Economist / Economist intelligence Unit.

Tong, D.A., Bartels, K.A., Honeyager, K.S., 2002. Adaptive reduction of motion artifact in the electrocardiogram, in: 24th Annual Conference and the Annual Fall Meeting of the Biomedical Engineering Society EMBS/BMES Conference, 2002. Proceedings of the Second Joint. IEEE, New York City, USA, Houston, Texas, USA, pp. 1403–04. doi:10.1109/IEMBS.2002.1106451

Tran, H.V., Charleux, F., Rachik, M., Ehrlacher, A., Ho Ba Tho, M.C., 2007. In vivo characterization of the mechanical properties of human skin derived from MRI and indentation techniques. Comput. Methods Biomech. Biomed. Engin. 10, 401–407. doi:10.1080/10255840701550287

Tseng, K.C., Lin, B.-S., Liao, L.-D., Wang, Y.-T., Wang, Y.-L., 2013. Development of a Wearable Mobile Electrocardiogram Monitoring System by Using Novel Dry Foam Electrodes. IEEE Syst. J. Early Access Online. doi:10.1109/JSYST.2013.2260620

Vos, W.K., Bergveld, P., Marani, E., 2003. Low frequency changes in skin surface potentials by skin compression: experimental results and theories. Arch. Physiol. Biochem. 111, 369–376. doi:10.3109/13813450312331337621

Webster, J., 2009. Medical Instrumentation: Application And Design, 3Rd Ed. Wiley India Pvt. Limited.

Webster, J.G., 1984. Reducing motion artifacts and interference in biopotential recording. IEEE Trans. Biomed. Eng. 31, 823–6. doi:10.1109/TBME.1984.325244

Wolthuis, R.A., Froelicher, V.F., Hopkirk, A., Fischer, J.R., Keiser, N., 1979. Normal electrocardiographic waveform characteristics during treadmill exercise testing. Circulation 60, 1028–1035.

Wu, J.Z., Dong, R.G., Smutz, W.P., Schopper, A.W., 2003. Modeling of time-dependent force response of fingertip to dynamic loading. J. Biomech. 36, 383–392. doi:10.1016/S0021-9290(02)00427-X

Yoo, J., Yan, L., Lee, S., Kim, H., Yoo, H.-J., 2009. A Wearable ECG Acquisition System With Compact Planar-Fashionable Circuit Board-Based Shirt. IEEE Trans. Inf. Technol. Biomed. 13, 897–902. doi:10.1109/TITB.2009.2033053

Zaunseder, S., Fischer, W.-J., Netz, S., Poll, R., Rabenau, M., 2007. Prolonged Wearable ECG Monitoring - a Wavelet Based Approach, in: 2007 IEEE Sensors. Presented at the 2007 IEEE Sensors, pp. 1197–1200. doi:10.1109/ICSENS.2007.4388623

Publications

Paper 1

Cömert A, Honkala M, Hyttinen J: Effect of pressure and padding on motion artifact of textile electrodes. *Biomed Eng Online* 2013, 12:26.

(An errata list is presented after Paper 4)

Paper 2

Cömert A, Hyttinen J: A motion artifact generation and assessment system for the rapid testing of surface biopotential electrodes. *Physiol Meas* 2015, 36:1.

(An errata list is presented after Paper 4)

Paper 3

Cömert A, Hyttinen J: Impedance spectroscopy of changes in skin-electrode impedance induced by motion. *BioMedical Engineering OnLine* 2014, 13:149.

(An errata list is presented after Paper 4)

Paper 4

Cömert A, Hyttinen J: Investigating the Possible Effect of Electrode Support Structure on Motion Artifact in Wearable Bioelectric Signal Monitoring. *BioMedical Engineering OnLine* 2015, 14:44

Errata of Publications

Paper 1

- Correct version of Figure 3 is presented below.

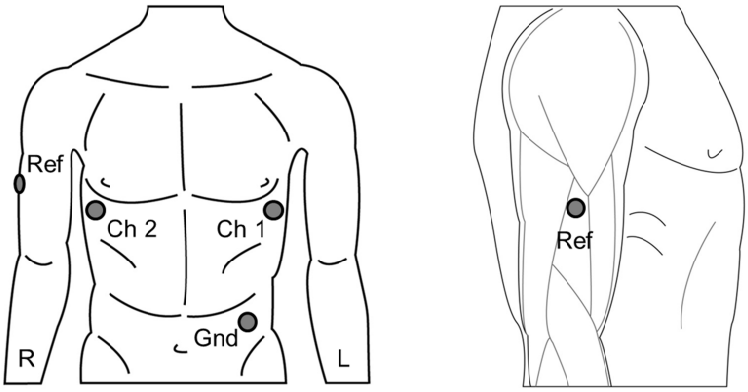

- In Figure 4 and the caption of Figure 4, the dimensions of the paddings are presented as diameters; however, the given numbers are for the radii of the paddings. “d” is corrected to be “r” and “diameter” is corrected to be “radius”

Paper 2

- Page 8: The text “ECG channel approximating the standard ECG channel aVR” is not accurate. An accurate definition of that channel is:
  “A channel that contains a strong ECG component”

Paper 3

- Page 5: The text “To achieve adequate resolution, the frequency band between 25 Hz and 1 MHz was divided into 24 logarithmically evenly distributed frequencies” is not correct.
  The correct description of the selected frequencies is: “To achieve adequate resolution, the frequency band between 30 Hz and 1 MHz was divided into 24 logarithmically evenly distributed frequencies”.
  In this setup, the lower three frequencies are 30, 47 and 74 Hz. Because the impedance measurement at 47 Hz is highly susceptible to 50Hz line noise, the lower two frequencies were changed to 25 and 34 Hz.
- It would be useful to point out that the effect of the interwoven arrangement of the frequency grouping can be observed the resistance plot presented in Figure 2: The same artifact is present at frequencies 74 , 289 and 1.1k Hz, pointing to a an artifact present in a measurement, and not a frequency band. (an artifact occurring in consecutive frequencies can easily be misattributed to a frequency dependent property, rather than an error in a measurement)

Tampereen teknillinen yliopisto
PL 527
33101 Tampere

Tampere University of Technology
P.O.B. 527
FI-33101 Tampere, Finland

ISBN 978-952-15-3563-5
ISSN 1459-2045